REACTIONS OF OSMIUM CLUSTERS

Steven J. Black

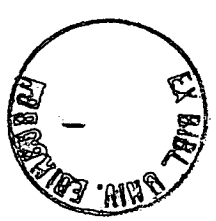

A Thesis presented for the degree of
Doctor of Philosophy in the Faculty of Science,
University of Edinburgh, 1994.

To my parents

Declaration

This thesis has not been submitted, in whole or in part, for any degree at this or any other institution. Furthermore all of the reactions reported here were carried out by me under the direct supervision of Professor B. F. G. Johnson and Dr S. G. D. Henderson. Any descriptions of work not carried out by me have been duly referenced.

CONTENTS

CONTENTS

CONTENTS

CONTENTS

CONTENTS

I would like to thank the following people, without whom this work would not have been possible.

First and foremost I would like to express my sincerest thanks to my supervisors Professor B. F. G. Johnson and Dr S. G. D. Henderson, for their invaluable assistance with the theoretical and practical aspects of this project, and their support through some of the more difficult times over the past three years. I would further like to thank Dr Henderson for help with glassblowing and for the tuition provided in basic glassblowing techniques and nmr spectrometer operation.

I would like to thank Dr D. Reed for his assistance and advice regarding the theory and practice of nmr spectroscopy. I would like to thank the following members of the University of Edinburgh technical staff for their assistance. Mr J. R. A. Millar and Mr W. Kerr for running some of the nmr spectra presented in this work, and for surrendering their spectrometers so frequently and graciously. Mr A. Taylor for running the mass spectra presented here and for his tolerance in running spectra at sometimes absurdly short notice.

Finally I acknowledge the award of a research studentship by the Earth and Physical Sciences Research Council and the provision of laboratory facilities by the University of Edinburgh.

Abbreviations

The following abbreviations are used in the text.

ir	Infra Red
ν	Frequency in cm^{-1}
s	Strong
m	Medium
w	Weak
EI	Electron Ionisation
FAB	Fast Atom Bombardment
MALDI	Matrix Assisted Laser Desorption Ionisation
M^+	Molecular ion peak
M/e	Mass to Charge ratio
nmr	Nuclear Magnetic Resonance
δ	Chemical shift values
$^nJ_{AB}$	n-bond A-B coupling constant, n = 1-3
M	Metal
L	Ligand
CO	Carbonyl
R	Alkyl, aryl or hydrogen
Me	Methyl
Et	Ethyl
i-Pr	Isopropyl
Ph	Phenyl
COD	Cyclo Octadiene

THF	Tetrahydrofuran
tlc	Thin Layer Chromatography
atm	Atmospheres
PES	Photoelectron Spectrum
eV	Electron Volts
N/A	Not Available
PSEP	Polyhedral Skeletal electron Pair
SEP	Skeletal Electron Pair
TEC	Total Electron Count
EAN	Effective Atomic Number
FIG	Figure

ABSTRACT

Previous studies of the ligand properties of primary, secondary and tertiary phosphines on metal monomers have been carried out. These studies investigated the properties of the phosphines in terms of the effects of their basicity and Tolman's cone angle on the metal substrate.

The reactions of $[Os_3(CO)_{10}(MeCN)_2]$ with a series of primary, secondary and tertiary phosphines (PR_xH_{3-x}) where R = Me, Et, i-Pr, Ph, were studied by variable temperature $^{31}P\{^1H\}$, and ^{31}P nmr. The reactions were monitored by nmr firstly after 24 hours at ambient temperature, the tubes were then heated to 60°C for 1 hour and the products studied by nmr, ir and mass spectroscopy. The products present included *mono* and disubstituted clusters. Also identified were inter- and intramolecular phosphinidene bridged species. The cluster bound products were initially identified on the basis of the $^1J_{PH}$ coupling constants - approximately 400Hz as opposed to approximately 200Hz for the free phosphines.

Stability studies were carried out on the triosmium benzene cluster system $[Os_3(CO)_9(\eta^2\eta^2\eta^2C_6H_6)]$. The cluster was reacted with a series of tertiary phosphines initially with heating and later uv irradiation to attempt to displace the benzene ligand. The ligand has proven to be strongly bound to the cluster as there was no displacement observed, though CO displacement occurs affording *mono-*, *bis-* and *tris*-phosphine cluster derivatives. The benzene ligand attached to the cluster also proved resistant to displacement *via* high vacuum pyrolysis.

Study of the mechanism for the thermal conversion of the raft cluster $[Os_6(CO)_{21}]$ with the species $[Os_6(CO)_{18}]$ under vacuum has been carried out *via* pressure monitoring, showing the loss of CO to be a stepwise process. During this reaction the formation of a novel ketenylidene species, $[Os_3(CO)_{11}CCO]$ has been observed. This species has been

characterised by high resolution FAB mass spectroscopy.

CHAPTER ONE

INTRODUCTION

INTRODUCTION

Metal Clusters

The study of transition metal clusters has provided several different definitions as to the nature of these species. The description given by Cotton[1], describes a cluster as "a finite group of metal atoms which are held together either entirely, mainly or at least to a significant degree by bonds between metal atoms, even though some non metal atoms may be associated intimately with the cluster".

The definition given by King[2], states that a cluster is "a network of metal atoms held together by at least two metal-metal bonds to each metal". This description however, rules out trinuclear species with one open edge.

Chini[3] states that "a cluster is a three dimensional network of metal atoms which is held together by metal-metal bonds and within which each metal atom forms at least 3 different metal-metal bonds". This definition, of course rules out all trinuclear clusters, any planar systems and any systems with edge bridging metal units.

This work will be mainly concerned with trinuclear and hexanuclear osmium carbonyl clusters and their reactions with phosphorus compounds. For the purposes of this work the definition of a cluster given by Cotton[1] will be adopted.

The study of metal clusters over the past 20 years has been both intensive and wide ranging[4-6]. These studies have shown that clusters may be regarded as small fragments of a bulk metal framework, with these fragments exhibiting packing similar to that observed for hexagonal close packed metal arrays in the bulk phase. Cluster polyhedra generally exhibit triangular faces, similar to the array observed for the metal 1,1,1 surface. Clusters may generally be subdivided by nuclearity into the tri- and tetranuclear species and a more encompassing group, the high nuclearity clusters.

Cluster Synthesis

Polynuclear metal carbonyl clusters may be synthesised in a number of ways;

(i) Preparation by autoclave reaction : The use of high pressure autoclave reactors to produce polynuclear metal species from monomers is perhaps the commonest method of synthesising clusters available. This method is used to produce the bulk of the "building block" clusters, mainly trinuclear cluster units, in use today.

(ii) Cluster condensation : The addition of highly reactive mononuclear metal species to clusters with vacant coordination sites offers a controlled route to cluster buildup.

(iii) Pyrolysis Reactions : The pyrolysis of trinuclear cluster species, either *in vacuo* or in high boiling solvents may be used to access clusters with, in the case of osmium, four to ten metal atoms.

Electron counting and cluster structure

In order that the bonding and geometries of metal clusters may be fully understood, it is first necessary to consider the bonding at a single metal centre. An isolated transition metal centre has nine atomic orbitals, each of which can hold two electrons. This forms the basis of the Effective Atomic Number, (EAN), or eighteen electron rule. The majority of transition metal centres conform to this rule, achieving a stable closed shell configuration whenever possible. The EAN rule makes several assumptions when applied to metal cluster systems.

(i) All M-M bonds correspond to polyhedral edge bonds.

(ii) All M-M bonds are two centre, two electron bonds.

(iii) Ligands serve solely as a source of electrons.

However, even with these considerations, the EAN rule breaks down when applied to high nuclearity cluster species primarily because polyhedral edges can no longer be considered to represent two centre, two electron bonds.

Wade's Rules and cluster structure

Recently much effort has been applied to deriving empirical methods for structure determination for cluster species, both of the transition elements and those of the main group. The original rules proposed for rationalisation of cluster structure were those for borane and carborane clusters derived by Wade[7]. Wade proposed that the gross geometrical features of the structures of these complexes could be rationalised by counting the number of electron pairs available to the cluster with respect to the number of vertices present. One of the problems with boron cage clusters is electron deficiency in that there are insufficient electrons present to permit the formation of two centre two electron bonds between all adjacent pairs of atoms. To rationalise this, a multicentre bonding approach must be employed. Wade proposed a set of rules for predicting the structures of these systems with the assumption that each B-H unit could supply three orbitals and two electrons to the cage framework, these rules are given below.

(i) For a $B_nH_n^{x-}$ species, the preferred structure is *closo*, an n-vertex polyhedron, with a preferred charge of 2-. There are n+1 pairs of electrons available to the framework. A *closo* structure, from the Greek *clovo* (cage), is defined as a closed polyhedron.

(ii) For a B_nH_{4+n} borane, where there are n+2 pairs of electrons available to the framework, a *nido* structure will be preferred. A *nido* structure, from the Latin *nidus* (nest), is defined as a polyhedron which lacks one vertex.

(iii) For a B_nH_m species based on a $B_nH_n^{6-}$ anion, an *arachno* structure will be preferred. There are n+3 pairs of electrons available to the framework. An *arachno* structure, from the Greek *arachnid* (spider), is defined as a polyhedron which lacks two adjacent vertices.

(iv) For a B_nH_m species based on a $B_nH_n^{8-}$ anion, a *hypho* structure will be preferred. There are n+**4**pairs of electrons available to the framework. A *hypho* structure, from the greek *hyphus* (net), is defined as a polyhedron which lacks three contiguous vertices.

The rules proposed by Wade give excellent results for borane and carborane clusters when predicted structure types are compared to those determined by spectroscopic methods, X-ray, nmr and so on. High nuclearity transition metal clusters are however, often structurally complex, and the presence of second and third row transition metals makes interpretation of their structures by conventional electron counting means difficult. This is a consequence of the separation of the s and p orbitals increasing on descending the periodic table and because of this, the possibility exists that fulfilment of the EAN rule is no longer required at each metal centre, making structure prediction by simple means difficult.

These rules, with some modifications form the basis of the now widely accepted polyhedral skeletal electron pair theory, (PSEP), for cluster structure prediction. By modification of the rules established for boron clusters by means of the isolobal theory[8-10] predictions may be made as to the structure of polynuclear metal clusters. Isolobal theory states that two molecular fragments are isolobal if number, symmetry, shapes and approximate energies of their frontier orbitals are the same. In the case of $M(CO)_3$ units which may be considered isolobal to B-H fragments the rules work well. However they do not function as well for $M(CO)_2$ and $M(CO)_4$ fragments, owing the significant symmetry differences between these fragments.

From this the comparison may be made between boranes/carboranes and high nuclearity metal clusters. Both of these classes of complex are unable to form two centre two electron bonds between all adjacent pairs of boron or metal atoms owing to electron deficiency. This allows the basic principles of electron counting for boron clusters to be applied to transition metal clusters. Subsequently several more elaborate treatments of PSEP have been derived for metal clusters[11-14]. However this discussion will be limited to the basic rules derived by Wade and some additional rules required to rationalise metal cluster structure.

With respect to metal clusters, the number of skeletal electron pairs, (SEP), is still the basis of the theory though other terms may be used, with the total electron count, (TEC), being the most common. The TEC is derived by adding up the electrons available for cluster bonding as follows;

(i) The total number of valence electrons available for each metal atom

(ii) Two electrons per CO ligand, regardless of coordination mode

(iii) One electron per unit of negative charge

(iv) The total number of valence electrons for each heteroatom associated with the cluster

The TEC for a cluster is based on the premise that each metal present will require twelve electrons for nonskeletal bonding to its associated ligands. For a *closo* structure with n vertices the TEC is given by the formula TEC = 12n + 2(n+1) electrons. Similarly for *nido, arachno* and *hypho* clusters, which are derived from a parent n vertex polyhedron the equations will require twelve, twenty four and thirty six less electrons respectively as the structure is based upon a parent polyhedron with missing vertices, not the number of vertices present in the cluster. Thus the equations for these structural types may be written as given overleaf.

nido TEC = 12(n-1) + 2(n+1) electrons

arachno TEC = 12(n-2) + 2(n+1) electrons

hypho TEC = 12(n-3) + 2(n+1) electrons

In practice, the TEC is usually determined by counting up the electrons for each metal/ligand fragment and subtracting twelve, with the remainder of the electrons constituting the SEP's available to the cluster framework. On the basis that for a *closo* n-vertex polyhedron the number of SEP's required is (n+1), for a *nido* structure (n+2) and so on, cluster structures may be predicted with a considerable degree of accuracy. e.g. for $[Rh_6(CO)_{16}]$, the TEC is 86, ({9x6} + {16x2}), and the number of SEP's may be determined by subtracting (12x6), leaving 14 electrons or 7 SEP. From this, the number of SEP is equal to (n+1), giving a *closo* structure for the complex, which agrees with the structure determined by X-ray study. For *nido, arachno* and *hypho* structures, a similar procedure is employed with the number of SEP's being equal to (n+2), (n+3) and (n+4) respectively.

One of the problems posed by polyhedral metal species is that they sometimes comprise a central metal core with one or more capping metal subunits. This necessitates the extension of the electron counting rules to include these complexes, as the central metal core electron count will be independent of the presence of a capping unit as it will still retain its basic structural configuration. This is facilitated by increasing the number of electrons required by twelve. The cluster $[Os_6(CO)_{18}]$ provides a convenient example for this, with the TEC being 84, ({6x8} + (18x2}). Subtracting (6x12) from this leaves the cluster with 6 SEP, indicating a *closo* five vertex polyhedron, with a capping metal unit. The structure of this complex is in fact a capped trigonal bipyramid[15], confirming the structural prediction made by electron counting.

Cluster Topology

Polynuclear clusters of the transition metals exhibit a vast range of structural forms. These range from the simple triangles observed for trinuclear species, through the square planar, butterfly and tetrahedral forms exhibited by tetranuclear clusters and on to the diverse forms of the higher nuclearity species.

Trinuclear clusters are simple triangular formations of metal atoms, either equilateral in nature as in $[Os_3(CO)_{12}]$[16] or an isosceles triangle as in $[H_2Os_3(CO)_{10}]$[17], (FIG 1.1). The species $[H_2Os_3(CO)_{10}]$ is electron deficient, as there are only forty six electrons available for the cluster framework, necessitating the presence of a M-M double bond in order to satisfy the EAN rule for all three metals. The cluster $[Os_3(CO)_{12}]$ is an electronically saturated species however, with forty eight electrons available to the metal framework and one M-M bond per cluster edge. This type of cluster is responsible for a large proportion of the study afforded cluster complexes owing to the ease of synthesis of these species and their diverse reactivity[18].

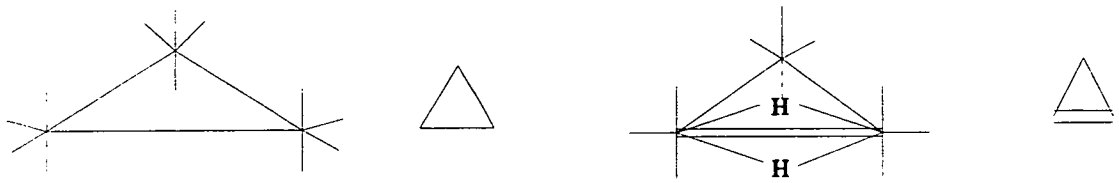

$[Os_3(CO)_{12}]$ $[H_2Os_3(CO)_{10}]$

Figure 1.1 : The Structures Of $[Os_3(CO)_{12}]$ And $[H_2Os_3(CO)_{10}]$

Tetranuclear clusters are common, with the predominant structural form observed being the tetrahedron as in $[Ir_4(CO)_{12}]$[19]. Tetrahedral clusters of this type are electronically saturated, with tetrahedral complexes requiring three M-M connectivities per metal to allow a closed shell configuration for all four metals to be achieved, with this distribution of bonds giving the cluster a total of sixty electrons involved in the framework. Other structural forms are known to exist however, with examples of butterfly and square planar complexes having been characterised[20], (FIG 1.2). These species are generally electron rich by comparison to the tetrahedron, having sixty two electrons, (butterfly) or sixty four electrons, (D_{4h} square planar).

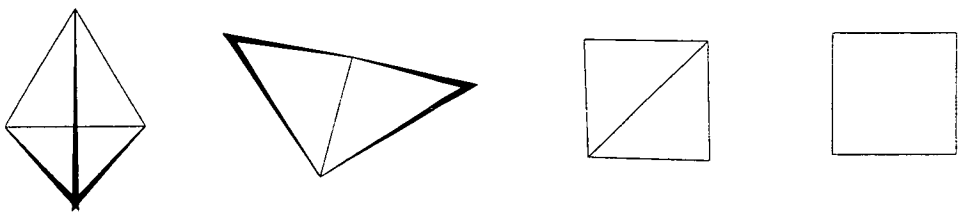

Tetrahedron Butterfly Square Planar - With And Without Diagonal Bond

Figure 1.2 : Some Polynuclear Structure Types Available For Tetranuclear Clusters

High nuclearity clusters

All clusters with five or more metal atoms may be included under this heading. The first high nuclearity cluster identified was $[Rh_6(CO)_{16}]$[21] in 1963. Since then the number of high nuclearity clusters known has grown to enormous proportions. In addition to the interest shown in these complexes purely for their chemical properties they are also studied in an attempt to elucidate how many metal atoms must come together before bulk metal properties may be observed. Although structural patterns for high nuclearity clusters are diverse structure types may be grouped into general classifications, as outlined below.

(i) Closed polyhedra : These are the most common type of high nuclearity cluster observed. Within this structural group the octahedron is certainly one of the most prevalent types observed. Octahedral clusters have been observed for most of the transition metals, *e.g.* $[Ru_6(CO)_{18}H_2]$[22], (FIG 1.3). Other closed polyhedra include the trigonal bipyramid, *e.g.* $[\{Ni_5(CO)_{12}\}^{2-}]$[23], (FIG 1.3), also known is the capped trigonal bipyramid, *e.g.* $[Os_6(CO)_{18}]$[15], (FIG 1.3). There are higher nuclearity clusters of this type known, *e.g.* $[Os_8(CO)_{22}]$[24] , (FIG 1.3), and $[\{Rh_{15}(CO)_{30}\}^{2-}]$[25]. Within this classification of clusters there are also a large number of mixed metal and heteronuclear species.

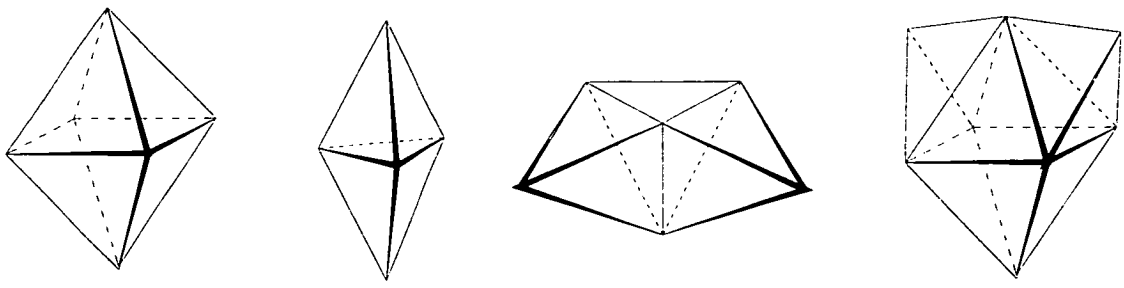

Octahedron Trigonal Bipyramid Capped Trigonal Bipyramid Bicapped Octahedron

Figure 1.3 : Some Examples Of Closed Polyhedral Structures

(ii) Stacked metallic arrays : These polymeric arrays of metal clusters form columns of metal atoms and are commonly observed for metals of the nickel triad, *e.g.* $[\{Pt_3(CO)_6\}_n]^{2-}$, (n=2-5)[26],(FIG 1.4), and $[\{Ni_3(CO)_6\}_2^{2-}]$[27]. In both of these cases the triangles stack in a slightly distorted trigonal prismatic fashion in that each layer is slightly rotated and offset from the lower one, presumably due to steric factors induced by overlap of CO ligands.

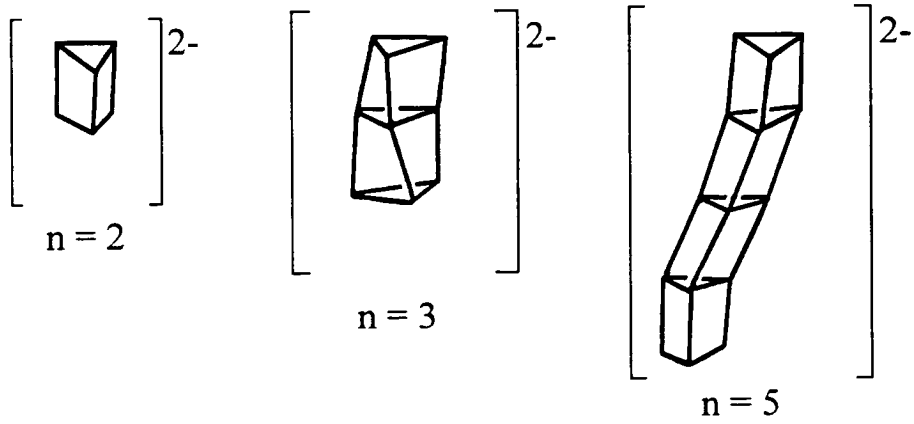

Figure 1.4 : Some Examples of Stacked Platinum Triangular Arrays

(iii) Close packed arrays : In these species the metal atoms are arrayed in a fashion analogous to that observed for bulk metals, *e.g.* $[\{Rh_{17}(CO)_{33}\}^{2-}]$[28]. In these clusters the metallic character of the complex increases as the number of metal atoms present increases, suggesting that a mimicking of true metallic properties may be possible via this type of array.

(iv) Raft structures : These complexes are planar triangulated arrays of metal atoms, to date only observed for osmium clusters, *e.g.* $[Os_6(CO)_{21}]$[29] and $[Os_9(CO)_{33}Hg_3]$[30], (FIG 1.5).

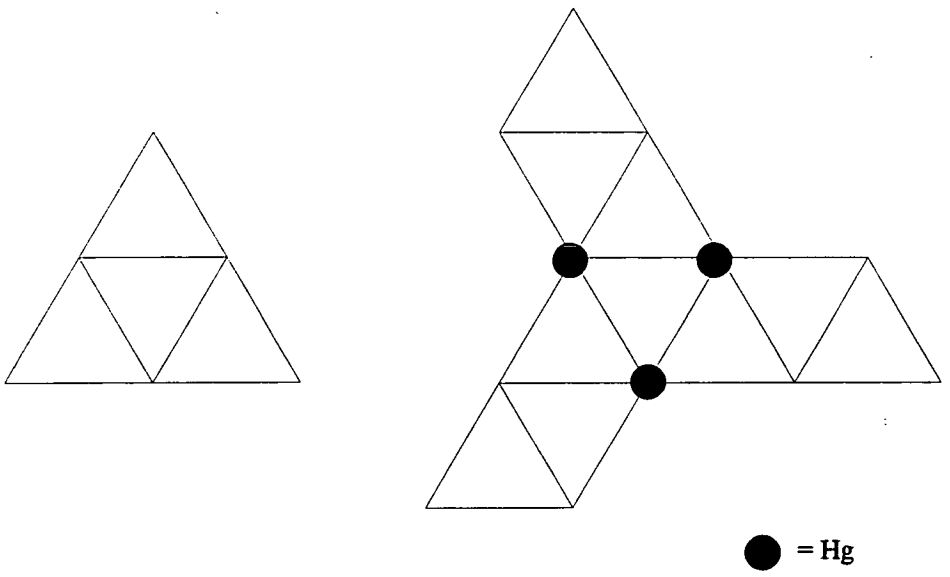

$[Os_6(CO)_{21}]$ $[Os_9Hg_3(CO)_{33}]$

Figure 1.5 : Some Structures Of Raft Clusters

(v) Clusters comprised of fused polyhedra : This type of species arises when small polyhedral complexes are joined together either by bridging ligands as in $[\{Co(CO)_9\}_2C_2]$[31], (FIG 1.6) or via vertex sharing between clusters, *e.g.* in $[Au_{11}(PPh_3)_7(SCN)_3]$[32], (FIG 1.6) where the structure is best described as a pentagonal bipyramid sharing a vertex with a square based pyramid.

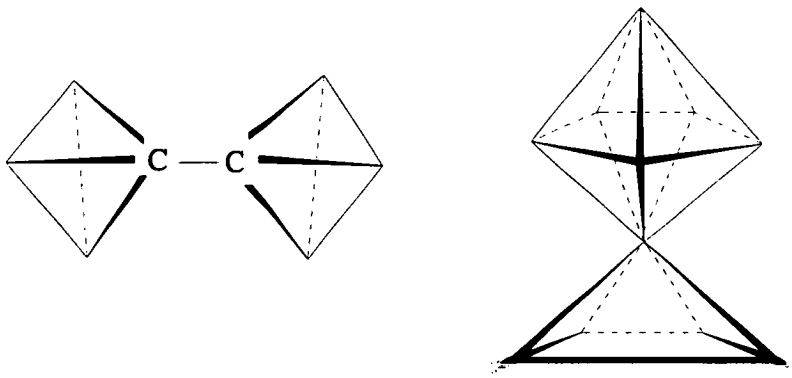

$[\{Co_3(CO)_9\}_2C_2]$ $[Au_{11}(PPh_3)_7(SCN)_3]$

Figure 1.6 : Structures Of Some Fused Polyhedra

(vi) Mixed metal clusters : polynuclear clusters of the transition metals which contain more than one type of metal are now well established. A wide range of mixed metal clusters of the transition elements are known, and are structurally similar to the homonuclear clusters discussed already. *e.g.* $[Os_3CoH_3(CO)_{12}]$[33], (FIG 1.7).

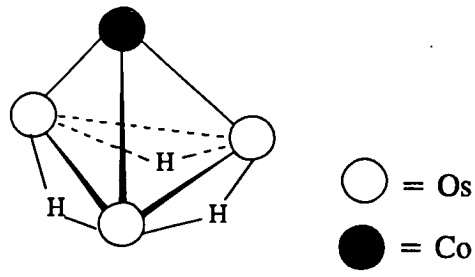

[Os 3CoH 3(CO) 12]

Figure 1.7 : The Structure Of $[Os_3CoH_3(CO)_{12}]$

Heteronuclear clusters

As well as mixed metal complexes, clusters are known which contain main group heteroatoms either as constituents of the cluster framework or encapsulated within the metal polyhedron, not simply as ligands. The most common types of heteronuclear cluster known are those containing either carbon or nitrogen. However, examples of clusters containing hydrogen, phosphorus and sulphur are also known.

(i) Carbido clusters : These are by far the most common type of heteronuclear cluster observed with examples known for iron, ruthenium, osmium, cobalt, nickel, rhodium and rhenium, as well as a few mixed metal carbido clusters. The carbon atom is generally encapsulated within the metal framework, allowing donation of four electrons to the cluster electron count. The source of the carbon atom in these clusters is generally via disproportionation of CO ligands to give C plus CO_2. However, other sources of carbon are known, *e.g.* $CHCl_3$ in the carbido cluster $[\{Rh_6C(CO)_{15}\}^{2-}]$[34]. Examples of carbido clusters include $[Fe_5C(CO)_{15}]$[35] where the carbon atom occupies the central site of the base of a square based pyramid of metals, (FIG 1.8). Fully encapsulated carbides are also known, *e.g.* $[Ru_6C(CO)_{17}]$[36], $[\{Co_6C(CO)_{15}\}^{2-}]$[37], (FIG 1.8).

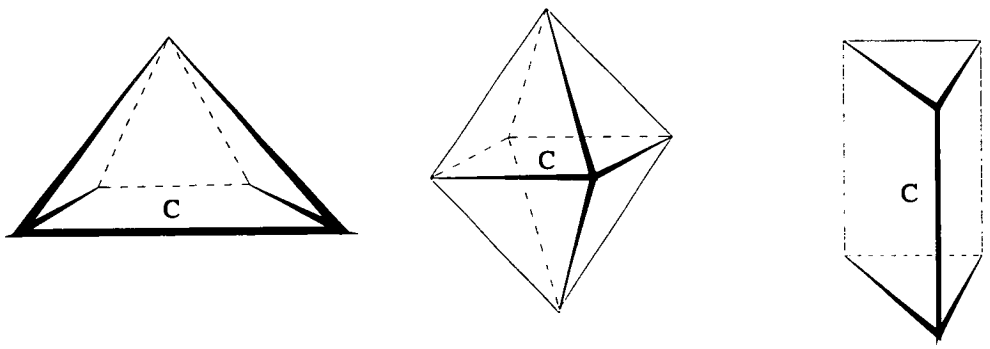

$[Fe_5C(CO)_{15}]$ $[Ru_6C(CO)_{17}]$ $[Co_6C(CO)_{15}]$

Figure 1.8 : The Structures Of Some Carbido Clusters

(ii) Nitrido clusters : These systems include nitrogen as an integral part of the cluster matrix, derived from NO in a similar fashion to the CO source of carbon in the carbido clusters, although other sources of nitrogen are available *e.g.* azides in the complex $[\{Ru_5N(CO)_{14}\}^{2-}]$[38]. As with the carbido clusters, the nitride is generally encapsulated within the metal framework, (FIG 1.9).

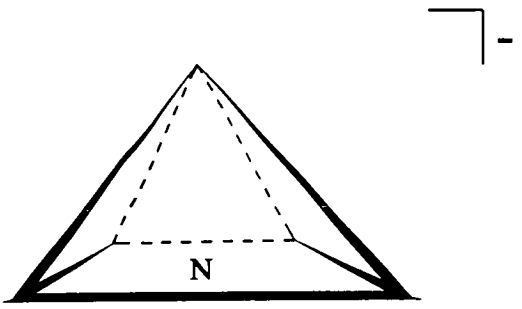

$[Ru_5N(CO)_{14}]^-$

Figure 1.9 : The Structure Of $[Ru_5N(CO)_{14}]^-$

(iii) Other heteronuclear clusters : The elements phosphorus, hydrogen and sulphur may also be encapsulated within a cluster framework, *e.g.* $[\{HCo_6(CO)_{15}\}^-]$[39], $[\{Rh_9P(CO)_{21}\}^{2-}]$[40] and $[\{Rh_{17}S_2(CO)_{32}\}^{3-}]$[41]. The source of the heteroatom in these clusters tends to be thermal decomposition of an incoming ligand, *e.g.* PPh_3 in $[\{Rh_9P(CO)_{22}\}^{2-}]$[40].

Reactions of metal clusters

The reactions that metal clusters may undergo are extremely diverse, however they may be grouped into general classifications; cluster expansion, cluster degradation, cluster oxidation, cluster reduction, oxidative addition and ligand substitution.

Cluster expansion

The mechanism of cluster expansion is not well understood, with several possibilities existing. The first is similar to that observed for polyhedral boron species in that a radical species, usually generated by photolysis or pyrolysis, *e.g.* $[Os(CO)_4]$ attacks a metal substrate leading to cluster expansion. Other mechanisms for this type of expansion include attack at chemically activated cluster sites by monomeric metal species *e.g.* the synthesis of $[Os_7(CO)_{20}H_2]$[42] which involves addition of an $[OsH_2(CO)_4]$ unit to $[Os_6(CO)_{17}(MeCN)]$, and then thermolysis to form an $(Os(CO)_4)$ bridge. Other methods include the placement of a monomeric metal unit over a triangular cluster face, once more by chemical activation of the cluster core. This allows generation of an additional tetrahedral unit fused to the metal core, giving a route into higher nuclearity cluster species, *e.g.* $[Os_6(CO)_{16}(PtCOD)_2]$[43]. Another possibility is the use of an intermolecular bridging ligand to hold two cluster units in close proximity and by use of thermochemical means close up the metal framework, as used in the formation of the heteronuclear cluster $[\{Os_6(CO)_{18}\mu_6\text{-}P\}^-]$[44]. Finally the catalytic dimerisation of triosmium units leads to the formation of the raft cluster $[Os_6(CO)_{21}]$[45]. All of these methods allow expansion of the cluster framework, but are not well understood, making it difficult to predict how cluster expansion will occur and therefore designing syntheses to allow controlled expansion of the metal framework is of limited use.

Cluster degradation

Degradation of a cluster framework generally takes place by initial ejection of an electronically saturated, (eighteen electrons), fragment, *e.g.* $Os(CO)_5$ or $Ru(CO)_5$ in the breakdown reactions of $[Os_3(CO)_{12}]$ and $[Ru_3(CO)_{12}]$[46]. These breakdown reactions are caused by the action of high pressures of CO gas on the binary cluster and are reversible at room temperature, though photolysis is required. Another mechanism which has been observed for cluster degradation is the disproportionation of $[Rh_2Co_2(CO)_{12}]$ to $[Rh_4(CO)_{12}]$ and $[Co_4(CO)_{12}]$[6]. For cluster breakdown to occur, there must first be sufficient CO ligands present to allow excited state formation where an electronically saturated fragment may be ejected, and this can be seen in $[Fe_3(CO)_{12}]$[47], which has two μ_2-CO groups arranged round the metal triangle. This would allow formation of $Fe(CO)_5$ via the cleavage of two M-M bonds, and samples of $[Fe_3(CO)_{12}]$ are almost always contaminated with $Fe(CO)_5$ supporting this hypothesis. Secondly the stability of the cluster in question must not be high, otherwise the high activation energy required would forbid this process. This may be seen in the conditions required for formation of $M(CO)_5$ in the iron triad, with $Fe(CO)_5$ forming apparently at room temperature, $Ru(CO)_5$ forming under 200atm CO at 160°C, with $Os(CO)_5$ requiring much higher temperatures, (290°C)[46]. This is consistent with the strengthening of M-M bonds upon descending the periodic table causing stabilisation of the heavier clusters.

Cluster oxidation

Reactions involving oxidation of the cluster framework are subdivided into two classes, those which incorporate the oxidant and those which do not. Reactions which involve incorporation of the oxidant include protonation of the cluster as in the series $[\{Os_6(CO)_{18}\}^{2-}]$, $[\{HOs_6(CO)_{18}\}^{-}]$ and $[H_2Os_6(CO)_{18}]$[48] where the successive oxidation of the cluster is accompanied by proton incorporation in the form of metal hydrides. This reaction is also accompanied by modification of the metal framework from a slightly distorted octahedron to a monocapped square pyramid. The addition of NO^+ or I^+ to anionic clusters are also examples of oxidant incorporation reactions, *e.g.* the reaction of $[\{Rh_6(CO)_{15}\}^{2-}]$ with I_2 yields $[\{Rh_6I(CO)_{15}\}^{-}]$ and I^-, the oxidant I^+ having been added to the cluster[49]. Similarly the addition of NO^+ to $[\{Co_6(CO)_{15}\}^{2-}]$ proceeds via addition of the NO ligand to the cluster, forming $[\{Co_6N(CO)_{15}\}^{2-}]$[50], via the intermediate species $[\{Co_6(NO)(CO)_{15}\}^{-}]$.

Oxidation reactions which do not involve incorporation of the oxidant are generally those which involve the action of Lewis acids such as $FeCl_3$ on the cluster. The reaction of $[\{Co_6C(CO)_{15}\}^{2-}]$ with $FeCl_3$ gives $[\{Co_6C(CO)_{14}\}^{-}]$, once more changing the geometry of the starting material, in this case from a trigonal prism to an octahedron[51]. For this type of oxidation $FeCl_3$/CO is the oxidant of choice, though success has been realised with other systems such as mercuric salts, though these may lead to the formation of clusters which incorporate mercury[52].

Cluster reduction

As with oxidation reactions the reduction of clusters may be accomplished with or without incorporation of the reducing species. Generally reactions with hard nucleophiles results in reduction of the cluster with no incorporation of the reductant, whereas soft nucleophiles will usually add to the cluster. Reactions which include the reductant in the cluster are often those leading to the buildup of clusters, *e.g.* the action of $[\{Rh_6(CO)_{15}\}^{2-}]$ on $[Rh_6(CO)_{16}]$ affords the reduced cluster species $[\{Rh_{12}(CO)_{30}\}^{2-}]$[53]. The addition of isocyanide ligands to $[Os_6(CO)_{18}]$ is another example of ligand incorporation during a reduction process, with a cleavage of three Os-Os bonds occurring to accommodate the extra six electrons. The addition of six electrons occurs because one isocyanide ligand is coordinated as a μ_3-η^4 bridging ligand, with the other a simple terminally coordinated species[54].

Reduction of clusters without incorporation of the reducing species almost invariably result in the loss of a CO ligand, sometimes with degradation of the cluster framework. The action of alkali metals on clusters commonly leads to the degradation of the cluster framework, *e.g.* the action of sodium on $[\{Co_6(CO)_{15}\}^{2-}]$ results in the formation of $[\{Co_6(CO)_{14}\}^{4-}]$, (90%) and $[\{Co(CO)_4\}^{-}]$, (10%)[55]. The actions of nucleophiles such as OH^- on clusters oxidise CO to CO_2 concurrently with cluster reduction in a similar fashion to that observed for monomeric metal complexes[56]. The reaction of R_3NO, (R = Me, Et), with $[Os_6(CO)_{18}]$ in the absence of MeCN gives the reduced cluster complex $[\{Os_6(CO)_{17}H\}^{-}]$[57]. This is thought to proceed via formation of an R_3N substituted cluster and then α-hydrogen transfer from the amine to the cluster. This is an example of a process whereby the reducing amine oxide is not incorporated directly into the cluster, but one of its components is.

Oxidative-addition at clusters

The classical definition of an oxidative-addition reaction at a metal is that the metal experiences a gain of two in charge and in coordination number[58]. This definition has been extended to cluster complexes by Deeming[59] to state that "if a molecule is reduced while entering the coordination sphere of a metal atom which is itself oxidised in the process, we say that the molecule has added oxidatively". The formation of $[Os_3X_2(CO)_{10}]$, (X = H, Cl), from the reaction of $[Os_3(CO)_{12}]$ with H_2 or Cl_2 both come under the heading of oxidative-addition, but follow radically different mechanisms with the addition of H_2 proceeding via CO loss and then addition of hydrogen[60]. The addition of Cl_2 is thought to proceed via initial M-M bond cleavage and then CO loss occurs allowing the cluster to reform the M-M bond[61]. Oxidative-addition at clusters may also occur via C-H cleavage in attached organic ligands[62] or via P-H cleavage in primary and secondary phosphines[63]. The ortho-metallation reaction has been observed on clusters for many ligands, *e.g.* PPh_3[64], where one of the ortho protons on a phenyl ring coordinates to the cluster directly and a $PPh_2(C_6H_4)$ bridge is also formed.

It is clear that there are some unique aspects of oxidative-addition with respect to

cluster chemistry. The main factor is the ability to ignore the necessity of five membered chelate ring formation which dominates monometallic systems. The simple oxidative-addition of hydrogen and halides will of course be unaffected by this. The wide range of C-H bond cleavage reactions observed for metal cluster/organic systems may be attributable to the ability of clusters to form coordinatively unsaturated intermediates, then allowing internal oxidative-addition to occur.

Substitution reactions of metal clusters

Substitution at cluster complexes is perhaps the most studied class of reactions for metal cluster complexes. The displacement of a CO ligand by a variety of ligands with no change in oxidation state at the cluster has given rise to a wide range of substituted clusters. The main problem associated with the early thermal substitution reactions of clusters were the highly energetic conditions required to remove a CO ligand, which led to complex mixtures of products, and made the observation of the basic substitution complexes, without further pyrolysis of attached ligand difficult. Recently the ability of R_3NO, (R = Me, Et), to active clusters chemically by oxidation of a CO ligand and then loss of the CO_2 group has made this field considerably easier.

Activated clusters are accessible by carrying out the amine oxide reactions in the presence of weakly coordinating ligands, *e.g.* MeCN, (C_8H_{14})[65]. These activated clusters have allowed many simple substitution complexes to be manufactured with two electron donors, *e.g.* phosphines[66-68], alkenes[69,70], alkynes[71-73]. Phosphine ligands have been shown to form simple substitution complexes with a wide range of metal clusters and upon pyrolysis, they may form metallated species. Primary and secondary phosphines have also demonstrated the ability to form phosphinidene bridges and phosphorus capped clusters. Addition of alkynes to clusters initially allows formation of simple donor complexes which may be further studied via thermolysis, exhibiting properties such as C-C bond cleavage, dimerisation and trimerisation[74-78].

Metal carbonyl binding

The most commonly observed ligand on clusters of the platinum metals is CO, which may bind to metal centres in a number of different ways[4]. The most common of these, and the simplest, is the terminal coordination to one metal atom. Other modes that are available include the μ_2 and μ_3 bridges, (FIG 1.10).

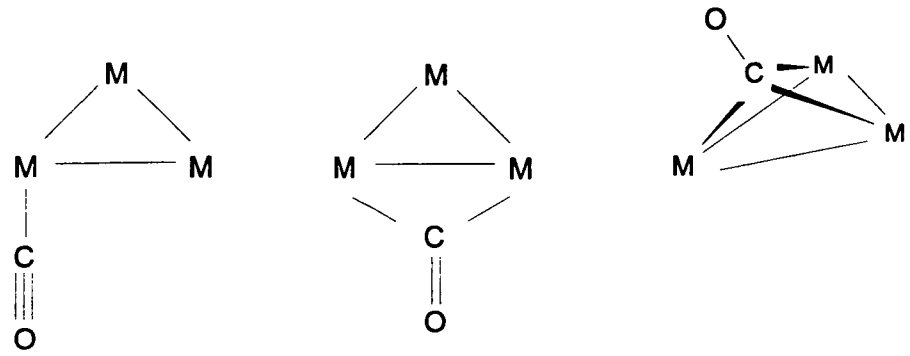

Figure 1.10 : Binding Modes Available To Carbonyl Ligands On Metal Clusters

The binding of CO to a metal atom involves both σ and π components, which are interdependent, forming a synergic bond[1]. The σ-component of this bond is formed by the donation of the lone electron pair of the carbon atom to a vacant metal hybrid bonding orbital. The π-component of the bond involves back donation of electrons from the metal d-orbitals to the vacant π^* orbitals of the CO ligand. Hence, the bond order of the carbon/oxygen bond of the CO ligand will decrease upon coordination to a metal ,with a subsequent lowering of the CO stretching frequency in the ir spectrum.

Interaction between a CO ligand and more than one metal atom will further decrease the bond order of the CO, as the hybridisation of the carbon will change in order to increase its coordination number, causing a decrease in the number of valence orbitals available to form the CO bond, and subsequently its ir stretching frequency will drop.

Ir spectroscopy and metal carbonyl clusters

Because of the nature of the interaction between metals and CO ligands it is generally possible to differentiate between the different binding modes of CO by ir spectroscopy from their characteristic stretching frequencies[1], (Table 1.1).

Table 1.1 : Characteristic carbonyl stretching frequencies	
Carbonyl Binding Mode	Frequency Range (cm^{-1})
Terminal	1900-2150
μ_2-Bridging	1750-1850
μ_3-Bridging	1500-1700

It is also possible to use the CO stretching frequencies and band intensities as a fingerprint for complex identification. Full analysis of the carbonyl region of the ir spectrum of a cluster is however difficult, with a full mode analysis being required. Full mode analysis is very difficult to carry out except for small, high symmetry clusters. This problem arises because of the large number of carbonyl stretching modes present in the larger, or lower symmetry clusters. This gives rise to overlapping bands and bands being obscured completely, making full resolution of the carbonyl region difficult, if not impossible. It is also possible via ir spectroscopy to recognise substitution patterns in clusters, *e.g.* a 1,2 substituted trinuclear cluster, by the number and relative positions and intensities of the bands. This is possible by analogy with fully characterised cluster species, ie those characterised by X-ray methods. Finally, ir spectroscopy may be useful in identifying other ligands bound to a metal cluster, by use of their fingerprint regions, *e.g.* the P-H stretching frequencies of primary and secondary phosphines[79], (~2250cm^{-1}).

Mass Spectroscopy

One of the principal methods used for the characterisation of clusters is mass spectroscopy. Early studies of higher nuclearity clusters by Electron Impact, (EI), mass spectroscopy allowed characterisation of these species, as microanalysis is inadequate, due to the small differences in carbon content present in these complexes. The spectra of these species generally shows an intense molecular ion[80], with sequential loss of carbonyl ligands. It is also possible to determine the nuclearity of clusters from the isotopic distribution within the peaks. However the highly energetic nature of this technique limits its usefulness, as the 'parent' peak observed may be that of a daughter product, not of the true parent species.

The advent of the softer ionisation technique, Fast Atom Bombardment (FAB), which operates by sputtering ions from an inert matrix has been shown to be a more suitable method for cluster study[81,82]. This method eliminates the problems of ligand loss from the parent species, allowing the true parent peak to be observed, as well as eliminating the problems of high temperatures associated with EI mass spectroscopy. eg. Clusters containing phosphine ligands will generally not show evidence of these in EI mass spectroscopy but will show them for FAB spectra.

Recently a further method has become available with the advent of Matrix Assisted Laser Desorption Ionisation (MALDI)[83,84]. This method uses passive and active matrix participation in the ionisation of the analyte, with time of flight, (TOF) monitoring of the ions formed. The sample under study is finely dispersed in a matrix of highly light absorbent species. The passive component of this technique is absorbence of energy from the laser by the matrix transferring this to the solid system, resulting in near instantaneous phase transition of a small amount of sample to the gas phase.

The active participation of the matrix is accomplished by further photoexcitation of the matrix, allowing proton transfer to the matrix to the analyte, and from the analyte to the matrix. For metal species, radical formation has also been observed to participate in the ionisation.

One of the problems associated with this technique is poor resolution, with isotopic distribution within peaks being impossible to observe. This is due to the presence of $(M+H)^+$, $(M-H)^-$ and $M^{\cdot+}$ fragments, making assignment of single peaks difficult. This factor, coupled with the intrinsic low resolution of TOF methods gives broad peaks, showing no internal resolution.

The nmr spectroscopic study of metal clusters

Nmr spectroscopy is one of the most powerful tools available for the study of metal clusters, both for observation of ligands and in some cases the metals themselves and for elucidation of exchange processes occurring on the cluster. The most commonly observed nuclei for transition metal clusters are ^{1}H, ^{13}C and ^{31}P.

^{1}H nmr spectroscopy

^{1}H nmr is useful for the detection of metal hydrides present on the cluster, especially due to their unique chemical shift ranges, (0-{-30ppm}). This range of chemical shift values is primarily due to shielding of the hydride nucleus by the non bonding electrons of the metal[7]. The use of ^{187}Os-^{1}H couplings has also proved useful in aiding structure determination of hydrido-osmium clusters[85,86]. ^{1}H nmr spectroscopy is also useful for detecting the presence of coordinated organic ligands. However, it is not usually possible to determine the coordination mode of an organic ligand purely from its proton spectrum. ^{1}H nmr may be used in some cases to distinguish the different coordination modes of arenes, *e.g.* benzene/benzyne coordination over a cluster face[87,88].

^{13}C nmr spectroscopy

^{13}C nmr may be used in cluster chemistry to differentiate between the different coordination modes of CO ligands on the cluster by virtue of their characteristic chemical shifts[89]. With the aid of variable temperature techniques ^{13}C nmr may also be used to observe and characterise some of the exchange processes which occur on clusters[90,91]. It should be noted here that it is often difficult to record ^{13}C nmr spectra for metal carbonyls as the relaxation time for the ^{13}C nuclei in these compounds can be very long, although this problem may be alleviated to some degree by the use of relaxation agents, *e.g. tris*-acetylacetonato-chromium(III), $[Cr(acac)_3]$[92].

^{31}P nmr spectroscopy

^{31}P nmr spectroscopy may be used to detect the presence of coordinated phosphorus ligands on a cluster which may occur in terminal, edge bridging and face capping modes. It is also useful in elucidating exchange processes on the cluster, by use of variable temperature techniques.

Chemical shifts and shielding

Chemical shifts arise from the interaction of a nucleus with a static field B_o. The strength of the interaction will vary with the degree of shielding the nucleus experiences from surrounding electrons. As the nucleus becomes less shielded it will interact more strongly with the applied field and will therefore resonate at higher frequency. The result of this is that as shielding of a nucleus decreases, its resonance frequency, and hence its chemical shift will increase.

Resonance signals which occur at lower frequency than H_3PO_4 are given negative chemical shift values, those occurring at higher frequency than H_3PO_4 are given positive chemical shift values.

The chemical shift range for phosphorus compounds is quite wide, (δ -400ppm to δ +900ppm), primarily due to the contribution of the phosphorus 3p and 3d orbitals to nuclear shielding. There has been a large amount of data gathered for chemical shifts for phosphorus[93,94] and the interpretation of this data has proven to be an arduous task. The factors which influence the chemical shifts of phosphorus compounds have long been known[95], but are not simple and any attempt at prediction of phosphorus shifts has met with little success, except for simple alkyl phosphine systems[94]. However it is possible to predict general trends for phosphorus compounds upon reaction with transition metals, as the shift of the phosphine will almost invariably move to higher frequency upon coordination to a metal species[94].

Factors affecting phosphorus chemical shifts

For three and four coordinate phosphorus compounds the chemical shift range tends to remain in the narrower, (δ -250ppm to δ +250ppm), range. For trivalent phosphorus complexes, PRR'R", with alkyl, aryl or hydrogen substituents the chemical shifts are generally in the negative range. The substituents directly attached to the phosphorus will affect the chemical shift value as follows;

(i) By changes in electronegativity with respect to phosphorus : An electronegative substituent, with respect to phosphorus, will withdraw electrons from the phosphorus, causing the shielding of the nucleus to drop. Electropositive substituents, with respect to phosphorus, will donate electrons to the phosphorus, causing shielding of the nucleus to increase[94].

eg. δPF_3 = +97ppm

δPH_3 = -239ppm.

(ii) Effects of increase in coordination number at the phosphorus : This is a consequence of the phosphorus 3p and 3d orbitals contributing to the hybrid orbitals forming the bond. The increase in coordination at the phosphorus will cause a drop in the occupancy of these orbitals, and a subsequent drop in nuclear shielding at the phosphorus[94].

eg. δPMe_3 = -62ppm

δPMe_4^+ = +25ppm.

It should be noted here that charge on a phosphorus species has little effect on the nuclear shielding at the phosphorus nucleus and hence has little effect on the chemical shift[94].

eg. $\delta(MeO)_3P{=}O$ = -2ppm

$\delta(MeO)_4P^+BF_4^-$ = -2ppm

(iii) The effects of the substituents on the geometry of the phosphorus : Geometry changes around the phosphorus nucleus will affect its electronic environment, causing shielding to vary. For example the two tricoordinate phosphorus complexes (cyclo-C_5H_8)PPh and (cyclo-C_6H_{10})PPh have chemical shift values of -15ppm and -23ppm respectively. As the phosphorus atom is coordinated to three carbon atoms in both cases and the ligands are approximately equal in electronegativity then the main contribution to the chemical shift difference must be the geometry at the phosphorus. (cyclo-C_5H_8)PPh is constrained towards planarity, with the bonding orbitals being of the sp^2 hybrid type, then the lone pair on the phosphorus must reside primarily in a p orbital. Whereas in (cyclo-C_6H_{10})PPh the phosphorus is more pyramidal in nature, with the lone pair residing more in an s orbital, shielding the nucleus more effectively, thus causing a lower resonance frequency, and subsequently a lower chemical shift[94].

Spin-Spin Coupling

If a molecule has two inequivalent groups of spinning nuclei present there may be an interaction between them known as spin-spin coupling. The consequence of this coupling is that the resonances in their nmr spectra will be split into multiple peaks. The distance between the peaks in these multiplets, given in Hz, is a measure of the strength of the interaction between the nuclei involved. For a purely first order spin system the distance between the peaks is known as the coupling constant, *J*.

For example a system with two protons H_A and H_B which are in non equivalent environments, and thus have different chemical shifts, the nuclei will couple as follows. The frequency of H_A is governed by the magnetic field acting upon it, and the primary influence will therefore be B_o. However, H_B can modify this to a small degree, since 50% of the protons in environment H_B will be aligned with B_o and the other 50% will oppose the field. H_A will therefore experience two different effective fields, ($B_o + H_B$ and $B_o - H_B$). Thus H_A will come to resonance at two different frequencies and two peaks will appear in the spectrum, one to higher frequency than the source chemical shift δH_A, and one to lower frequency. H_B will experience a similar effect, also appearing as a doublet. In simple terms H_A and H_B will both "see" two different environments, causing the splitting to occur.

It is generally accepted that there are two main causes of spin-spin couplings as follows;

(i) Interaction of the magnetic moment of a nucleus with the magnetic field caused by the orbital motions in its surrounding electrons. For example, consider a spinning system containing two nuclei A+B. This interaction arises because of the secondary field set up in the electrons surrounding a nucleus, A, due to the

spin of that nucleus.

This secondary field will then perturb the electrons in the bond between A+B, causing an effect to be felt in the electrons surrounding B, and therefore at the nucleus of B. The result of this is that both nuclei will experience coupling to one another via their bonding electrons. This effect is known as scalar or contact coupling[95].

(ii) Dipole-dipole interactions between magnetic moments of the nuclei involved and the electron spin magnetic moments of spinning electrons around these nuclei. The presence of a group of spins surrounding a spinning nucleus may give rise to a number of interactions between these nuclei. The interaction of a spin with the dipolar field caused by another spinning nucleus is the most important of these. The energy of this interaction between two magnetic moments, μ_1 and μ_2 is given by the equation below.

$$E = \frac{\mu_1 . \mu_2}{r^3} - \frac{3(\mu_1 . r)(\mu_2 . r)}{r^5}$$

Where r is the vector connecting these nuclei. A quantum mechanical hamiltonian can be formulated by treating μ_1 and μ_2 as operators :

$$\mu_1 = \gamma_1 \hbar I_1$$

$$\mu_2 = \gamma_2 \hbar I_2$$

The general hamiltonian for the spins then becomes :

$$\hbar_{vd} = \frac{1}{2}\sum_{j=1}^{N}\sum_{k=1}^{N}\left[\frac{\mu j.\mu k}{r^3_{jk}} - \frac{3(\mu j.r_{jk})(\mu k.r_{jk})}{r^5_{jk}}\right]$$

For a system with two spins A+B, the approximate Hamiltonian then becomes :

$$\hbar_{vd} = \frac{1}{2}\frac{\gamma_I \gamma_{S.}^2}{r^3}(1-3\cos^2\theta)(3I_zS_z - I.S)$$

Where θ is the angle between the internuclear vector, of length r and the applied field. This term is averaged to zero in solution because all possible values of θ exist due to rotational motion. The value of $\cos^2\theta$ is thus ⅓, and the dipolar coupling will average to zero[95].

Hybridisation and coupling constants

The contact contribution to coupling depends on the probability of an electron being at the nucleus. However only electrons in s orbitals have any electron density at the nucleus. Thus any consideration of scalar coupling need only consider the contribution of the valence atomic s orbitals for the coupled nuclei. From this it may be seen that the coupling between nuclei will have a pronounced dependence on the s character of the hybrid orbitals forming the bond between the nuclei[96].

P-H Coupling Constants

The magnitudes of $^1J_{PH}$ coupling values cover an extremely wide range of approximately 1000Hz. For the purposes of this work only three and four coordinate phosphorus ligands will be considered, which have $^1J_{PH}$ ranges of 180Hz to 230Hz and 250Hz to 730Hz respectively[94].

The reason behind this large range of coupling constant values lies with the orbital hybridisation around the phosphorus centre.

Three coordinate phosphorus

For tricoordinate phosphorus, the bonding orbitals are predominantly comprised of p orbitals. This is a consequence of the orbital hybridisation in tricoordinate phosphorus species, in which the phosphorus uses its p orbitals for bonding and its lone pair predominantly resides in an s orbital. The result of this is that the scalar coupling interaction between the phosphorus nucleus and its attached protons is weak, giving small $^1J_{PH}$ couplings. Due to the small amount of s character in the bonding orbitals, changes in the substituents on the phosphorus has little effect on the $^1J_{PH}$ value.

Four coordinate phosphorus

For four coordinate phosphorus the bonding orbitals are made up of an sp^3 hybrid system, with approximately 25% s character. This leads to much stronger scalar coupling interactions with neighbouring protons, hence the $^1J_{PH}$ coupling constant increases. This also means that the substituents directly attached to the phosphorus will have a more profound effect on $^1J_{PH}$ values, as the s orbital will be more directly affected by changes in the electron donor or acceptor characteristics of a substituent.

Phosphorus(III) Ligands

The number of species known with a metal-phosphorus bond is vast, and rapidly expanding[97]. However it is the metal in these complexes which tends to be the focus of study, not the phosphorus ligands. The object of this study it to keep the metal centre under study constant and to vary the phosphorus ligands in order to observe their behaviour, and to study the consequences of their coordination to the metal, in terms of their effect on the metal substrate characteristics.

Phosphorus binding

Undoubtedly the most controversial point in phosphorus chemistry recently has been the subject of the use of the phosphorus 3d orbitals for π-bonding. The use of the 3d orbitals for σ-bonding is now an established fact. The wide acceptance of 3d orbitals being involved in σ-bonding arises because it would not be possible to have more than four ligands present on a phosphorus centre without the use of the 3d orbitals in the bonding orbital hybrids. The postulate that the 3d orbitals are involved in σ-bonding is reinforced by the increase in maximum coordination number observed upon going from the first to second rows of the periodic table, which may be explained by allowing the d orbitals to participate in hybrid bonding orbital formation, therefore increasing the maximum number of valence orbitals available[94].

π-Bonding at phosphorus

The original postulate that phosphorus could engage in π-bonding via its 3d orbitals arose when the very obvious disparity between bonding of the first and second row elements was noticed, *e.g.* in the case of N=O and P=O bonding the relative strengths of the bonds are in an approximately 1:2 ratio. This discrepancy cannot be explained purely by the use of a σ-bonding theory, and recourse to π-bonding explanations must be made. It has been suggested that the phosphorus has the ability to use its 3d orbitals to reaccept some of the electron density it has given the oxygen via its coordinate σ-bond. This is of course something nitrogen is unable to do, leading to a more polar, weaker bond then the phosphorus is capable of producing via π-acceptance[98].

Further evidence is available by study of trivalent phosphorus donor ability. Where no π-bonding is possible, donor ability follows the order expected on the basis of σ-donation capability, and is in the order $R_3P > (RO)_3P > Cl_3P > F_3P$. However when the phosphorus ligands are coordinated to a central atom which has π-bonding capability, *e.g.* a transition metal, then the donor ability order is reversed[98].

This suggests that the metal is somehow able to release some of its excess electron density via π-back donation to the phosphorus, in a similar fashion to the synergic bond observed for CO ligands on transition metals. This ability is of course enhanced by the presence of strongly electron withdrawing groups on the phosphorus, which cause contraction of the 3d orbitals, making them more accessible to π-bonding. This explains the reversal of the series well, as the important factor is now not σ-donor ability but π-acceptor ability with respect to the ligand.

Binding of Phosphorus(III) ligands to metals

The study of M-P binding has shown parallels to M-CO binding, in terms of the formation of some form of synergic bond system. Chatt[99] observed that the strength of the dipole observed in M-P bonds for PX_3 systems was much less than could be explained by σ-bonding alone. He proposed that the σ-bond formed between the metal and the phosphorus ligand was reinforced by π-back bonding to the phosphorus, causing the dipole to drop.

Whilst phosphorus ligands are not as effective in π bonding terms as CO they nevertheless have the ability to stabilise low valency states for metals, a property evident in all of the π-acid ligands. There are few systems in existence in which a metal is solely coordinated to phosphorus ligands. Complexes of this type do exist, however, and $Ni(PPh_3)_4$[100] and $Pt(PPh_3)_4$[101] are both known. Both of these complexes are unstable at room temperature and will dissociate to yield $Ni(PPh_3)_3 + PPh_3$ and $Pt(PPh_3)_3 + PPh_3$ respectively. There are also platinum clusters known which are coordinated to solely by phosphorus ligands, *e.g.* $Pt_3(PPh_3)_6$ and $Pt_4(PPh_3)_4$[101]. Accordingly phosphorus ligands are associated with the group of ligands known as π-acids, *e.g.* CO.

Phosphorus(III) π-bonding to metals

The evidence in support of π-bonding at phosphorus is considerable. Perhaps the most convincing piece of evidence comes from the photoelectron spectrum of $Ni(PF_3)_4$[102]. This spectrum clearly shows the presence of electrons in a π-bonding environment. The photoelectron spectrum of free PF_3 however, shows that the lowest energy transition is that attributed to the lone pair electrons on the phosphorus, at 12.31eV. The spectrum of $Ni(PF_3)_4$ shows these electrons at 13.09eV, consistent with their presence in a σ-bond system between nickel and phosphorus. There are two lower energy bands present in the spectrum at 9.55eV and 10.58eV which can only arise from electrons present in a π-bonding system. Above 15eV, the photoelectron spectrum of $Ni(PF_3)_4$ is identical to the spectrum of the free ligand, indicating that no further modification of the molecule has occurred. Moreover this study has shown that PF_3 is a more efficient π-acceptor ligand than CO.

Another piece of evidence for the presence of π-bonding at phosphorus comes from study of bond lengths observed when phosphorus ligands are varied on identical metal centres. Comparison of the bond lengths of $Cr\text{-}PPh_3$ and $Cr\text{-}P(OPh)_3$ have shown that it is in fact the phosphite which has the shorter, stronger bond not the phosphine as would be expected purely on the basis of σ-donation[103]. Cotton and Wilkinson[1] have placed a great deal of faith in this observation. The Cr-P bond lengths as well as the Cr-C bond lengths in the complexes shown below, (FIG 1.11), give good correlation with the presence of a M-P π-bonding system. The CO ligand *trans* to the phosphorus ligand should be largely unaffected by the presence of a purely σ-bound ligand, and should show a drop in the value of νCO when a more basic phosphorus ligand is coordinated.

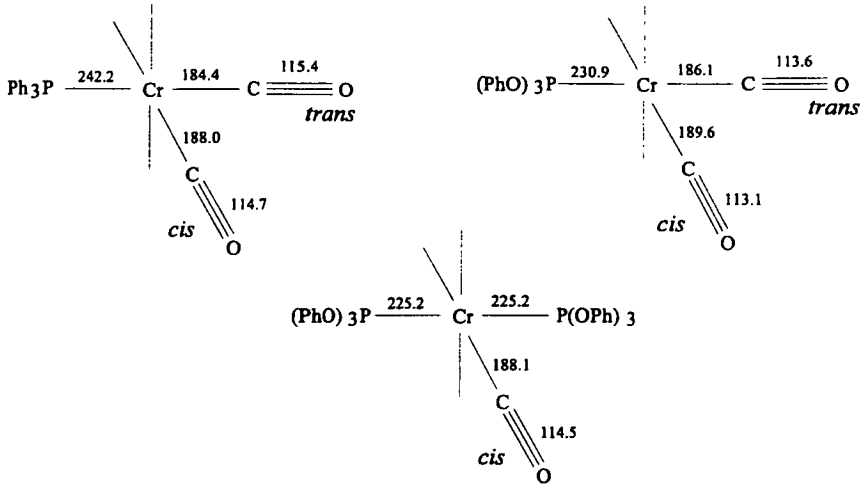

Figure 1.11 : Cr-P Bond Length Comparison For PPh_3 And $P(OPh)_3$

In fact it is the opposite case which holds, in that the coordination of the phosphite ligand causes an increase in the Cr-C bond length and a decrease in the C-O bond length. This suggests that the CO ligand does not compete as successfully for the π-electrons of the metal when *trans* to the $P(OPh)_3$ ligand than when *trans* to the PPh_3. This is further supported by the observation that when two phosphite ligands are *trans* to one another that their M-P bond lengths increase with respect to *cis* coordination in the same system, *e.g.* $M(CO)_4P_2$. This piece of evidence is important as it rules out the possibility that the bond length discrepancies were attributable to steric factors.

The π-acceptor ability of a given phosphine ligand is unlikely to vary to any great extent between metal systems, at least with low valent metal systems. This has given rise to the study of 'constant' metal environments with a variety of phosphines in an attempt to assign some form of π-acceptor ranking for phosphorus ligands. The most commonly employed probe to study these systems is the νCO value of a metal carbonyl, allowing the established synergic bond system to act as an indicator of π-acceptor strength of a coordinated phosphine.

The studies carried out on $Ni(CO)_3P$ by Tolman[104] allowed a relationship to be derived between the values of the A_1 νCO vibration mode and the groups attached to the phosphorus ligand. This relationship assigned an arbitrary value of χ_i to all of the phosphines under study, seventy in all, which then allowed empirical calculations of νCO to be calculated. The calculated stretching frequencies obtained from this study were in excellent agreement with experimental results, ($<0.3cm^{-1}$ accuracy), and have allowed calculation of νCO values for inaccessible complexes to be made, *e.g.* $Ni(CO)_3PH_3$; $\nu CO=2081.0cm^{-1}$. However, Tolman was unwilling to assign these effects to π-bonding, or for that matter to purely σ-bonding considerations.

Graham[105] attempted to utilise force constants to apportion electronic effects into σ- and π-components of a bond system. He used the complexes $Mo(CO)_5P$ and $Mo(CO)_5(NH_2C_6H_{11})$ to compare values of *k* (force constant), assuming that the $Mo(CO)_5(NH_2C_6H_{11})$ system was incapable of π-bonding through the amine ligand, therefore allowing it to be used as a control. Graham used the equations given below to assign relative σ- and π-effects to the ligands under study.

$\Delta k(trans) = \Delta\sigma + 2\Delta\pi$

$\Delta k(cis) = \Delta\sigma + \Delta\pi$

The terms are of course related to the CO ligands which are *trans* and *cis* to the phosphorus ligand respectively. The $\Delta\sigma$ values obtained appeared to be of little use, however the $\Delta\pi$ values allowed a meaningful assignment of π-acceptor capacity to be assigned to the phosphorus ligands under study. There are however some major discrepancies in this theory as the $\Delta\pi$ values rank $P(OPh)_3$ and PBu^t_3 together, which conflicts with experimental results.

It was suggested by Cotton[106] that variance in νCO of a metal carbonyl substrate was not as reliable a guide to the π-acceptor capability of phosphorus ligands as force constant values. He proposed a simplified method of calculating force constants for $ML_n(CO)_{6-n}$ for M=Cr, Mo, W. This method of calculation allowed a π-acceptor ranking to be assigned to the phosphines under study. These calculations provided a slightly different ranking of π-acceptor capacity than that proposed by Graham[105]. This series not only assigned phosphorus ligands in the same ranking as would be expected from experimental results, they also showed PF_3 to be 1.32 times better at π-acceptance than CO, which is confirmed by the photoelectron spectrum of $Ni(PF_3)_4$[102].

There has been considerable opposition to the idea of M-P π-bonding as well, with one of the main protagonists being Angelici. Angelici[107] carried out a similar study to Graham, using tungsten rather than molybdenum. This study proposed that variance in νCO with different phosphines could be attributed to changes in pKa within the range of phosphorus ligands studied. This postulate was borne out by varying the amine ligands in the complex $W(CO)_5(NL_3)$, demonstrating a similar νCO variation over a wide pKa range. Given that it is impossible for an amine ligand to engage in π-bonding with a metal, Angelici proposed that the νCO variation could be explained in terms of σ-donation alone.

Bigorne[108] also suggested that νCO variations in the complexes $Ni(CO)_3P$ and $Ni(CO)_2P_2$ could be explained without resorting to a π-bonding system. He proposed that all of the variations could be explained *via* use of the taft inductive constants, (σ^*), of the groups attached to the phosphorus. He observed a linear relationship between the σ^* values and νCO, concluding from this that all of the observed differences could be explained by the diversity of σ^* values for the groups attached to the phosphorus ligand.

However Tolman[104] showed that the variations in σ^* values could not be used as a reliable guide to νCO differences in the case of primary and secondary phosphines, PH_3, or halo-phosphines. He ascribed this to the fact that the taft constants relied on transmission of inductive effects through carbon, and could not explain their behaviour when directly attached to a phosphorus centre.

Some degree of understanding of the π-bonding ability of phosphorus ligands has been attained from studies carried out by Giering et al.[109-112] on QALE, (Quantitative Analysis of Ligand Effects). It has been proposed that in order to achieve any sort of π-bonding interaction the phosphorus ligand must contain either a P-O or P-F bond. Without either of these conditions being fulfilled Giering[112] has proposed that a phosphorus ligand may only act as a σ-donor. These studies are based upon the premise that a M-P bond is described by both σ- and π-components. These components may be plotted as potential energy curves, which may be superimposed to give a modified internuclear distance/potential energy curve, as shown below, (FIG 1.12).

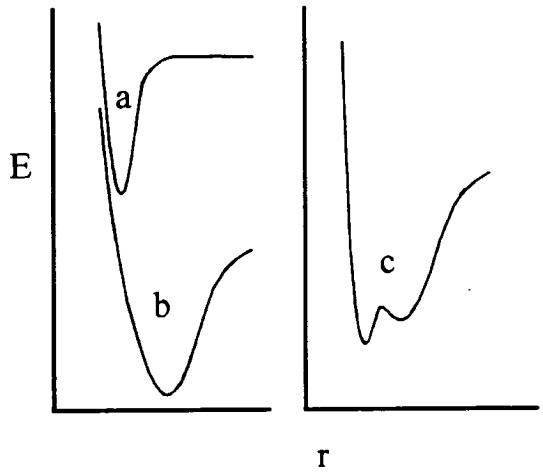

Figure 1.12 : Potential Energy Curves With π-Bonding Interactions Included For Phosphorus(III) Ligands, a = purely π-bound, b = purely σ-bound, c = combined σ/π-binding system

From this curve it may be seen that a M-P multiple bond will only form when the stabilisation given by the π-component of the bond is greater than the destabilisation caused by the decrease in internuclear distance. These studies have shown that for a given M-P bond system the π-component of the interaction may be destabilised by either steric interactions or by reduced π-acidity of the ligand. If the ligand parameters cause the multiple bond energy minimum to rise above the σ-bond energy minimum, then the bond formed will be purely σ-donor in nature.

These studies have also shown the existence of steric thresholds, which are values of θ, (Cone angle), above which the formation of complexes between metals and phosphines becomes endothermic. These thresholds vary between complexes, but are well defined within any single system.

From the results obtained by Giering it was concluded that in the absence of steric and π-bonding effects, the length of a M-P bond is virtually constant. By judicious study of the M-P bond lengths for 'constant' metal systems with varied phosphine ligands it has been possible to separate phosphorus ligands into two classes. The first class comprises the pure σ-donors and the second class comprises the σ-donor/π-acceptors. The ligands of the pure σ-donor type are the alkyl, aryl and mixed alkyl/aryl phosphines, ie the poor π-acids. The ligands with any significant π-acceptor quality tend to be those with either a P-F or P-O bond present.

1 F. A. Cotton and G. A. Wilkinson, *"Advanced Inorganic Chemistry" 5th Edition,* Wiley- Interscience, 1988.

2 R. B. King, *"Progress in Inorganic Chemistry", 1972, 15, 287.*

3 P. Chini and B. T. Heaton, *Topics Curr Chem, 1977, 71, 1.*

4 B. F. G. Johnson, *"Transition Metal Clusters"*, Wiley-Interscience, 1980.

5 M. D. Vargas and J. N. Nicholls, *Adv Inorg Chem and Radiochem, 1986, 30,123.*

6 B. F. G. Johnson and J. Lewis, *Adv Inorg Chem and Radiochem, 1980, 24, 225.*

7 *K. Wade, Adv Inorg Chem and Radiochem, 1976, 18, 1.*

8 R. Hoffmann, *Angew chem, int Ed, 1982, 21, 711.*

9 D. M. P. Mingos, *J. Chem Soc, Chem Comm, 1983, 706.*

10 D. G. Evans and D. M. P. Mingos, *Organometallics, 1983, 2, 435.*

11 D. M. P. Mingos, *Inorg Chem, 1985, 24, 114.*

12 D. M. P. Mingos, *J. Chem Soc, Chem Comm, 1985, 1352.*

13 R. L. Johnston and D. M. P. Mingos, *Inorg Chem, 1986, 25, 1661.*

14 M. MacPartlin, *Polyhedron, 1984, 3, 1279.*

15 R. Mason, K. M. Thomas and D. M. P. Mingos, *J Am Chem Soc, 1973, 95, 3802.*

16 E. R. Corey and L. F. Dahl, *Inorg Chem, 1962, 1, 521.*

17 G. T. Orpen, A. V. Rivera, E. G. Bryan, D. Pippard and G. M. Sheldrick, *J. Chem Soc, Chem Comm, 1978, 723.*

18 A. J. Deeming, *Adv Orgmet Chem, 1986, 26, 1.*

19 M. R. Churchill and J. P. Hutchinson, *Inorg Chem, 1978, 17, 3258.*

20 F. W. B. Einstein *et al.*, *J Am Chem Soc, 1986, 108, 338.*

21 W. Beck, E. R. Corey and L. F. Dahl, *J Am Chem Soc, 1963, 85, 1202.*

22 M. R. Churchill and J. Wormald, *J Am Chem Soc, 1971, 93, 5670.*

23 P. Chini, L. F. Dahl, G. Longolini and L. D. Lower, *J Am Chem Soc, 1975, 97, 5034.*

24 P. F. Jackson, B. F. G. Johnson, J. Lewis, W. J. H. Nelson, M. A. Pearsall, P. R. Raithby and M. D. Vargas, *J. Chem Soc, Dalton Trans, 1987 - page #?.*

25 L. A. Kapicak, , J. M. Troup and J. L. Vidal, *J. Orgmet, 1981, 215, C11.*

26 J. C. Calabrese, L. F. Dahl, P. Chini, G. Longoni, and S. Martinengo, *J Am Chem Soc, 1974, 96, 2614.*

27 J. C. Calabrese, L. F. Dahl, A. Cavalieri, P. Chini, G. Longoni, and S. Martinengo, *J Am Chem Soc, 1974, 96, 2616.*

28 G. Ciani, S. Martinengo, A. Magni and A. Sironi, *J. Chem Soc, Chem Comm, 1981, 1280*

29 D. H. Farrar, P. F. Jackson, B. F. G. Johnson, J. Lewis and J. N. Nicholls, *J. Chem Soc, Dalton Trans, 1982, 1395.*

30 M. Fajardo, H. D. Holden, B. F. G. Johnson, J. Lewis and P. R. Raithby, *J. Chem Soc, Chem Comm, 1984, 24.*

31 M. D. Brice, R. J. Dellaca, B. R. Penfold and J. L. Spencer, *J. Chem Soc, Chem Comm, 1971, 72.*

32 M. M^{c}Partlin, R. Mason and L. Malatesta, *J. Chem Soc, Chem Comm, 1969, 334.*

33 S. Badhuri, B. F. G. Johnson, J. Lewis, P. R. Raithby and D. J. Watson, *J. Chem Soc, Chem Comm, 1978, 343.*

34 V. G. Albano, P. Chini, S. Martinengo and V. G. Sansoni, *J. Chem Soc, Dalton Trans, 1973, 651.*

35 E. H. Braye, L. F. Dahl, W. Hubel and D. S. Wampler, *J Am Chem Soc, 1962, 84, 4633.*

36 E. Benedetti, M. Bianchi and A. Sirugi, *J. Chem Soc, Chem Comm, 1969, 596.*

37 V. G. Albano, D. Braga, P. Chini, S .Martinengo and D. Strumolo, *J. Chem Soc, Dalton Trans, 1985, 35.*

38 M. L. Blohm and W. L. Gladfelter, *Organometallics, 1985, 4, 45.*

39 R. Bau, S. Campanella, P. Chini, D. W. Hart, T. F. Koetzle, G. Longini, R. G. Teller and C. Y. wei, *J Am Chem Soc, 1981, 103, 1458.*

40 R. L. Pruett, R. C. Schoening, J. L. Vidal and W. E. Walker, *Inorg Chem, 1979, 18, 129.*

41 L. A. Cosby, R. A. Fiato, R. L. Pruett and J. L. Vidal, *Inorg Chem, 1978, 17, 2574.*

42 E. J. Deitzel, H. D. Holden, B. F. G. Johnson, J. Lewis, A. Saunders and M. J. Taylor, *J. Chem Soc, Chem Comm, 1982, 1373.*

43 M. T. Camellini, M. Lanfranchi, E. Sappa and A. Tiripicchio, *J. Chem Soc, Chem Comm, 1981, 995.*

44 C. J. Cardin, S. B. Colbran, B. F. G. Johnson, F. J. Lahoz and J. Lewis, *J. Chem Soc, Dalton Trans, 1988, 173.*

45 R. J. Goudsmit, J. G. Jeffrey, B. F. G. Johnson, J. Lewis, R. C. S. M^{c}Queen, A. J. Whitmire and J. C. Lui, *J. Chem Soc, Chem Comm, 1986, 24.*

46 P. Rushman, G. N. van Buuren, M. Shirallan and R. K. Pomeroy, *Organometallics, 1983, 2, 693.*

47 F. A. Cotton and J. M. Troup, *J Am Chem Soc, 1974, 96, 4155.*

48 C. R. Eady, B. F. G. Johnson, J. Lewis and M. M^{c}Partlin, *J. Chem Soc, Chem Comm, 1976, 883.*

49 V. G. Albano, P. L. Bellon and M. Sansoni, *J Am Chem Soc, 1971, A, 678.*

50 G. Ciani, B. T. Heaton, S. Marinengo, J. Mason and A. Sironi, *J Am Chem Soc, 1979, 101, 7095.*

51 V. G. Albano, P. Chini, G. Ciani, S. Marinengo and M. Sansoni, *J. Chem Soc, Dalton Trans, 1980, 163.*

52 S. R. Drake, K. Henrick, B. F. G. Johnson, J. Lewis and M. McPartlin, *J. Chem Soc, Chem Comm, 1986, 928.*

53 V. G. Albano, W. M. Anker, A. Ceriotti, P. Chini, G. Ciani and S. Martinengo, *J. Chem Soc, Chem Comm, 1975, 859.*

54 M. B. Hursthouse, A. V. Rivera and G. M. Sheldrick, *Acta Cryst, 1978, B34, 1985.*

55 V. G. Albano, P. Chini and G. Longini, *J. Orgmet, 1976, 14, 285.*

56 M. Hofler, T. Kruck and M. Noack, *Chem Ber, 1966, 99, 1153.*

57 B. F. G. Johnson, *Unpublished results.*

58 S. G. D. Henderson, PhD Thesis, Edinburgh 1986.

59 A. J. Deeming, *Chapter VI, "Transition Metal Clusters"*, Wiley-Interscience, 1980.

60 S. A. R. Knox, J. W. Koepke, M. A. Andrews and H. D. Kaesz, *J. Am Chem Soc, 1975, 97, 3942.*

61 A. J. Deeming, B. F. G. Johnson and J. Lewis, *J. Chem Soc, A, 1970, 897.*

62 A. J. Deeming and M. Underhill, *J. Chem Soc, Dalton Trans, 1974, 1415.*

63 F. Iwasaki, M. J. Mays, P. R. Raithby, P. L. Taylor and P. J. Wheatley, *J. Orgmet, 1981, 213, 185.*

64 C. W. Bradford and R. S. Nyholm, *J. Chem Soc, Dalton Trans, 1973, 529.*

65 M. Tachikawa and J. R. Shapley, *J. Orgmet, 1977, 124, C25.*

66 A. J. Deeming, S. Donovan-Muunzi, S. E. Kabir and P. J. Manning, *J. Chem Soc, Dalton Trans, 1985, 1037.*

67 S. B. Colbran, B. F. G. Johnson, J. Lewis and R. M. Sorrell, *J. Orgmet, 1985, 296, C1.*

68 C. Couture, D. H. Farrar, M. P. Gomez-Sal, B. F. G. Johnson, R. A. Kamarudin, J. Lewis and P. R. Raithby, *Acta Cryst, 1986, C42, 163.*

69 B. F. G. Johnson, J. Lewis and D. Pippard, *J. Orgmet, 1978, 145, C4.*

70 E. G. Bryan, B. F. G. Johnson and J. Lewis, *J. Chem Soc, Dalton Trans, 1977, 1328.*

71 A. J. Carty, S. A. M^{c}Glaughlin and N. J. Taylor, *J. Orgmet, 1981, 204, C27.*

72 M. P. Gomez-Sal, B. F. G. Johnson, R. A. Kamarudin, J. Lewis and P. R. Raithby, *J. Chem Soc, Chem Comm, 1985, 1622.*

73 J. G. Jeffrey, B. F. G. Johnson, J. Lewis, P. R. Raithby and D. A. Welch, *J. Chem Soc, Chem Comm, 1986, 318.*

74 R. B. King and C. A. Harmon, *Inorg Chem, 1976, 15, 879.*

75 W. Hubel, *"Organic synthesis via metal carbonyls"*, vol 1, Interscience, 1968.

76 R. P. Dodge and V. Schomaker, *J. Orgmet, 1965, 3, 274.*

77 G. Cetini,R. P. Ferrari, O. Gambino, and G. A. Vaglio, *Inorg Chim Acta, 1973, 7, 193.*

78 G. Cetini,R. P. Ferrari, O. Gambino, and G. A. Vaglio, *J. Chem Soc, A, 1972, 1998.*

79 S. Cradock, E. A. V. Ebsworth and D. W .H. Rankin, *"Structural Methods In Inorganic Chemistry"*, Blackwell Scientific Publications, 1987.

80 C. R. Eady, B. F. G. Johnson and J. Lewis, *J. Chem Soc, Dalton Trans, 1975, 2606.*

81 J. M. Miller, *Adv Inorg Chem and Radiochem, 1984, 28, 1.*

82 T. Blumenthal, M. I. Bruce and O. B. Shawkataly, *J. Orgmet, 1984, 269, C10.*

83 U. Bahr, M. Karas and F. Hillenkamp, *Fresenius, J. Anal Chem, 1994, 783.*

84 P. Juhasz and C. E. Costello, *Rapid Comm in Mass Spectrometry, 1993, 343.*

85 E. C. Constable, B. F. G. Johnson. J. Lewis, G. N. Pain and M. J. Taylor, *J. Chem Soc, Chem Comm, 1982, 754.*

86 J. S. Holmgren, and J. R. Shapley, *J. Organomet Chem, 1985, 284, C5.*

87 M. P. Gomez-sal, B. F. G. Johnson, J. Lewis, P. R. Raithby and A. H. Wright, *J. Chem Soc, Chem Comm, 1985, 1682.*

88 R. J. Goudsmit, B. F. G. Johnson, J. Lewis, P. R. Raithby and M. J. Rosales, *J. Chem Soc, Dalton Trans, 1983, 2257.*

89 B. E. Mann and B. F. Taylor, *"^{13}C NMR data for Organometallic Compounds"*, Academic Press, London, 1981.

90 A. Forester, B. F. G. Johnson, J. Lewis, T. W. Matheson, B. H. Robinson, and W. G. Jackson, *J Chem Soc, Chem Comm, 1974, 1042.*

91 B. F. G. Johnson, J. Lewis, B. E. Reichert and K. T. Schorpp, *J Chem Soc, Chem Comm, 1976, 1043.*

92 O. A. Ganslow, A. R. Burke and G. N. Lamar, *J Chem Soc, Chem Comm, 1972, 456.*

93 E. J. Griffith and M. Grayson, *"Topics In Phosphorus Chemistry"*, Interscience, New York, 1967.

94 J. Emsley and D. Hall, *"The Chemistry Of Phosphorus"*, Harper and Row, London, 1976.

95 S. W. Homans, *"A Dictionary of Concepts in Nmr"*, Oxford Science Publications, Oxford, 1993.

96 R. Lynden-Bell and R. K. Harris, *"NMR Spectroscopy"*, Pitman Press, London, 1969.

97 eg *"Inorganic Chemistry of the Transition Elements"*, Specialist Periodical Reports, vols 1 + 2 (1972-73), Chemical Society, London.

98 B. J. Walker, *"Organophosphorus Chemistry"*, Penguin Books ltd, Middlesex, 1972.

99 J. Chatt, *Nature, 1950, 165, 637.*

100 C. A. Tolman, W. C. Seidel and D. H. Gerlach, *J Am Chem Soc, 1972, 94, 2669.*

101 R. D. Gillard, R. Ugo, F. Caviati, S. Ceneni and F. Bonati, *J. Chem Soc, 1966, 869.*

102 J. H. D. Eland, J. C. Green and D. I. King, *J Chem Soc, Chem Comm, 1970, 1121.*

103 H. J. Plastas, J. M. Stewart and S. O. Grim, *J Am Chem Soc, 1969, 91, 4326.*

104 C. A. Tolman, *J Am Chem Soc, 1970, 92, 2953.*

105 W. A. Graham, *Inorg Chem, 1968, 7, 315.*

106 F. A. Cotton and C. S. Kraihanzel, *J Am Chem Soc, 1962, 98, 4432.*

107 R. J. Angelici and M. D. Malone, *Inorg Chem, 1967, 6, 1731.*

108 M. Bigorgne, *J. Inorg Nucl Chem,* 1964, 26, 107.

109 J. E. Belmonte, M. N. Golovin, M. Rahman and W. P. Giering, *Organometallics, 1985, 4, 1981.*

110 H. Y. Lui, A. Prock, M. Rahman and W. P. Giering, *Organometallics, 1987, 6, 650.*

111 K. Eriks, H. Y. Lui, A. Prock, M. Rahman and W. P. Giering, *Organometallics, 1989, 8, 1.*

112 K. Eriks, H. Y. Lui, A. Prock and W. P. Giering, *Organometallics, 1990, 9, 1758.*

CHAPTER TWO

SOME REACTIONS OF TRIOSMIUM CLUSTERS WITH PHOSPHINES

Triosmium clusters : An overview

Triosmium dodecacarbonyl, $[Os_3(CO)_{12}]$, was first reported by Heiber in 1942[1], when it was incorrectly identified as $[Os_2(CO)_9]$. It was synthesised by the action of HI on OsO_4 forming an oxyiodide species, which upon treatment with silver powder under 200atm of CO gas, gave $[Os_3(CO)_{12}]$ in poor yield. The modern synthesis[2] utilises autoclave techniques to form $[Os_3(CO)_{12}]$ in good yield, by the reaction of OsO_4 with CO in ethanol, (80 atm CO/175°C/4 hours).

The cluster $[Os_3(CO)_{12}]$ is a highly symmetrical molecule, having D_{3h} symmetry in the solid phase, which is maintained in other phases[3,4]. The molecule has six CO ligands in the plane of the metal triangle, with three each above and below the plane of the metal triangle, perpendicular to that plane, (FIG 2.1).

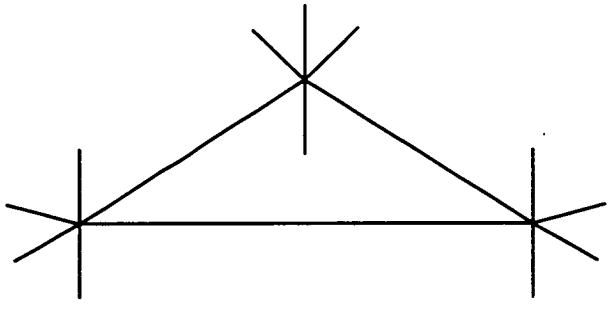

$[Os_3(CO)_{12}]$

Figure 2.1 : The Molecular Structure Of $[Os_3(CO)_{12}]$

The reactivity of $[Os_3(CO)_{12}]$

The species $[Os_3(CO)_{12}]$ is known to readily undergo nuclearity changes upon gain or loss of CO. The gain of CO will cause decomposition of the cluster[5] to form $Os(CO)_5$ which may be converted back to $[Os_3(CO)_{12}]$ under irradiation by sunlight at 80°C[5]. Loss of CO occurs under high vacuum pyrolysis conditions, causing cluster buildup to occur, allowing a high yield route to higher nuclearity osmium cluster species, e.g. $[Os_6(CO)_{18}]$[6]. Reaction with both electrophilic and nucleophilic reagents occurs with $[Os_3(CO)_{12}]$, with electrophiles attacking the metal triangle[7] and nucleophiles attacking at carbon atoms of the CO ligands[8]. Reaction of $[Os_3(CO)_{12}]$ with common reagents requires elevated temperatures (>100°C), to facilitate reaction. This may lead to problems with decomposition of thermally unstable ligand species, or to loss of highly volatile reagents. Irradiation to labilise CO loss is of limited usefulness as breakdown of the cluster will occur with dienes or acrylates to form mononuclear species. Irradiation may also lead to problems with respect to breakdown of ligands, e.g. secondary phosphines.

Cluster activation by chemical means

The use of trimethylamine oxide, Me_3NO, to labilise CO ligands on $[Os_3(CO)_{12}]$ occurs *via* attack at a CO ligand to form $-CO_2(NMe_3)$, which will readily eliminate in the presence of more strongly coordinating ligands, *e.g.* MeCN[9]. The treatment of $[Os_3(CO)_{12}]$ with one or two equivalents of Me_3NO, in the presence of MeCN gives rise to the isolable, activated clusters, $[Os_3(CO)_{11}(MeCN)]$[10] and $[Os_3(CO)_{10}(MeCN)_2]$[11,12] respectively. These activated clusters allow easy routes to substituted triosmium species, due to the highly labile nature of the MeCN ligand.

The mono acetonitrile substituted cluster, $[Os_3(CO)_{11}(MeCN)]$, allows only the formation of simple substitution complexes of *e.g.* pyridine[10] or NH_3[13]. Whereas the *bis*-acetonitrile derivative, $[Os_3(CO)_{10}(MeCN)_2]$, allows oxidative-addition to occur, in the case of pyridine forming, $[Os_3H(CO)_{10}(NC_5H_4)]$ and upon reaction with NH_3, $[Os_3H(CO)_{10}(NH_2)]$ is produced. Chemical activation of $[Os_3(CO)_{12}]$ may also be accomplished by the use of chelating dienes coordinated to the cluster, which allows substitutuion of more than one ligand to occur at an osmium atom upon displacement of the diene, *e.g.* by the use of 1,3-butadiene, which coordinates to one metal at an axial and an equatorial site[14-16].

On heating $[Os_3(CO)_{12}]$ in toluene under reflux in the presence of tertiary phosphines or arsines gives a mixture of $[Os_3(CO)_{11}L]$, $[Os_3(CO)_{10}L_2]$ and $[Os_3(CO)_9L_3]$. All three of these derivatives have been observed for PEt_3[17], PEt_2Ph[17], $AsMe_2Ph$[18], PMe_2Ph[19] and for $AsMe_2Ar$, (Ar = variously substituted phenyl groups)[20,21]. The thermal reaction of $[Os_3(CO)_{12}]$ does not give rise to any products with more than one phosphine or arsine ligand on any one osmium atom. However, the use of $[Os_3(CO)_{10}(MeCN)_2]$ allows the selective formation of the 1,2 substituted species to occur under less forcing conditions than those requires for substititution via thermolysis of $[Os_3(CO)_{12}]$.

Reactions of triosmium clusters with phosphines

Previous studies of the products of the reaction of $[Os_3(CO)_{12}]$ with tertiary phosphines have concentrated on study of isolable products of these reactions, without study of the bulk reaction mixtures. Also previous studies have been carried out using only commercially avaialable or readily synthesised phosphines.

Reaction with tertiary phosphines

The reactions of triosmium clusters with tertiary phosphines yields only simple substitution complexes, as described above[17,19]. However, thermolysis of these species may lead to P-C bond cleavage to form *e.g.* the alkyne substituted triosmium cluster $[Os_3(CO)_9(\mu_2\text{-}H)(PEt_2)(HCCH)]$[17]. These complexes may, upon thermolysis, also allow ortho-metallation to occur, *via* C-H bond cleavage of the phenyl groups on coordinated phosphines, and have been used as a route into benzyne substituted triosmium clusters, *via* P-C bond cleavage[18].

Reaction with secondary phosphines

The reaction of triosmium clusters with secondary phosphines appears to have been limited by the lack of availability of these ligands. The reactions which have been studied involve those with PCy_2H and PBu^t_2H have been carried out *via* photolytic activation of $[Os_3(CO)_{12}]$ and yield a mixture of terminally bound and phosphinidene-bridged clusters[22]. The reaction of $[Os_3(CO)_{11}(MeCN)]$ with PPh_2H has yielded the terminally bound phosphine species $[Os_3(CO)_{11}(PPh_2H)]$[23]. Upon deprotonation, the anionic species $[Os_3(CO)_{10}(\mu_2\text{-}PPh_2)]^-$ has been identified which will readily protonate to form the phosphinidene-bridged cluster $[Os_3(CO)_{10}(\mu_2\text{-}H)(\mu_2\text{-}PPh_2)]$. P-C bond cleavage has also been observed for the perfluoro substituted phosphine $P(C_6F_5)_2H$[24].

Reaction with primary phosphines

The reactions of primary phosphines with triosmium clusters has been limited to the study of derivatives of $PCyH_2$ and $PPhH_2$. These ligands give rise to three types of substituted cluster, the terminally bound species, similar in nature to those observed for teriary phosphines, the bridged species as observed for the secondary phosphines and the μ_3-PR capped species. These complexes have been formed in a number of different ways, by pyrolysis of $[Os_3(CO)_{12}\}$[25,26], via direct activation by Me_3NO[27] and by reaction with the activated precursor molecule $[Os_3(CO)_{11}(MeCN)]$[23]. In all cases the terminally bound and bridged species are intermediates to the formation of the capped species as evidenced by pyrolysis of these species. Heating of the cluster containing the terminally bound PRH_2 ligand in refluxing toluene gives rise to the phosphinidene-bridged complexes, $[Os_3(CO)_{10}(\mu_2\text{-}H)\mu_2\text{-}PHR]$. Further pyrolysis of the μ-P bridged cluster prompts formation of the capped species, $[Os_3(CO)_9(\mu_2\text{-}H)_2(\mu_3\text{-}PR)]$. These reactions are all facilitated by oxidative-addition *via* P-H bond cleavage and are irreversible, indicating that the capped complexes are the most stable of the three types observed.

Under pyrolysis conditions however, the capped species may be forced to open, creating a vacant coordination site on the cluster and a reactive lone pair on the phosphorus[28]. This has been utilised as a route to cluster condensation by addition of another trinuclear cluster to the reaction mixture, causing coordination firstly by the phosphine ligand to the incoming cluster. The phosphine in this system then acts as a hinge allowing the two clusters to link up, forming hexanuclear clusters with phosphinidene bridges incorporated into the framework.

In the case of phosphine itself, (PH_3), the cluster condensation reaction may be taken one step further. This is possible as the capping ligand contains a further P-H bond which may be cleaved allowing the phosphorus to be encapsulated by the metal framework of the cluster in a μ_6-P fashion[29].

The intention of this work is to systematically synthesise and characterise a range of primary, secondary and tertiary phosphine derivatives of $[Os_3(CO)_{12}]$. The characterisation of these complexes will primarily be carried out in the bulk reaction mixture by variable temperature ^{31}P nmr. These reactions will be studied under milder reaction conditions than previously utilised, relying on chemical activation of the cluster via the complexes $[Os_3(CO)_{11}(MeCN)]$ and $[Os_3(CO)_{10}(MeCN)_2)]$.

Fluxional behaviour of substituted $[Os_3(CO)_{12}]$ complexes

To date phosphine ligands in substituted complexes of $[Os_3(CO)_{12}]$ have only exhibited equatorial coordination. This has been proved by nmr[30] and by X-ray study[31,32]. The nature of ligand exchange on metal clusters has seen intensive study[33-35], and occurs *via* one of five mechanisms as shown below.

(i) Exchange *via* a 'turnstile' mechanism around one metal atom, with axial-equatorial exchange occuring via a rotational motion of ligands, (FIG 2.2)

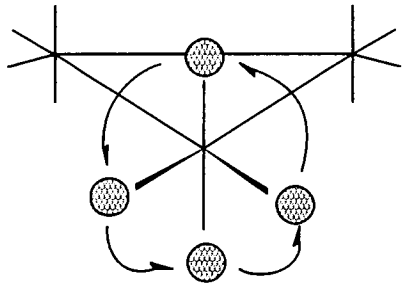

Figure 2.2 : Turnstile Ligand Exchange Mechanism For $[Os_3(CO)_{12}]$

(ii) Exchange *via* a two centre 'merry go round' mechanism with a di-μ_2-CO bridged intermediate species, similar in structure to $[Fe_3(CO)_{12}]$, (FIG 2.3).

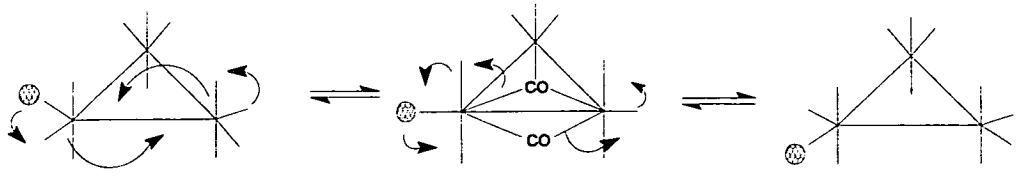

Figure 2.3 : Two Centre Merry Go Round Ligand Exchange Mechanism For $[Os_3(CO)_{12}]$

(iii) Exchange *via* a three centre 'merry go round' process involving six equatorial CO ligands, with an intermediate with three μ_2-CO ligands in the plane of the metal triangle, (FIG 2.4).

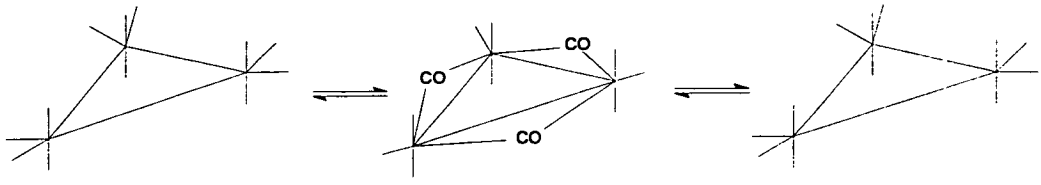

Figure 2.4 : Equatorial Three Centre Merry Go Round Exchange Mechanism For $[Os_3(CO)_{12}]$

(iv) Exchange *via* a three centre 'merry go round' process involving three axial CO ligands, with an intermediate with three μ_2-CO ligands in a conical surface on the same face of the metal triangle, (FIG 2.5).

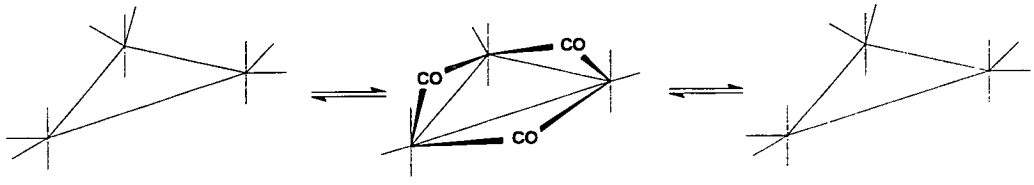

Figure 2.5 : Axial Three Centre Merry Go Round Exchange Mechanism For $[Os_3(CO)_{12}]$

(v) Overall motion of the CO polyhedron about the metal triangle, this is known as the "Ligand Polyhedron Model"[30].

The reaction of $PMeH_2$ with $[Os_3(CO)_{10}(MeCN)_2]$:

The nmr tube containing the reactants was left for 24 hours at 293K, after which time the $^{31}P\{^1H\}$ nmr was recorded, showing that no reaction had occurred. The tube was then heated to 333K for 1 hour, after which time the $^{31}P\{^1H\}$ nmr was run again, showing that reaction had occurred.

The spectrum exhibited four resonances, with the lowest frequency resonance at (δ -161ppm) being assigned as unreacted $PMeH_2$ on the basis of its chemical shift. The other 3 resonances present are separated into 2 distinct groups. The lower frequency set comprises a broad resonance at (δ -140ppm) with a second, sharper peak at (δ -136ppm). The highest frequency peak at (δ -70ppm) is a sharp singlet.

The proton coupled ^{31}P nmr spectrum shows $^1J_{PH}$ couplings present for all of the peaks in the spectrum. The lowest frequency resonance at (δ -161ppm) exhibits a triplet coupling with a $^1J_{PH}$ value of 199Hz, consistent with a three coordinate phosphorus centre, confirming that this peak is attributable to unreacted $PMeH_2$.

The peaks at (δ -140ppm) and (δ -136ppm) show triplet couplings with a $^1J_{PH}$ value of 380Hz . The peak at (δ -70ppm) exhibits a doublet coupling and has a $^1J_{PH}$ value of 416Hz. All of the peaks present also exhibited a narrow quartet coupling of 14Hz, this has been assigned as arising from the $^2J_{PH}$ to the methyl protons present on the phosphine.

On the basis of this data the resonance at (δ -140ppm) has been assigned as a coordinated $PMeH_2$ group. The resonance at (δ -70ppm) has been assigned as a PMeH bridge. The table below, (Table 2.1), summarises the nmr data obtained.

Table 2.1 : Room temperature nmr parameters for the reaction of $PMeH_2$ with $[Os_3(CO)_{10}(MeCN)_2]$ in dichloromethane			
δP (ppm)	$^1J_{PH}$ (Hz)	Multiplicity	Assignment
-161	199	Triplet of quartets	Unreacted $PMeH_2$
-140	380	Triplet of quartets	Cluster bound $PMeH_2$
-136	380	Triplet of quartets	Cluster bound $PMeH_2$
-70	416	Doublet of quartets	PMeH Bridge

The fact that the resonance at (δ -140ppm) was very broad suggests that some sort of fluxional process may be occurring. In order to investigate this further the tube was cooled to 213K and the spectrum rerun. The $^{31}P\{^1H\}$ spectrum showed no change for the peaks at (δ -161ppm), (δ -136ppm) and (δ -70ppm), however the broad peak at (δ -140ppm) splits into three separate resonances at (δ -142ppm), (δ -138ppm) and (δ -137ppm).

The proton coupled ^{31}P nmr spectrum once more showed $^1J_{PH}$ values indicative of 4 coordinate phosphorus groups, except for the free phosphine. The three resonances which have been resolved fully all show triplet couplings in the order of 380Hz. All of the resonances present also show the 14Hz $^2J_{PH}$ couplings to the methyl protons. The table below, (Table 2.2), summarises the data obtained for the low temperature nmr spectra.

Table 2.2 : Low temperature nmr parameters for the reaction of $PMeH_2$ with $[Os_3(CO)_{10}(MeCN)_2]$ in dichloromethane			
δP (ppm)	$^1J_{PH}$ (Hz)	Multiplicity	Assignment
-161	199	Triplet of quartets	Unreacted $PMeH_2$
-142	377	Triplet of quartets	Cluster bound $PMeH_2$
-138	374	Triplet of quartets	Cluster bound $PMeH_2$
-137	382	Triplet of quartets	Cluster bound $PMeH_2$
-136	381	Triplet of quartets	Cluster bound $PMeH_2$
-70	416	Doublet of quartets	PMeH Bridge

The assignment of these resonances has been made primarily on the basis of the $^{1}J_{PH}$ and $^{2}J_{PH}$ values obtained. From the nmr data obtained it is impossible to say whether the bridge is intermolecular or intramolecular.

The nmr tube containing the products was then broken open under a nitrogen atmosphere and the products were separated by tlc, eluent 60% n-hexane, 40% dichloromethane. The ir and mass spectra of the products were recorded, the results of these are summarised in the table below, (Table 2.3).

Table 2.3 : ir and mass spectral parameters for the reaction of $PMeH_2$ with $[Os_3(CO)_{10}(MeCN)_2]$

tlc band #	Mass spectrum (Obs/Calc)	ir (νCO/cm^{-1}) (dichloromethane)	Assignment
1	934/934	2105.8(w), 2051.9(s), 2028.7(m), 2016.0(s), 1982.7(w), 1967.7(w) νCN 2360.1(s), 2340.3(s)	Unreacted $[Os_3(CO)_{10}(MeCN)_2]$
2	947/946	2090.3(w), 2030.1(w), 2011.0(s), 2002.1(s), 1966.5(m),1956.3(m), 1931.3(m)	$[Os_3(CO)_{10}(PMeH_2)_2]$ (1)
3	926/926	2110.5(w), 2068.9(w), 2057.2(s), 2036.2(m), 2020.1(s), 1977.6(w)	$[Os_3(CO)_{11}(PMeH_2)]$ (2)
4	898/898	2107.1(w), 2068.9(m), 2062.3(m),2039.7(m), 2023.5(s),2002.1(m), 1995.4(w)	$[Os_3(CO)_{10}(\mu_2\text{-}H)(\mu_2\text{-}PMeH)]$ (3)

The assignment of these complexes has been confirmed by room temperature nmr studies on the isolated products, as well as the mass spectral and ir data. The ir data are all consistent with the types of complexes described in terms of number, intensities and relative positions of bands. The proposed structures of these complexes are given below (FIG 2.6).

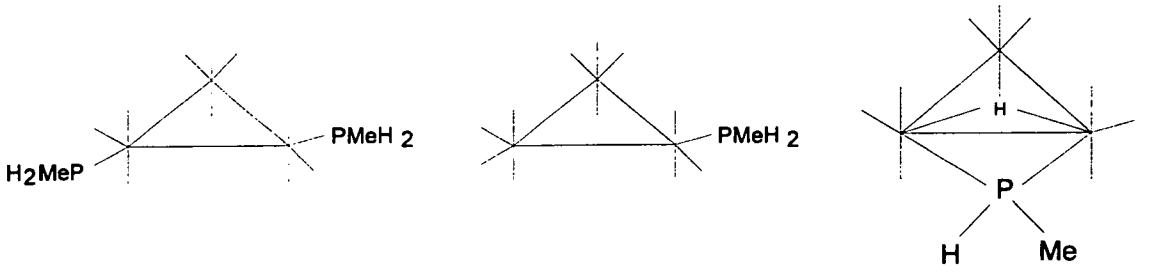

(1) (2) (3)

Figure 2.6 : The Proposed Structures of $[Os_3(CO)_{10}(PMeH_2)_2]$ (1), $[Os_3(CO)_{11}(PMeH_2)]$ (2) And $[Os_3(CO)_{10}(\mu_2\text{-}H)(\mu_2\text{-}PMeH)]$ (3)

With the mass spectral and ir evidence it is possible to assign the peaks in the nmr spectrum to individual products. Complex (1) gives rise to the exchange system observed at (δ -140ppm), which spits into three peaks, as seen above. The exchange system is thought to involve an intermediate with two bridging carbonyl groups in as shown below (FIG 2.7).

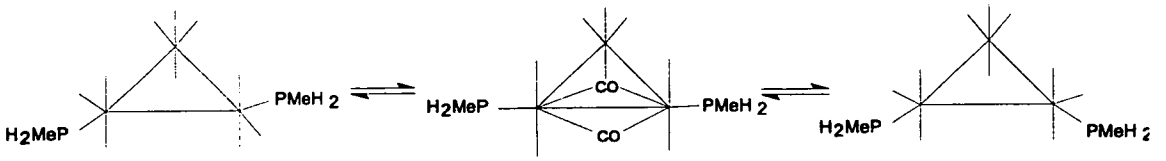

(1a) (1b)

Figure 2.7 : Proposed Exchange System For Complex (1)

The three resonances observed in the low temperature spectrum have been assigned as follows. The two outer peaks at (δ -137ppm) and (δ -142ppm) have been assigned to complex (1a). This has been assigned as the two phosphines present are not magnetically equivalent. The central peak at (δ -138ppm) arises from complex (1b), as the two phosphine environments are identical. The isomeric form with 2 adjacent phosphines on the same edge of the cluster cannot be ruled out but this has been regarded as unlikely for steric reasons. The resonance at (δ -136ppm) has been assigned to complex (2). This is assumed to arise from the presence of a small amount of $[Os_3(CO)_{11}(MeCN)]$ contaminant present in the $[Os_3(CO)_{10}(MeCN)_2]$ starting material. The bridged species, (3), has been assigned to the resonance observed at (δ -136ppm). The mass spectral data indicates that the bridge present is in fact intramolecular in nature, not intermolecular.

It did not prove possible to observe the requisite bridging hydride group in the ^1H nmr spectrum. The low intensity of such signals, coupled with the problems of quad images generated by other signals may account for this. Reaction with $PMeD_2$ should resolve this problem by observing the ^2H nmr spectrum, but time did not permit this experiment to be carried out.

The reaction of $P(i\text{-}Pr)H_2$ with $[Os_3(CO)_{10}(MeCN)_2]$:

Initial reaction occurred at 298K, with the $^{31}P\{^1H\}$ nmr spectrum showing two resonances. The lowest frequency peak at (δ -86ppm) was broad with a sharper peak to slightly higher frequency (δ -86ppm). The proton coupled ^{31}P nmr spectrum shows triplet couplings with $^1J_{PH}$ values of 400Hz for the peaks at (δ -86ppm) and (δ -84ppm). The peaks at (δ -86ppm) and (δ -84ppm) also showed a doublet coupling of 15Hz, which has been assigned to $^2J_{PH}$ to the CH part of the (i-Pr) group attached to the phosphorus. The $^3J_{PH}$ coupling to the $-CH_3$ groups of the (i-Pr) group were not observed. On the basis of this data the resonance at (δ -86ppm) has been assigned as a coordinated $P(i\text{-}Pr)H_2$ group. The table below, (Table 2.4), summarises the nmr data obtained.

Table 2.4 : The room temperature nmr parameters for the reaction of $P(i\text{-}Pr)H_2$ with $[Os_3(CO)_{10}(MeCN)_2]$ in dichloromethane

δP (ppm)	$^1J_{PH}$ (Hz)	Multiplicity	Assignment
-86	400	Triplet of doublets	Cluster bound $P(i\text{-}Pr)H_2$
-84	398	Triplet of doublets	Cluster bound $P(i\text{-}Pr)H_2$

The temperature of the probe was then lowered to 213K to ascertain whether or not the broad peak at (δ -86ppm) was due to an exchanging system. In the $^{31}P\{^1H\}$ nmr spectrum this peak was observed to split into three separate resonances at (δ -90ppm) , (δ -87ppm) and (δ -86ppm). The ^1H coupled spectrum once more showed triplet couplings with $^1J_{PH}$ values of the order of 400Hz for these three resonances. All three of these resonances also exhibit narrow doublet couplings with $^2J_{PH}$ values of 15Hz.

The sample was then warmed to 333K, and the $^{31}P\{^{1}H\}$ nmr spectrum recorded. This spectrum showed the presence of an extra resonance at (δ -5ppm), and the resonance at (δ -84ppm) showed an intensity loss of approximately 10% with respect to the original peaks present in the spectrum.

The proton coupled ^{31}P nmr spectrum showed a doublet coupling for the new peak exhibiting a $^{1}J_{PH}$ value of 412Hz, and a $^{2}J_{PH}$ value of 13Hz. From this data the new resonance has been assigned as arising from a P(i-Pr)H bridge. At this stage it is impossible to differentiate between an intermolecular and intramolecular bridge system. The probe was once more cooled to 213K, and the $^{31}P\{^{1}H\}$ nmr spectrum recorded. The new resonance at (δ -5ppm), showed no change. The table below, (Table 2.5), summarises the nmr data for the 213K spectrum.

Table 2.5 : The low temperature nmr parameters for the reaction of $P(i\text{-}Pr)H_2$ with $[Os_3(CO)_{10}(MeCN)_2]$ in dichloromethane

δP (ppm)	$^{1}J_{PH}$ (Hz)	Multiplicity	Assignment
-90	399	Triplet of doublets	Cluster bound $P(i\text{-}Pr)H_2$
-87	404	Triplet of doublets	Cluster bound $P(i\text{-}Pr)H_2$
-86	401	Triplet of doublets	Cluster bound $P(i\text{-}Pr)H_2$
-84	398	Triplet of doublets	Cluster bound $P(i\text{-}Pr)H_2$
-5	412	Doublet of doublets	P(i-Pr)H Bridge

The nmr tube containing the products was then broken open under a nitrogen atmosphere and the products were separated by tlc, eluent 60% n-hexane, 40% dichloromethane. The ir and mass spectra of the products were run, the results of these are summarised in the table below, (Table 2.6).

Table 2.6 : The ir and mass spectral parameters for the reaction of $P(i\text{-}Pr)H_2$ with $[Os_3(CO)_{10}(MeCN)_2]$ in dichloromethane

tlc band #	Mass spectrum (Obs/Calc)	ir ($\nu CO/cm^{-1}$) (dichloromethane)	Assignment
1	934/934	2105.8(w), 2051.9(s), 2028.7(m), 2016.0(s), 1982.7(w), 1967.7(w) νCN 2360.1(s),-2340.3(s)	Unreacted $[Os_3(CO)_{10}(MeCN)_2]$
2	1004/1002	2088.5(w), 2029.9(s), 2010.5(s), 2001.2(s), 1965.6(m), 1955.2(w), 1930.3(w)	$[Os_3(CO)_{10}(P(i\text{-}Pr)H_2)_2]$ (4)
3	956/954	2108.3(w), 2067.8(w), 2055.8(s), 2034.0(m), 2018.6(s), 1975.6(w)	$[Os_3(CO)_{11}(P(i\text{-}Pr)H_2)]$ (5)
4	925/926	2104.0(w), 2067.8(m), 2060.5(s), 2037.9(m), 2019.5(s), 1999.8(m), 1991.6(w)	$[Os_3(CO)_{10}(\mu_2\text{-}H)(\mu_2P(i\text{-}Pr)H)]$ (6)

The assignment of these complexes has been confirmed by room temperature nmr studies as well as the mass spectral and ir data obtained. The ir data are all consistent with the types of complexes described, in terms of number, intensities and relative positions of bands. The proposed structure of these complexes are given overleaf (FIG 2.8).

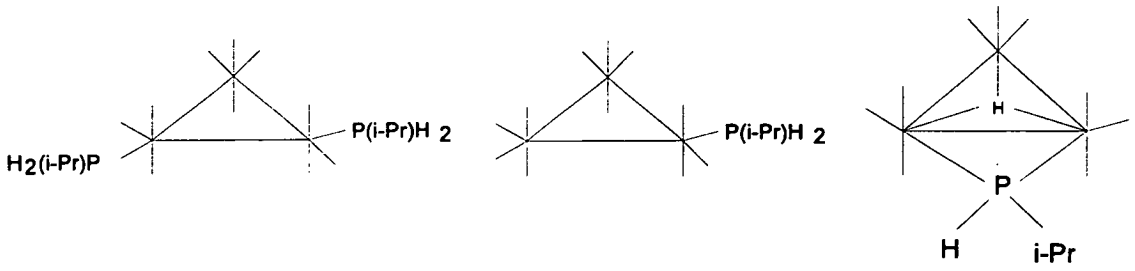

(4) (5) (6)

Figure 2.8 : The Proposed Structures of $[Os_3(CO)_{10}(P(i\text{-}Pr)H_2)_2]$ (4), $[Os_3(CO)_{11}(P(i\text{-}Pr)H_2)]$ (5) And $[Os_3(CO)_{10}(\mu_2\text{-}H)(\mu_2P(i\text{-}Pr)H)]$(6)

With the mass spectral and ir evidence it is possible to assign the peaks in the nmr spectrum to individual products. Complex (4) gives rise to the exchange system observed at (δ -140ppm), which spits into three peaks, as seen above. The exchange system is presumed to be analogous to that proposed for the methyl phosphine case, (FIG 2), above. The peak at (δ -84ppm) has been assigned to complex (5), a *mono* substituted cluster, presumably derived from some $[Os_3(CO)_{11}(MeCN)]$ present in the starting material. The peak at (δ -5ppm) has been assigned to the phosphinidene bridged species (6), once again the mass spectrum indicates that the bridge in this species is intramolecular in nature, not intermolecular.

The room temperature proton nmr spectrum of this species shows 2 separate signals attributable to metal hydrides at (δ -21.4ppm) and (δ -19.5ppm), exhibiting doublet couplings with $^2J_{PH}$ values of 9.6Hz and 14.9Hz respectively. From this data it has been concluded that there are two isomers of the phosphinidene bridge present, one with the i-Pr group coordinated in an axial fashion, and the second isomer coordinated in an equatorial fashion. From the coupling information available it is impossible to assign the hydride resonances to individual isomers. The proposed conformations of these isomers are given below, (FIG 2.9).

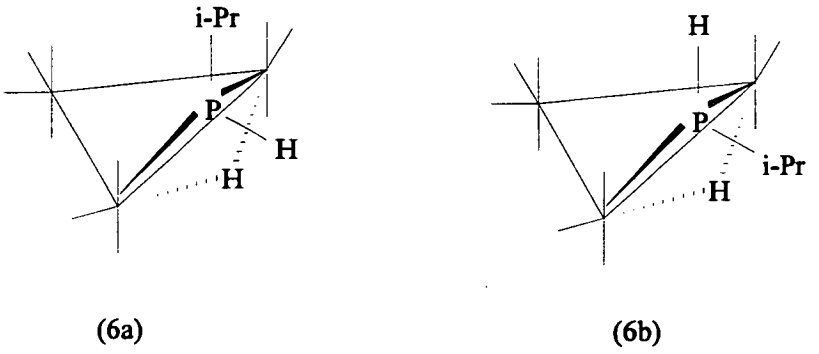

(6a) (6b)

Figure 2.9 : The Proposed Phosphine Conformations Of "Axial"-$[Os_3(CO)_{10}(\mu_2\text{-}H)(\mu_2P(i\text{-}Pr)H)]$, (6a), And "Equatorial"-$[Os_3(CO)_{10}(\mu_2\text{-}H)(\mu_2P(i\text{-}Pr)H)]$, (6b).

The reaction of $PEtH_2$ with $[Os_3(CO)_{10}(MeCN)_2]$:

Initial reaction occurred at 298K, with the $^{31}P\{^1H\}$ nmr spectrum showing three resonances at (δ -111ppm), (δ -48ppm) and (δ -35ppm). The resonance at (δ -111ppm) was broad, presumably due to some fluxional process.

The proton coupled ^{31}P nmr spectrum shows a triplet coupling with a $^1J_{PH}$ value of 372Hz for the resonance at (δ -111ppm), whilst the two higher frequency resonances exhibited doublet couplings of 367Hz, (δ -48ppm), and 395Hz, (δ -35ppm). It was not possible to elucidate any $^2J_{PH}$ couplings from the spectrum, as the resonances present were very broad. This broadening is assumed to arise from couplings to the methyl protons of the ethyl group attached to the phosphorus. On the basis of this data the resonance at (δ -48ppm) has been assigned as a cluster bound $PEtH_2$ unit whilst the two higher frequency resonances have been assigned as arising from PEtH bridges. The table below, (Table 2.7), summarises the nmr data obtained.

Table 2.7 : The room temperature nmr parameters for the reaction of $PEtH_2$ with $[Os_3(CO)_{10}(MeCN)_2]$ in dichloromethane

δP (ppm)	$^1J_{PH}$ (Hz)	Multiplicity	Assignment
-111	372	Triplet	Cluster bound $PEtH_2$
-48	367	Doublet	PEtH Bridge
-35	395	Doublet	PEtH Bridge

The temperature was then lowered to 213K to investigate the possibility that the broad signal at (δ -111ppm) was associated with an exchanging system. The $^{31}P\{^1H\}$ nmr spectrum showed that this was indeed the case with this resonance resolving into 3 separate peaks at (δ -113ppm), (δ -109ppm) and (δ -108ppm).

The proton coupled ^{31}P nmr spectrum shows triplet couplings for all of the peaks in the resolved system with $^{1}J_{PH}$ values of 367Hz, (δ -113ppm), 372Hz, (δ -109ppm), and 366Hz, (δ -108ppm). The two high frequency resonances show no change at this temperature. The table below, (Table 2.8), summarises the low temperature nmr data obtained.

Table 2.8 : The low temperature nmr parameters for the reaction of $PEtH_2$ with $[Os_3(CO)_{10}(MeCN)_2]$ in dichloromethane

δP (ppm)	$^{1}J_{PH}$ (Hz)	Multiplicity	Assignment
-113	367	Triplet	Cluster bound $PEtH_2$
-109	372	Triplet	Cluster bound $PEtH_2$
-108	366	Triplet	Cluster bound $PEtH_2$
-48	367	Doublet	PEtH Bridge
-35	395	Doublet	PEtH Bridge

The fluxional system observed is presumed to arise from the exchange already observed for the 1,2 substituted products observed for $PMeH_2$ and $P(i\text{-}Pr)H_2$, above.

The nmr tube was then heated to 333K and the $^{31}P\{^{1}H\}$ nmr spectrum recorded again. The two bridged species showed a 2 fold increase in intensity under these conditions with a resultant loss of intensity for the low frequency resonance. There was no evidence of free $PEtH_2$ in solution however and it is assumed that any free phosphine present will rapidly react with free $[Os_3(CO)_{10}(MeCN)_2]$ in solution.

As there are two bridged species present then the possibility arises that one of these is intermolecular in nature. The postulate behind the existence of an intermolecular phosphinidene bridge is twofold.

Firstly, the signal at (δ -48ppm) is lower in intensity than the other bridged species, which would be expected for steric reasons. It is assumed that it is considerably easier for a phosphine to cleave a P-H bond and form a bridge along one edge of a metal triangle than it is for a second cluster to come into close aligment to link up in an intermolecular fashion. Secondly, a phosphine ligand bound along one edge of a metal triangle will interact more strongly with the cluster framework than one bridging two clusters. The result of this is that the intermolecular species will have less shielding on the phosphorus atom and consequently a higher chemical shift value.

There is of course another possibility for the presence of two separate resonances arising from bridging phosphines. That is the presence of two confomers similar in nature to those observed for $P(i\text{-}Pr)H_2$, ie one axially coordinated and one equatorially coordinated species. The two different coordination modes would of course have different geometries at the phosphorus, imposed by the other ligands present on the cluster, causing the chemical shift difference to arise.

The nmr tube was then broken open under a N_2 atmosphere and the solvent removed. The mixture was then separated by tlc, eluent 60% n-hexane, 40% dichloromethane, and the ir and mass spectra of the products taken. The results of these studies are given in the table below, (Table 2.9).

Table 2.9 : The ir and mass spectral parameters for the reaction of $PEtH_2$ with $[Os_3(CO)_{10}(MeCN)_2]$

tlc band #	Mass spectrum (Obs/Calc)	ir (νCO/cm^{-1}) (dichloromethane)	Assignment
1	934/934	2105.8(w), 2051.9(s), 2028.7(m), 2016.0(s), 1982.7(w), 1967.7(w) νCN 2360.1(s), 2340.3(s)	Unreacted $[Os_3(CO)_{10}(MeCN)_2]$
2	974/974	2088.3(w), 2060.8(w), 2029.6(m), 2006.5(s), 2000.9(s), 1965.3(m), 1952.7(w)	$[Os_3(CO)_{10}(PEtH_2)_2]$ (7)
3	912/912	2103.9(w), 2076.9(m), 2067.7(m), 2060.5(s), 2052.1(m), 2020.0(s), 2002.5(w), 1990.0(m)	$[Os_3(CO)_{10}(\mu_2\text{-}H)(\mu_2\text{-}PEtH)]$ (8)

The fluxional system observed in the nmr spectra has been assigned to the 1,2 substituted cluster, (7). The fact that there are two bridged systems observed in the nmr but only one found in the mass spectrum suggests that it is unlikely that an intramolecular bridged species that was observed, but that the two bridged species observed are conformational isomers. The first one with the ethyl group on the phosphorus coordinated axially, and one with the ethyl group coordinated equatorially.

As there is no evidence to support the existence of an intermolecular bridged species it has been ruled more likely that the species observed in the nmr spectra are the two conformational isomers of the intramolecular bridged species. It is impossible however, to eliminate the possibility of an intermolecular phosphine bridged cluster species. Study of the isolated intramolecular bridged cluster, (8), by ^{31}P nmr spectroscopy only shows evidence of a resonance at (δ -35ppm). From this information the resonance present at (δ -48ppm) may only be assigned as an intermolecular phosphine bridged species. The proposed structures of these complexes are given below (FIG 2.10).

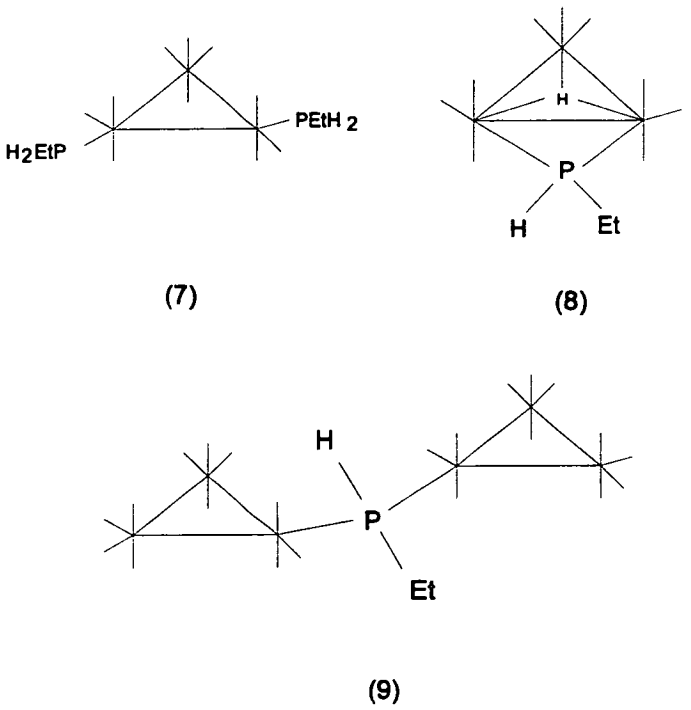

Figure 2.10 : The Proposed Structures of $[Os_3(CO)_{10}(PEtH_2)_2]$ (7), $[Os_3(CO)_{10}(\mu_2\text{-}H)(\mu_2\text{-}PEtH)]$(8) And $[\{Os_3(CO)_{11}\}_2(\mu_2\text{-}PEtH)]$ (9)

The reaction of $PPhH_2$ with $[Os_3(CO)_{10}(MeCN)_2]$:

Initial reaction occurred at 298K, with the $^{31}P\{^1H\}$ nmr spectrum exhibiting five resonances at (δ -112ppm), (δ -109ppm), (δ -108ppm), (δ -56ppm) {very low intensity}, and (δ -35ppm). The resonances observed at (δ -112ppm) and (δ -109ppm) were broad, presumably due to some fluxional process.

The proton coupled ^{31}P nmr spectrum showed triplet couplings for the three low frequency resonances at (δ -112ppm), (δ -109ppm) and (δ -108ppm) with $^1J_{PH}$ values of 374Hz, 380Hz and 398Hz respectively. These values are approximate due to the broad, ill defined nature of the peaks. Of the two high frequency resonances at (δ -56ppm) and (δ -35ppm) only the peak at (δ -35ppm) exhibited a doublet coupling with a $^1J_{PH}$ value of 407Hz, with the second high frequency resonance, (δ -56ppm), broadening sufficiently that it was impossible to locate in the baseline noise. There were no $^3J_{PH}$ couplings to the ortho protons on the phenyl group observed. The table below, (Table 2.10) summarises the nmr data obtained.

Table 2.10 : The room temperature nmr parameters for the reaction of $PPhH_2$ with $[Os_3(CO)_{10}(MeCN)_2]$ in dichloromethane

δP (ppm)	$^1J_{PH}$ (Hz)	Multiplicity	Assignment
-112	374	Triplet	Cluster bound $PPhH_2$
-109	374	Triplet	Cluster bound $PPhH_2$
-108	380	Triplet	Cluster bound $PPhH_2$
-56	Not Observed	Not Observed	N/A
-35	407	Doublet	PPhH Bridge

The sample was then cooled to 213 K and the $^{31}P\{^1H\}$ nmr spectrum rerun. This showed the peaks at (δ -112ppm) and (δ -109ppm) resolving into a 3 peak system, with resonances at (δ -113ppm), (δ -109ppm) and (δ -108.9ppm), with the resonance present at (δ -108ppm) showing no change.

The proton coupled ^{31}P nmr spectrum showed triplet couplings for all of the low frequency peaks, with $^{1}J_{PH}$ values in the order of 390Hz. The high frequency peaks showed no change at this temperature, although it was possible to elucidate a doublet coupling for the peak at (δ -56ppm) with a $^{1}J_{PH}$ value of 387Hz. Again no couplings to the ortho protons of the phenyl group were observed. The table below, (Table 2.11), summarises the low temperature nmr data obtained.

Table 2.11 : The low temperature nmr parameters for the reaction of $PPhH_2$ with $[Os_3(CO)_{10}(MeCN)_2]$ in dichloromethane

δP (ppm)	$^{1}J_{PH}$ (Hz)	Multiplicity	Assignment
-113	391	Triplet	Cluster bound $PPhH_2$
-109	380	Triplet	Cluster bound $PPhH_2$
-108.9	400	Triplet	Cluster bound $PPhH_2$
-108	412	Triplet	Cluster bound $PPhH_2$
-56	387	Doublet	PPhH Bridge
-35	407	Doublet	PPhH Bridge

From the nmr data obtained the low frequency peaks have been assigned to cluster bound $PPhH_2$ ligands and the high frequency resonances to PPhH bridges.

As discussed in the case of $PEtH_2$ there is no evidence available to prove or disprove the existence of an intermolecular phosphine bridge. However it is regarded as more likely that the two bridged species observed are simply isomeric forms of the intramolecular bridged species.

The fluxional system observed has been assigned to the 1,2 phosphine substituted cluster, $[Os_3(CO)_{10}(PPhH_2)_2]$, (10). The resonance at (δ -108ppm) has been assigned to the *mono* substituted cluster, $[Os_3(CO)_{11}(PPhH_2)]$, (11). The two bridged species have been assigned as the intramolecular bridge, $[Os_3(CO)_{10}(\mu_2\text{-}H)(\mu_2\text{-}PPhH)]$, (12), (δ -35ppm) and the intermolecular bridge, $[\{Os_3(CO)_{11}\}_2(\mu_2\text{-}PPhH)]$, (13), (δ -56ppm). The proposed structures of these complexes are given below, (FIG 2.11).

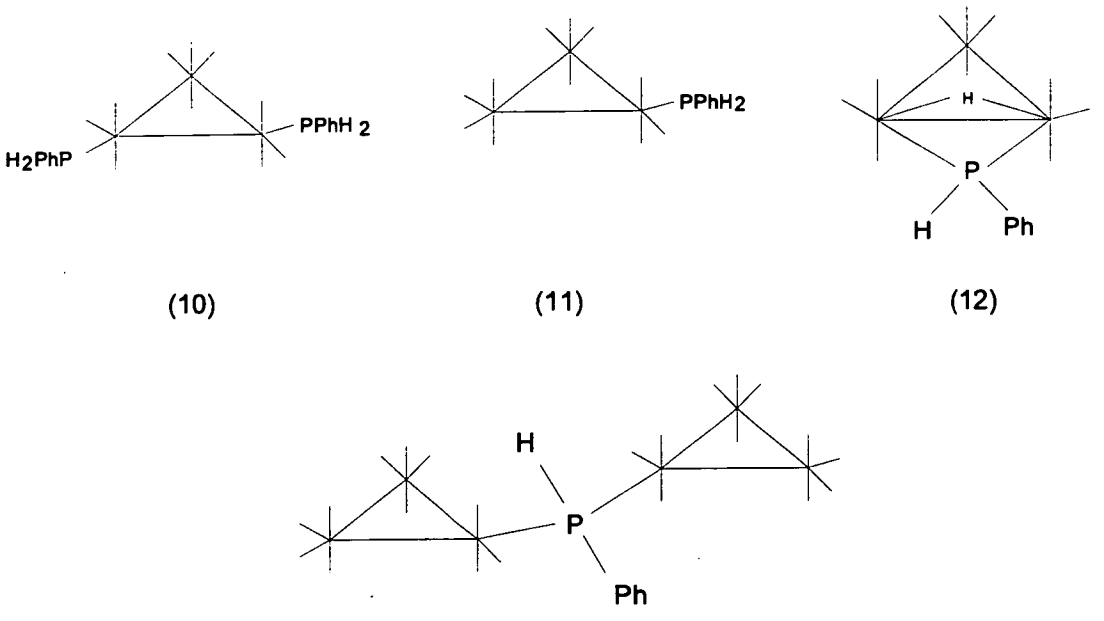

(10) (11) (12)

(13)

Figure 2.11 : The Proposed Structures Of $[Os_3(CO)_{10}(PPhH_2)_2]$, (10), $[Os_3(CO)_{11}(PPhH_2)]$, (11), $[Os_3(CO)_{10}(\mu_2\text{-}H)(\mu_2\text{-}PPhH)]$, (12) And $[\{Os_3(CO)_{11}\}_2(\mu_2\text{-}PPhH)]$, (13)

The nmr tube was then broken open under a N_2 atmosphere and the products were separated by tlc, eluent 60% n-hexane, 40% dichloromethane. The ir and mass spectra of these complexes were taken, the results of which are summarised in the table below, (Table 12).

Table 2.12 : The ir and mass spectral parameters for the reaction of $PPhH_2$ with $[Os_3(CO)_{10}(MeCN)_2]$

tlc band #	Mass spectrum (Obs/Calc)	ir (νCO/cm^{-1}) (dichloromethane)	Assignment
1	1071/1070	2090.1(w), 2032.7(m), 2009.5(m), 2003.9(s), 1968.3(m), 1957.4(w), 1935.2(w)	$[Os_3(CO)_{10}(PPhH_2)_2]$ (10)
2	988/988	2095.0(w), 2067.8(m), 2056.2(m),2034.5(m), 2018.3(s), 1992.4(w)	$[Os_3(CO)_{11}(PPhH_2)]$ (11)
3	960/960	2104.5(w), 2067.8(s), 2062.3(s), 2033.8(m), 2022.0(m), 1995.5(w), 1991.2(w)	$[Os_3(CO)_{10}(\mu_2\text{-}H)(\mu_2\text{-}PPhH)]$ (12)

Study of the isolated products by nmr, coupled with the mass spectral and ir data allows full assignment of the resonances in the nmr spectrum to individual products.

The exchange system observed at (δ -112ppm) and (δ -109ppm) has been assigned to the 1,2 substituted cluster, (10). The *mono* substituted product (11) has been assigned to the peak at (δ -108ppm). The intramolecular bridged species has been assigned to the resonance at (δ -35ppm). There is no evidence in the mass spectra or ir spectra for the intermolecular bridged species (13).

The room temperature ^{1}H nmr spectrum of (12) shows evidence of the presence of a metal hydride. The hydride species shows a doublet of doublets in the proton spectrum, centred around (δ -19.4ppm). The large doublet coupling of 22Hz has been assigned to the $^{2}J_{PH}$ couple to the bridging phosphine. The smaller doublet coupling of 4Hz (±0.7Hz), has been assigned to the $^{3}J_{HH}$ to the proton present on the bridging phosphine. From the fact that only one hydride resonance was observed for this species it has to be assumed that there are not two isomeric forms of the intramolecular bridge preesent. From this it may be concluded that the resonance observed at (δ -56ppm) is attributable to the intermolecular phosphinidene bridged species, (13).

The reaction of PMe_2H with $[Os_3(CO)_{10}(MeCN)_2]$:

Reaction initially occurred at room temperature with the $^{31}P\{^1H\}$ nmr spectrum showing five peaks at (δ -97ppm), (δ -92ppm), (δ -90ppm), (δ -63ppm), and (δ -38ppm). The peaks at (δ -97ppm), and (δ -38ppm), have been assigned as free PMe_2H and $OPMe_2H$ respectively on the basis of their chemical shifts. It was observed that the peaks present at (δ -92ppm) and (δ -90ppm) were broad and ill defined.

The proton coupled ^{31}P nmr spectrum was then recorded showing doublet couplings for the all of the peaks present. The $^1J_{PH}$ values of 191Hz and 348Hz confirm the assignments of the peaks at (δ -97ppm) and (δ -38ppm), as being the free phosphine and phosphine oxide respectively. The other peaks present show doublet couplings of 378Hz, (δ -92ppm), 394Hz (δ -90ppm), and 360Hz, (δ -63ppm). All of these values are consistent with metal bound PMe_2H ligands.

In addition to this all of the peaks in the proton coupled spectrum exhibit poorly resolved septet couplings to the methyl protons with $^2J_{PH}$ values in the order of 12Hz. The table below, (Table 2.13) summarises the nmr data obtained at room temperature.

Table 2.13 : The room temperature nmr parameters for the reaction of PMe_2H with $[Os_3(CO)_{10}(MeCN)_2]$ in dichloromethane

δP (ppm)	$^1J_{PH}$ (Hz)	Multiplicity	Assignment
-97	191	Doublet of Septets	Free PMe_2H
-92	378	Doublet of Septets	Cluster bound PMe_2H
-90	394	Doublet of Septets	Cluster bound PMe_2H
-63	360	Doublet of Septets	Cluster bound PMe_2H
-38	348	Doublet of Septets	$OPMe_2H$

The tube was then warmed to 333K for 2 hours and the $^{31}P\{^{1}H\}$ nmr spectrum recorded, once more at 213K. This spectrum showed the presence of an additional peak at (δ -27ppm). The proton coupled ^{31}P nmr spectrum showed no $^{1}J_{PH}$ coupling present for the new species, only a septet coupling with a $^{2}J_{PH}$ value of 13Hz. The temperature of the probe was then lowered to 213K in an attempt to resolve the broad peaks present at (δ -92ppm) and (δ -90ppm). The $^{31}P\{^{1}H\}$ nmr spectrum showed that these peaks resolved into three separate peaks at (δ -95ppm), (δ -92ppm), and (δ -90ppm). None of the other resonances present showed any change at this temperature.

The proton coupled ^{31}P nmr spectrum showed doublet couplings for all three of these peaks with $^{1}J_{PH}$ values of approximately 380Hz. The table below, (Table 2.14) summarises the nmr parameters obtained for this reaction.

Table 2.14 : The low temperature nmr parameters for the reaction of PMe_2H with $[Os_3(CO)_{10}(MeCN)_2]$ in dichloromethane

δP (ppm)	$^{1}J_{PH}$ (Hz)	Multiplicity	Assignment
-97	191	Doublet of Septets	Free PMe_2H
-95	378	Doublet of Septets	Cluster bound PMe_2H
-92	375	Doublet of Septets	Cluster bound PMe_2H
-90	394	Doublet of Septets	Cluster bound PMe_2H
-63	360	Doublet of Septets	Cluster bound PMe_2H
-38	348	Doublet of Septets	$OPMe_2H$
-27	-	Septet	PMe_2H Bridge

From the nmr evidence available the resonances present have been assigned as follows; The broad peaks at (δ -92ppm) and (δ -90ppm) have been assigned to the 1,2 substituted cluster $[Os_3(CO)_{10}(PMe_2H)_2]$, (14). The peak at (δ -63ppm) has been assigned to the *mono* substituted cluster $[Os_3(CO)_{11}(PMe_2H)]$, (15).

The peak present at (δ-27ppm) has been assigned to a phosphinidene-bridged species, although at this time it is impossible to say whether the bridge is inter- or intramolecular in nature. However, for steric reasons it is more likely that the bridged species will be intramolcular in nature, therefore this species has been tentatively assigned as $[Os_3(CO)_{10}(\mu_2\text{-}H)(\mu_2\text{-}PMe_2)]$, (16). The proposed structures of these species are given below, (FIG 2.12).

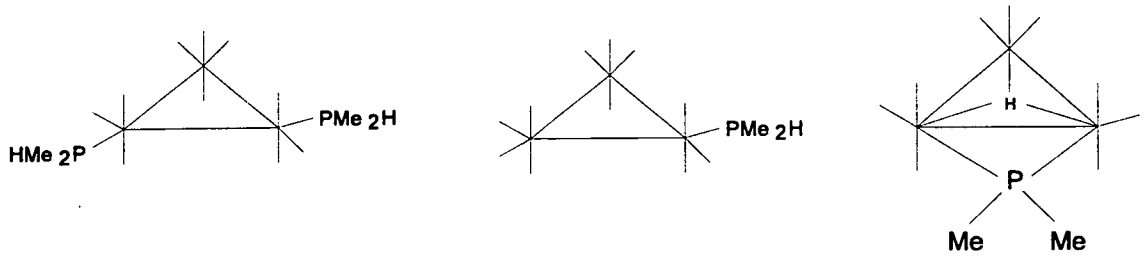

(14) (15) (16)

Figure 2.12 : The Proposed Structures Of $[Os_3(CO)_{10}(PMe_2H)_2]$, (14), $[Os_3(CO)_{11}(PMe_2H)]$, (15) And $[Os_3(CO)_{10}(\mu_2\text{-}H)(\mu_2\text{-}PMe_2)]$, (16).

The nmr tube containing the products was then broken open under N_2 and the mixture separated by tlc, eluent 60% n-hexane, 40% dichloromethane. The ir and mass spectra of these complexes were taken, the results of which are summarised in the table below, (Table 2.15).

Table 2.15 : The ir and mass spectral parameters for the reaction of PMe_2H with $[Os_3(CO)_{10}(MeCN)_2]$

tlc band #	Mass spectrum (Obs/Calc)	ir (νCO/cm^{-1}) (dichloromethane)	Assignment
1	975/974	2106.4 (w), 2084.8(w), 2068.2(m), 2053.3(m), 2038.4(m), 2024.4(s), 1997.8(s), 1974.0(w)	$[Os_3(CO)_{10}(PMe_2H)_2]$ (14)
2	940/940	2107.4(w), 2067.8(w), 2053.0(s), 2031.3(m), 2017.5(s), 2001.8(w), 1984.2(w), 1974.0(w)	$[Os_3(CO)_{11}(PMe_2H)]$ (15)
3	914/912	2101.4(w), 2067.9(m), 2056.0(s), 2047.5(m), 2033.3(m), 2016.0(s), 2003.9(w), 1985.7(w)	$[Os_3(CO)_{10}(\mu_2\text{-}H)(\mu_2\text{-}PMe_2)]$ (16)

Specific nmr studies coupled with the ir and mass spectral data allows the assignment of individual products to the observed resonances.

The broad resonances present at (δ -92ppm) and (δ -90ppm) have been confirmed as arising from the 1,2 substituted cluster $[Os_3(CO)_{10}(PMe_2H)_2]$, (14). The resonance present at (δ -63ppm) has been attributed to the *mono* substituted cluster $[Os_3(CO)_{11}(PMe_2H)]$, (15).

The mass spectral data has confirmed that the bridged species is intramolecular in nature. The ^1H nmr spectrum shows the presence of a metal hydride on this species. This shows as a doublet resonance at (δ -18.5ppm), with a $^2J_{PH}$ value of 18.5Hz. On the basis of this data it has been confirmed that the peak present at (δ -63ppm) arises from the phosphinidene bridged cluster, $[Os_3(CO)_{10}(\mu_2\text{-}H)(\mu_2\text{-}PMe_2)]$, (16).

The Reaction of $P(i\text{-}Pr)_2H$ with $[Os_3(CO)_{10}(MeCN)_2]$:

The nmr tube containing the reactants was left at room temperature for 24 hours, after which time the $^{31}P\{^1H\}$ nmr spectrum was recorded, this showed that no reaction had occurred. The tube was then heated to 333K for two hours and the nmr spectrum rerecorded. This spectrum showed a mixture of products, all previously observed, attributable to the reactions of $P(i\text{-}Pr)H_2$ and $P(i\text{-}Pr)_3$ with $[Os_3(CO)_{10}(MeCN)_2]$. It is evident from this that the phosphine has undergone disproportionation, to form the primary and tertiary isopropyl phosphine derivatives.

A pure sample of $P(i\text{-}Pr)_2H$ was then subjected to heating to 333K for two hours and the ^{31}P nmr spectrum recorded. This showed the same disproportionation had occurred. It has been concluded that this phosphine is thermally unstable in solution, and given its lack of reaction at room temperature, unsuitable for this cluster study.

The Reaction of PEt_2H with $[Os_3(CO)_{10}(MeCN)_2]$:

The nmr tube containing the reactants was left at room temperature for 24 hours after which time the $^{31}P\{^1H\}$ nmr spectrum was run. This spectrum showed no indication that any phosphorus bearing species was present in solution. The reaction was repeated, again showing no phosphine present in the tube after 24 hours. In both cases the tube contained an insoluble yellow powder, commonly observed after phosphine decomposition has occurred. The precipitate was insoluble in all common solvents and is assumed to be some form of polymeric $(PEtH)_n$ species. It has been concluded that this phosphine is unstable in the presence of triosmium clusters in solution, and is therefore unsuitable for use in cluster related studies.

The reaction of PPh_2H with $[Os_3(CO)_{10}(MeCN)_2]$:

The nmr tube was left at room temperature for 24 hours, after which time the $^{31}P\{^1H\}$ nmr spectrum was recorded, this showed that no reaction had occurred. The tube was then heated to 333K for 2 hours, and the $^{31}P\{^1H\}$ nmr spectrum rerun.

The spectrum showed five peaks at room temperature at (δ-40ppm), (δ-38ppm), (δ-36ppm), (δ+21ppm) and (δ+51ppm). The peak at (δ-40ppm) has been assigned as free PPh_2H on the basis of its chemical shift, and the peak at (δ+21ppm) has been assigned as $OPPh_2H$, once more on the basis of its chemical shift. The resonance at (δ-38ppm) is broad, suggesting an exchange system.

The proton coupled ^{31}P nmr spectrum was then recorded. The peaks at (δ-38ppm) and (δ-36ppm) both showed doublet couplings with $^1J_{PH}$ values of 380Hz, although the value for the resonance at (δ-38ppm) is approximate due to the broad nature of the peak. The peaks at (δ-40ppm) and (δ+21ppm) both showed doublet couplings with $^1J_{PH}$ values of 214Hz and 480Hz respectively, confirming their assignment as free phosphine and phosphine oxide. The resonance at (δ+51ppm) did not exhibit any $^1J_{PH}$ coupling. There were no $^3J_{PH}$ couplings observed to the ortho protons on the phenyl groups for any of the peaks. On the basis of this data the peaks at (δ-38ppm) and (δ-36ppm) have been assigned as cluster bound PPh_2H units and the peak at (δ+51ppm) has been assigned as a PPh_2 bridge. It is impossible to say at this time whether the bridging ligand forms an inter- or intramolecular bridge. The table overleaf, (Table 2.16), summarises the nmr data obtained.

Table 2.16 : The room temperature nmr parameters for the reaction of PPh_2H with $[Os_3(CO)_{10}(MeCN)_2]$ in dichloromethane			
δP (ppm)	$^1J_{PH}$ (Hz)	Multiplicity	Assignment
-40	214	Doublet	Free PPh_2H
-38	380	Doublet	Cluster bound PPh_2H
-36	380	Doublet	Cluster bound PPh_2H
+21	480	Doublet	$OPPh_2H$
+51	-	Singlet	PPh_2 Bridge

The probe temperature was then lowered to 213K, and the $^{31}P\{^1H\}$ nmr spectrum recorded. This showed the resonance at (δ-38ppm) splitting into three separate peaks at (δ-39ppm), (δ-38ppm) and (δ-37ppm), none of the other peaks showed any change at this temperature.

The proton coupled $^{31}P\{^1H\}$ nmr spectrum was then recorded, showing doublet couplings for all three of the peaks involved in the exchanging system with $^1J_{PH}$ values of 387Hz, 380Hz and 390Hz respectively. The table below, (Table 2.17), summarises the low temperature nmr data obtained.

Table 2.17: The low temperature nmr parameters for the reaction of PPh_2H with $[Os_3(CO)_{10}(MeCN)_2]$ in dichloromethane			
δP (ppm)	$^1J_{PH}$ (Hz)	Multiplicity	Assignment
-40	214	Doublet	Free PPh_2H
-39	387	Doublet	Cluster bound PPh_2H
-38	380	Doublet	Cluster bound PPh_2H
-37	390	Doublet	Cluster bound PPh_2H
-36	380	Doublet	Cluster bound PPh_2H
+21	480	Doublet	$OPPh_2H$
+51	-	Singlet	PPh_2 Bridge

On the basis of this data the peak at (δ-38ppm) has been assigned as the 1,2 substituted cluster $[Os_3(CO)_{10}(PPh_2H)_2]$, (17). The resonance at (δ-36ppm) has been assigned as the *mono* substituted cluster $[Os_3(CO)_{110}(PPh_2H)]$, (18), presumably derived from a small amount of $[Os_3(CO)_{11}(MeCN)]$ contaminating the starting material. The resonance present at (δ+51ppm) has been tentatively assigned as the bridged species $[Os_3(CO)_{10}(\mu_2\text{-}H)(\mu_2\text{-}PPh_2)]$, (19). The proposed structures of these complexes are given below (FIG 2.13).

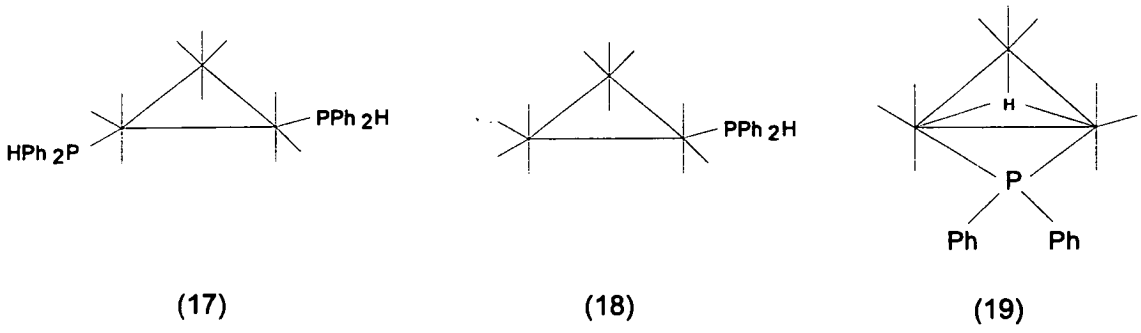

(17) (18) (19)

Figure 2.13 : the Proposed Structures of $[Os_3(CO)_{10}(PPh_2H)_2]$ (17), $[Os_3(CO)_{11}(PPh_2H)]$ (18) and $[Os_3(CO)_{10}(\mu_2\text{-}H)(\mu_2\text{-}PPh_2)]$ (19).

The nmr tube containing the products was then broken open and the mixture separated by tlc, eluent 60% dichloromethane/40% n-hexane. The ir and mass spectra of these products were then recorded. The results of these studies are summarised below, (Table 2.18).

Table 2.18 : The ir and mass spectral parameters for the reaction of PPh_2H with $[Os_3(CO)_{10}(MeCN)_2]$

tlc band #	Mass spectrum (Obs/Calc)	ir (νCO/cm^{-1}) (dichloromethane)	Assignment
1	1220/1222	2087.3(w), 2067.9(w), 2029.9(m), 2008.2(s), 2002.2(m), 1966.1(m), 1951.2(w)	$[Os_3(CO)_{10}(PPh_2H)_2]$ (17)
2	1065/1063	2092.7(w), 2067.7(m), 2054.3(m),2032.1(m), 2017.9(s), 1991.2(w)	$[Os_3(CO)_{11}(PPh_2H)]$ (18)
3	1035/1035	2108.2(m), 2067.9(m), 2054.9(s), 2034.0(s), 2019.3(s), 1987.1(m), 1976.3(w)	$[Os_3(CO)_{10}(\mu_2\text{-}H)(\mu_2\text{-}PPh_2)]$ (19)

Study of the isolated products by nmr, coupled with the mass spectral and ir data allows full assignment of the resonances in the nmr spectrum to individual products.

The exchange system observed at (δ -38ppm) has been assigned to the 1,2 substituted cluster, (17). The *mono* substituted product, (18), has been assigned to the peak at (δ -36ppm). The bridged species, (19), has been assigned to the resonance present at (δ +51ppm). From the mass spectral data it can be seen that the bridge involved is intramolecular in nature.

The reaction of PMe_3 with $[Os_3(CO)_{10}(MeCN)_2]$:

The nmr tube containing the reactants was left at room temperature for 24 hours, after which time the $^{31}P\{^1H\}$ nmr spectrum was recorded. This showed that no reaction had occurred. The tube was then heated to 333K for two hours, after which time the $^{31}P\{^1H\}$ nmr spectrum was rerecorded, showing that reaction had occurred.

The spectrum showed 3 resonances at (δ -62ppm), (δ -54ppm), and (δ -51ppm) with the resonance at (δ -62ppm) being assigned as free PMe_3 on the basis of its chemical shift. The resonance present at (δ -62ppm) was broad and ill defined, suggesting that some form of exchange was taking place.

The proton coupled ^{31}P nmr spectrum was recorded, showing poorly defined ten line pattern for all of the peaks with $^2J_{PH}$ values of approximately 14Hz. On the basis of this data the peaks at (δ -54ppm) and (δ -51ppm) have been assigned as cluster bound PMe_3 groups. The table below, (Table 2.19) summarises the room temperature nmr data obtained for this reaction.

Table 2.19 : The room temperature nmr parameters for the reaction of PMe_3 with $[Os_3(CO)_{10}(MeCN)_2]$ in dichloromethane

δP (ppm)	$^2J_{PH}$ (Hz)	Multiplicity	Assignment
-62	14	Dectet	Free PMe_3
-54	16	Dectet	Cluster bound PMe_3
-51	15	Dectet	Cluster bound PMe_3

The temperature of the probe was then lowered to 213K in an attempt to resolve the broad peak at (δ -54ppm) and the $^{31}P\{^{1}H\}$ nmr spectrum recorded. The resonance at (δ -54ppm) resolved into three peaks at (δ -57ppm), (δ -55ppm) and (δ -52ppm).

The proton coupled spectrum at this temperature once more showed dectet coupling with $^{2}J_{PH}$ values of the order of 15Hz. The table below, (Table 2.20) summarises the low temperature nmr data for this reaction.

Table 2.20 : The low temperature nmr parameters for the reaction of PMe_3 with $[Os_3(CO)_{10}(MeCN)_2]$ in dichloromethane

δP (ppm)	$^{2}J_{PH}$ (Hz)	Multiplicity	Assignment
-62	14	Dectet	Free PMe_3
-57	16	Dectet	Cluster bound PMe_3
-55	15	Dectet	Cluster bound PMe_3
-52	16	Dectet	Cluster bound PMe_3
-51	15	Dectet	Cluster bound PMe_3

From this data the broad resonance at (δ -54ppm) has been assigned as arising from the 1,2 substituted cluster $[Os_3(CO)_{10}(PMe_3)_2]$, (20). The resonance at (δ -51ppm) has been assigned as arising from the *mono* substituted cluster $[Os_3(CO)_{11}(PMe_3)]$, (21), this presumably arises from the presence of a small amount of $[Os_3(CO)_{11}(MeCN)]$ in the starting material. The proposed structures of these species are given overleaf (FIG 2.14).

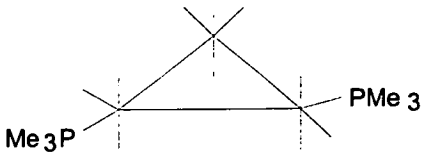

(20)

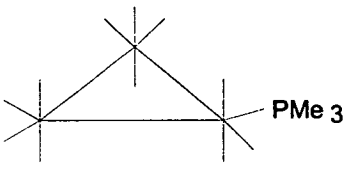

(21)

Figure 2.14 : The Proposed Structures Of $[Os_3(CO)_{10}(PMe_3)_2]$, (20), And $[Os_3(CO)_{11}(PMe_3)]$, (21)

The nmr tube containing the reactants was then broken open under a N_2 atmosphere, and the products were separated by tlc, eluent 60% dichloromethane/40% n-hexane. The table below, (Table 2.21) summarises the ir and mass spectroscopic data obtained.

Table 2.21 : The ir and mass spectral parameters for the reaction of PMe_3 with $[Os_3(CO)_{10}(MeCN)_2]$

tlc band #	Mass spectrum (Obs/Calc)	ir (νCO/cm^{-1}) (dichloromethane)	Assignment
1	1002/1002	2081.0(w), 2069.0(w), 2033.5(w), 2019.9(m), 2000.0(s), 1994.7(s), 1974.1(w), 1957.0(w)	$[Os_3(CO)_{10}(PMe_3)_2]$ (20)
2	954/954	2105.9(w), 2063.8(w), 2050.8(s), 2028.2(m), 2015.1(s), 1996.4(w), 1982.7(w), 1973.0(w)	$[Os_3(CO)_{11}(PMe_3)]$ (21)

Study of the isolated products by nmr, coupled with the mass spectral and ir data allows confirmation of the nmr assignment of the individual products.

The broad resonance at (δ -54ppm) is attributable to the 1,2 substituted cluster $[Os_3(CO)_{10}(PMe_3)_2]$, (20). The resonance at (δ -51ppm) is attributable to the *mono* substituted cluster $[Os_3(CO)_{11}(PMe_3)]$, (21).

The reaction of $P(i\text{-}Pr)_3$ with $[Os_3(CO)_{10}(MeCN)_2]$:

The nmr tube containing the reactants was left at room temperature for 24 hours, after which time the $^{31}P\{^1H\}$ nmr spectrum was recorded. This showed that no reaction had occurred. The tube was then warmed to 333K for 2 hours and the $^{31}P\{^1H\}$ nmr spectrum rerecorded This spectrum indicated that reaction had occurred.

The $^{31}P\{^1H\}$ nmr spectrum showed eight resonances, separated into two distinct groups, one set of three to low frequency at (δ +8ppm), (δ +13ppm) and (δ +20ppm). The high frequency set comprised five peaks at (δ +35ppm), (δ +40ppm), (δ +45ppm), (δ +48ppm) and (δ +53ppm). The lowest frequency peak, (δ +8ppm), has been assigned as free $P(i\text{-}Pr)_3$ on the basis of its chemical shift. The resonance at (δ +15ppm) is broad suggesting that some form of exchange is taking place.

The resonances occurring to high frequency have been assigned as arising from the presence of $OP(i\text{-}Pr)_3$ contaminant in the phosphine. The resonance at (δ +35ppm) has been assigned as free $OP(i\text{-}Pr)_3$ and the peaks to higher frequency as arising from the products of its reaction with the cluster.

The proton coupled ^{31}P nmr spectrum shows evidence of fine couplings to the proton on the tertiary carbon atom of the i-Pr group, however these are not well resolved at room temperature. The table overleaf, (Table 2.22), summarises the room temperature nmr data obtained.

Table 2.22 : The room temperature nmr parameters for the reaction of $P(i\text{-}Pr)_3$ with $[Os_3(CO)_{10}(MeCN)_2]$ in dichloromethane		
δP (ppm)	Multiplicity	Assignment
+8	Singlet	Free $P(i\text{-}Pr)_3$
+15	Singlet (Broad)	Cluster bound $P(i\text{-}Pr)_3$
+20	Singlet	Cluster bound $P(i\text{-}Pr)_3$
+35	Singlet	Free $OP(i\text{-}Pr)_3$
+40	Singlet	Cluster bound $OP(i\text{-}Pr)_3$
+45	Singlet	Cluster bound $OP(i\text{-}Pr)_3$
+48	Singlet	Cluster bound $OP(i\text{-}Pr)_3$
+53	Singlet	Cluster bound $OP(i\text{-}Pr)_3$

The high frequency resonances are well resolved at room temperature, presumably due to the large steric bulk of the phosphine oxide preventing ligand mobility. The resonances present at (δ +40ppm), (δ +45ppm) and (δ +48ppm) are distributed in a fashion similar to that seen for the 1,2 substituted clusters observed previously, except that this is resolved at ambient temperature. From this the system has been assigned as arising from the 1,2 substituted cluster $[Os_3(CO)_{10}(OP(i\text{-}Pr)_3)_2]$. The highest frequency peak, (δ +53ppm), has been assigned to the *mono* substituted cluster species $[Os_3(CO)_{11}(OP(i\text{-}Pr)_3)]$.

The probe was then cooled to 213K in an attempt to resolve the broad resonance at (δ +15ppm). At this temperature the resonance at (δ +15ppm) resolves into a three peak system, with resonances at (δ +10ppm), (δ +14ppm) and (δ +16ppm). The peak at (δ +20ppm) shows no change at this temperature. The resonances to high frequency showed no further resolution at this temperature.

The proton coupled ^{31}P nmr spectrum at low temperature allows the $^{2}J_{PH}$ couplings to be elucidated. For the resonances arising from $P(i\text{-}Pr)_3$ ligands bound to the cluster all of the peaks show quartet couplings with $^{2}J_{PH}$ values of 13-14Hz. The $OP(i\text{-}Pr)_3$ ligands bound to the cluster still show no resolvable couplings at this temperature. The table below, (Table 2.23) summarises the low temperature nmr data available for this reaction.

Table 2.23 : The low temperature nmr parameters for the reaction of $P(i\text{-}Pr)_3$ with $[Os_3(CO)_{10}(MeCN)_2]$ in dichloromethane

δP (ppm)	$^{2}J_{PH}$ (Hz)	Multilpicity	Assignment
+8	15	Quartet	Free $P(i\text{-}Pr)_3$
+10	13	Quartet	Cluster bound $P(i\text{-}Pr)_3$
+14	13	Quartet	Cluster bound $P(i\text{-}Pr)_3$
+16	13	Quartet	Cluster bound $P(i\text{-}Pr)_3$
+20	14	Quartet	Cluster bound $P(i\text{-}Pr)_3$
+35	-	Singlet	Free $OP(i\text{-}Pr)_3$
+40	-	Singlet	Cluster bound $OP(i\text{-}Pr)_3$
+45	-	Singlet	Cluster bound $OP(i\text{-}Pr)_3$
+48	-	Singlet	Cluster bound $OP(i\text{-}Pr)_3$
+53	-	Singlet	Cluster bound $OP(i\text{-}Pr)_3$

On the basis of this data the broad resonance present at (δ +15ppm) has been assigned as arising from the 1,2 substituted cluster, $[Os_3(CO)_{10}(P(i\text{-}Pr)_3)_2]$, (22). The peak at (δ +20ppm) has been assigned to the *mono* substituted cluster $[Os_3(CO)_{11}(P(i\text{-}Pr)_3)]$, (23). The high frequency resonances at (δ +40ppm), (δ +45ppm) and (δ +48ppm) have been assigned to the 1,2 substituted cluster $[Os_3(CO)_{10}(OP(i\text{-}Pr_3)_2]$, (24). The highest frequency resonance at (δ +532ppm) has been assigned to the *mono* substituted cluster $[Os_3(CO)_{11}(OP(i\text{-}Pr_3)]$, (25). The proposed structures of these species are shown below, (FIG 2.15).

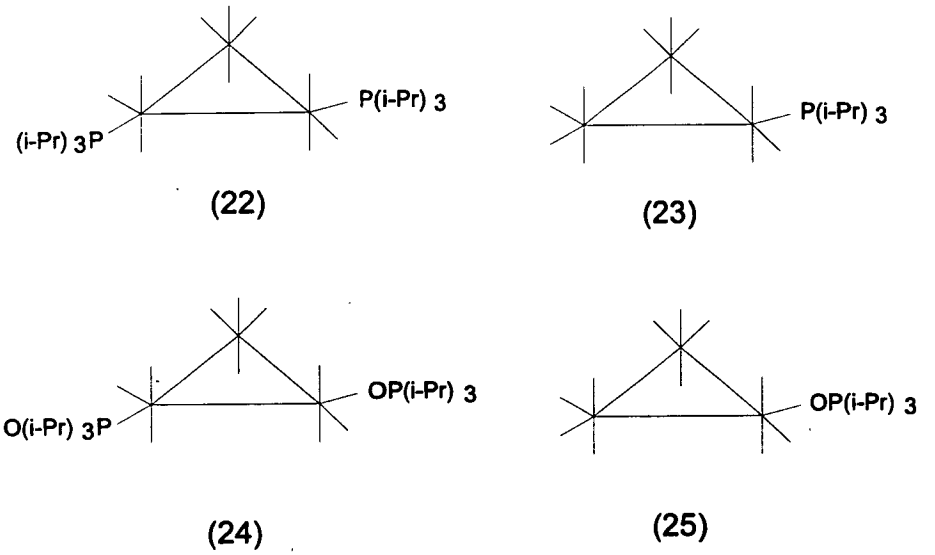

Figure 2.15 : The Proposed Structures Of $[Os_3(CO)_{10}(P(i\text{-}Pr)_3)_2]$, (22), $[Os_3(CO)_{11}(P(i\text{-}Pr)_3)]$, (23), $[Os_3(CO)_{10}(OP(i\text{-}Pr_3)_2]$, (24) And $[Os_3(CO)_{11}(OP(i\text{-}Pr_3)]$, (25)

The nmr tube containing the products was then broken open under N_2, and the products separated by tlc, eluent 60% dichloromethane/40% n-hexane. The ir and mass spectra of the products were recorded, these results are summarised on the table below, (Table 2.24).

Table 2.24 : The ir and mass spectral parameters for the reaction of $P(i\text{-}Pr)_3$ with $[Os_3(CO)_{10}(MeCN)_2]$

tlc band #	Mass spectrum (Obs/Calc)	ir (νCO/cm^{-1}) (dichloromethane)	Assignment
1	1202/1202	2095.9(w), 2067.6(m), 2034.1(m), 2017.7(s), 1996.3(m), 1981.6(m), 1964.9(m), 1955.4(w)	$[Os_3(CO)_{10}(OP(i\text{-}Pr_3)_2]$ (24)
2	1170/1170	2088.3(w), 2064.2(w), 2021.1(m), 1993.8(s), 1958.3(m), 1942.8(w)	$[Os_3(CO)_{10}(P(i\text{-}Pr_3)_2]$ (22)
3	1071/1070	2105.8(w), 2066.5(w), 2052.5(m), 2027.4(m), 2016.2(s), 1996.9(w), 1983.8(w)	$[Os_3(CO)_{11}(OP(i\text{-}Pr_3)]$ (25)
4	1040/1038	2103.5(w), 2064.2(w), 2051.7(m), 2026.2(m), 2015.6(s), 1995.3(w), 1978.6(w)	$[Os_3(CO)_{11}(P(i\text{-}Pr_3)]$ (23)

Study of the isolated products by nmr, coupled with the mass spectral and ir data allows full assignment of the resonances in the nmr spectrum to individual products.

The broad resonance at (δ +15ppm) has been assigned to the 1,2 substituted cluster $[Os_3(CO)_{10}(P(i\text{-}Pr_3)_2]$, (22). The resonance present at (δ +20ppm) has been assigned to the *mono* substituted cluster $[Os_3(CO)_{11}(P(i\text{-}Pr_3)]$, (23), this species is assumed to have formed from reaction with some $[Os_3(CO)_{11}(MeCN)]$ contaminant present in the starting material.

The high frequency resonances at (δ +40ppm), (δ +45ppm) and (δ +48ppm) have been assigned to the 1,2 substituted cluster $[Os_3(CO)_{10}(OP(i\text{-}Pr_3)_2]$, (24). The highest frequency resonance at (δ +53ppm) has been assigned to the *mono* substituted cluster $[Os_3(CO)_{11}(OP(i\text{-}Pr_3)]$, (25), this species is assumed to have formed from reaction with some $[Os_3(CO)_{11}(MeCN)]$ contaminant present in the starting material.

The Reaction of PEt_3 with $[Os_3(CO)_{10}(MeCN)_2]$:

The nmr tube containing the reaction mixture was left at room temperature for 24 hours, after which time the $^{31}P\{^1H\}$ nmr spectrum was recorded. This spectrum showed only the presence of free PEt_3 in solution. The tube was then warmed to 333K for two hours, after which time the nmr spectrum was recorded once more. This spectrum indicated that reaction had occurred.

The spectrum showed three peaks at (δ -20ppm), (δ -16ppm) and (δ -13ppm), with the resonance at (δ -20ppm) being assigned as free PEt_3 on the basis of its chemical shift. The resonance at (δ -16ppm) was broad, suggesting that some form of fluxional process was occurring.

The proton coupled ^{31}P nmr spectrum was recorded, showing significant broadening for all three peaks in the spectrum. This broadening is due to the large number of similar couplings present due to the ethyl groups, and is not easily resolved. On the basis of this data the peaks at (δ -16ppm) and (δ -13ppm) have been assigned as arising from cluster bound PEt_3 ligands. The table below, (Table 2.25) summarises the room temperature nmr data obtained for this reaction.

Table 2.25 : The room temperature nmr parameters for the reaction of PEt_3 with $[Os_3(CO)_{10}(MeCN)_2]$ in dichloromethane

δP (ppm)	$^2J_{PH}$ (Hz)	Multiplicity	Assignment
-20	-	Broad Singlet	Free PEt_3
-16	-	Broad Singlet	Cluster bound PEt_3
-13	-	Broad Singlet	Cluster bound PEt_3

The temperature of the probe was then lowered to 213K, with the intention of resolving the broad resonance at (δ -16ppm). This resonance resolved into three peaks at (δ -18ppm), (δ -17ppm) and (δ -14ppm). The other resonance present showed no change at this temperature.

The proton coupled ^{31}P nmr spectrum was recorded, once more showing broadening of all of the peaks present. the table below, (Table 2.26) summarises the low temperature nmr data obtained.

Table 2.26 : The low temperature nmr parameters for the reaction of PEt_3 with $[Os_3(CO)_{10}(MeCN)_2]$ in dichloromethane

δP (ppm)	$^2J_{PH}$ (Hz)	Multiplicity	Assignment
-20	-	Broad Singlet	Free PEt_3
-18	-	Broad Singlet	Cluster bound PEt_3
-17	-	Broad Singlet	Cluster bound PEt_3
-14	-	Broad Singlet	Cluster bound PEt_3
-13	-	Broad Singlet	Cluster bound PEt_3

On the basis of this data the broad resonance present at (δ -16ppm) has been assigned as the 1,2 substituted cluster $[Os_3(CO)_{10}(PEt_3)_2]$, (26). The peak at (δ -13ppm) has been assigned to the *mono* substituted cluster $[Os_3(CO)_{11}(PEt_3)]$, (27). This species is presumed to be derived from a small amount of $[Os_3(CO)_{11}(MeCN)]$ in the starting material. The proposed structures of these species are given overleaf, (FIG 2.16).

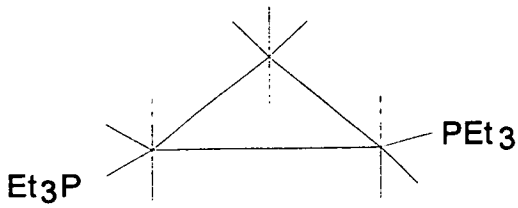

(26)

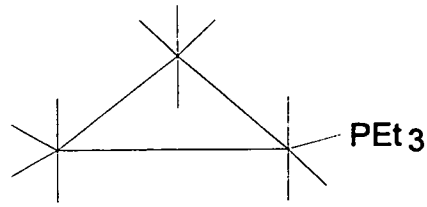

(27)

Figure 2.16 : The Proposed Structures Of $[Os_3(CO)_{10}(PEt_3)_2]$, (26), $[Os_3(CO)_{11}(PEt)_3)]$, (27)

The nmr tube containing the products was then broken open under N_2 and the mixture separated by tlc, eluent 60% dichloromethane/40% n-hexane. The ir and mass spectra of the products obtained were recorded. These results are summarised on the table below, (Table 2.27).

Table 2.27 : The ir and mass spectral parameters for the reaction of PEt_3 with $[Os_3(CO)_{10}(MeCN)_2]$

tlc band #	Mass spectrum (Obs/Calc)	ir (νCO/cm^{-1}) (dichloromethane)	Assignment
1	934/934	2105.8(w), 2051.9(s), 2028.7(m), 2016.0(s), 1982.7(w), 1967.7(w) νCN 2360.1(s), 2340.3(s)	Unreacted $[Os_3(CO)_{10}(MeCN)_2]$
2	1086/1086	2081.9(w), 2065.3(w), 2021.6(m), 1995.1(s), 1957.5(m), 1940.4(w)	$[Os_3(CO)_{10}(PEt_3)_2]$ (26)
3	997/996	2104.6(w), 2065.8(w), 2053.5(m), 2028.1(m), 2016.9(s), 1998.1(w), 1979.9(w)	$[Os_3(CO)_{11}(PEt_3)]$ (27)

Study of the isolated products by nmr, coupled with the mass spectral and ir data available allows full assignment of the resonances in the nmr spectrum to individual products.

The broad resonance at (δ -16ppm) has been assigned to the 1,2 substituted cluster $[Os_3(CO)_{10}(PEt_3)_2]$, (26). The resonance present at (δ -13ppm) has been assigned to the *mono* substituted cluster $[Os_3(CO)_{11}(PEt_3)]$, (27), this species is assumed to have formed from reaction with a small amount of $[Os_3(CO)_{11}(MeCN)]$ contaminant present in the starting material.

Summary

The following tables contain a summary of the nmr, ir and mass spectral data available for the species produced in this study, (Tables 2.28 and 2.29).

Table 2.28 : Collated ^{31}P nmr data for all complexes				
Complex	δP/ppm	Multiplicity	$^{1}J_{PH}$/Hz	$^{2}J_{PH}$/Hz
$[Os_3(CO)_{10}(PMeH_2)_2]$ (1)	-140	Triplet of Quartets	380	14
$[Os_3(CO)_{11}(PMeH_2)]$ (2)	-136	Triplet of Quartets	380	14
$[Os_3(CO)_{10}(\mu_2\text{-}H)(\mu_2\text{-}PMeH)]$ (3)	-70	Doublet of Quartets	416	14
$[Os_3(CO)_{10}(P(i\text{-}Pr)H_2)_2]$ (4)	-86	Triplet of Doublets	400	15
$[Os_3(CO)_{11}(P(i\text{-}Pr)H_2)]$ (5)	-84	Triplet of Doublets	398	15
$[Os_3(CO)_{10}(\mu_2\text{-}H)(\mu_2\text{-}P(i\text{-}Pr)H)]$ (6)	-5	Doublet of Doublets	412	13
$[Os_3(CO)_{10}(PEtH_2)_2]$ (7)	-111	Triplet	372	-
$[Os_3(CO)_{10}(\mu_2\text{-}H)(\mu_2\text{-}PEtH)]$ (8)	-35	Doublet	395	-
$[\{Os_3(CO)_{11}\}_2(\mu_2\text{-}PEtH)]$ (9)	-48	Doublet	367	-
$[Os_3(CO)_{10}(PPhH_2)_2]$ (10)	-112/-109	Triplet	374	-
$[Os_3(CO)_{11}(PPhH_2)]$ (11)	-108	Triplet	380	-
$[Os_3(CO)_{10}(\mu_2\text{-}H)(\mu_2\text{-}PPhH)]$ (12)	-35	Doublet	387	-
$[(Os_3(CO)_{11})_2(\mu_2\text{-}PPhH)]$ (13)	-56	Doublet	407	-
$[Os_3(CO)_{10}(PMe_2H)_2]$ (14)	-92/-90	Doublet of Septets	378/394	12
$[Os_3(CO)_{11}(PMe_2H)]$ (15)	-63	Doublet of Septets	360	12
$[Os_3(CO)_{10}(\mu_2\text{-}H)(\mu_2\text{-}PMe_2)]$ (16)	-27	Septet	-	13
$[Os_3(CO)_{10}(PPh_2H)_2]$ (17)	-38	Doublet	380	-
$[Os_3(CO)_{11}(PPh_2H)]$ (18)	-36	Doublet	380	-
$[Os_3(CO)_{10}(\mu_2\text{-}H)(\mu_2\text{-}PPh_2)]$ (19)	+61	Singlet	-	-
$[Os_3(CO)_{10}(PMe_3)_2]$ (20)	-54	Dectet	-	16
$[Os_3(CO)_{11}(PMe_3)]$ (21)	-51	Dectet	-	15
$[Os_3(CO)_{10}(P(i\text{-}Pr_3)_2]$ (22)	+15	Quartet	-	13
$[Os_3(CO)_{11}(P(i\text{-}Pr_3)]$ (23)	+20	Quartet	-	14
$[Os_3(CO)_{10}(OP(i\text{-}Pr_3)_2]$ (24)	+40/45/48	Singlet	-	-
$[Os_3(CO)_{11}(OP(i\text{-}Pr_3)]$ (25)	+53	Singlet	-	-
$[Os_3(CO)_{10}(PEt_3)_2]$ (26)	-16	Singlet	-	-
$[Os_3(CO)_{11}(PEt_3)]$ (27)	-13	Singlet	-	-

Table 2.29 : Collated mass spectral and ir data for all complexes		
Complex	Parent ion	νCO (cm^{-1}) in CH_2Cl_2
$[Os_3(CO)_{10}(PMeH_2)_2]$ (1)	947	2090.3(w), 2030.1(w), 2011.0(s), 2002.1(s), 1966.5(m),1956.3(m), 1931.3(m)
$[Os_3(CO)_{11}(PMeH_2)]$ (2)	926	2110.5(w), 2068.9(w), 2057.2(s), 2036.2(m), 2020.1(s), 1977.6(w)
$[Os_3(CO)_{10}(\mu_2\text{-}H)(\mu_2\text{-}PMeH)]$ (3)	898	2107.1(w), 2068.9(m), 2062.3(m),2039.7(m), 2023.5(s),2002.1(m), 1995.4(w)
$[Os_3(CO)_{10}(P(i\text{-}Pr)H_2)_2]$ (4)	1004	2088.5(w), 2029.9(s), 2010.5(s), 2001.2(s), 1965.6(m), 1955.2(w), 1930.3(w)
$[Os_3(CO)_{11}(P(i\text{-}Pr)H_2)]$ (5)	956	2108.3(w), 2067.8(w), 2055.8(s), 2034.0(m), 2018.6(s), 1975.6(w)
$[Os_3(CO)_{10}(\mu_2\text{-}H)(\mu_2\text{-}P(i\text{-}Pr)H)]$ (6)	925	2104.0(w), 2067.8(m), 2060.5(s), 2037.9(m), 2019.5(s), 1999.8(m), 1991.6(w)
$[Os_3(CO)_{10}(PEtH_2)_2]$ (7)	974	2088.3(w), 2060.8(w), 2029.6(m), 2006.5(s), 2000.9(s), 1965.3(m), 1952.7(w)
$[Os_3(CO)_{10}(\mu_2\text{-}H)(\mu_2\text{-}PEtH)]$ (8)	912	2103.9(w), 2076.9(m), 2067.7(m), 2060.5(s), 2052.1(m), 2020.0(s), 2002.5(w), 1990.0(m)
$[\{Os_3(CO)_{11}\}_2(\mu_2\text{-}PEtH)]$ (9)	N/A	N/A
$[Os_3(CO)_{10}(PPhH_2)_2]$ (10)	1071	2090.1(w), 2032.7(m), 2009.5(m), 2003.9(s), 1968.3(m), 1957.4(w), 1935.2(w)
$[Os_3(CO)_{11}(PPhH_2)]$ (11)	988	2095.0(w), 2067.8(m), 2056.2(m),2034.5(m), 2018.3(s), 1992.4(w)
$[Os_3(CO)_{10}(\mu_2\text{-}H)(\mu_2\text{-}PPhH)]$ (12)	960	2104.5(w), 2067.8(s), 2062.3(s), 2033.8(m), 2022.0(m), 1995.5(w), 1991.2(w)
$[(Os_3(CO)_{11})_2(\mu_2\text{-}PPhH)]$ (13)	N/A	N/A
$[Os_3(CO)_{10}(PMe_2H)_2]$ (14)	975	2106.4 (w), 2084.8(w), 2068.2(m), 2053.3(m), 2038.4(m), 2024.4(s), 1997.8(s), 1974.0(w)
$[Os_3(CO)_{11}(PMe_2H)]$ (15)	940	2107.4(w), 2067.8(w), 2053.0(s), 2031.3(m), 2017.5(s), 2001.8(w), 1984.2(w), 1974.0(w)
$[Os_3(CO)_{10}(\mu_2\text{-}H)(\mu_2\text{-}PMe_2)]$ (16)	914	2101.4(w), 2067.9(m), 2056.0(s), 2047.5(m), 2033.3(m), 2016.0(s), 2003.9(w), 1985.7(w)
$[Os_3(CO)_{10}(PPh_2H)_2]$ (17)	1220	2087.3(w), 2067.9(w), 2029.9(m), 2008.2(s), 2002.2(m), 1966.1(m), 1951.2(w)
$[Os_3(CO)_{11}(PPh_2H)]$ (18)	1065	2092.7(w), 2067.7(m), 2054.3(m),2032.1(m), 2017.9(s), 1991.2(w)
$[Os_3(CO)_{10}(\mu_2\text{-}H)(\mu_2\text{-}PPh_2)]$ (19)	1035	2108.2(m), 2067.9(m), 2054.9(s), 2034.0(s), 2019.3(s), 1987.1(m), 1976.3(w)

Table 2.29 (Continued) : Collated mass spectral and ir data for all complexes		
Complex	Parent ion	νCO (cm^{-1}) in CH_2Cl_2
$[Os_3(CO)_{10}(PMe_3)_2]$ (20)	1002	2081.0(w), 2069.0(w), 2033.5(w), 2019.9(m), 2000.0(s), 1994.7(s), 1974.1(w), 1957.0(w)
$[Os_3(CO)_{11}(PMe_3)]$ (21)	954	2105.9(w), 2063.8(w), 2050.8(s), 2028.2(m), 2015.1(s), 1996.4(w), 1982.7(w), 1973.0(w)
$[Os_3(CO)_{10}(P(i\text{-}Pr_3)_2]$ (22)	1170	2088.3(w), 2064.2(w), 2021.1(m), 1993.8(s), 1958.3(m), 1942.8(w)
$[Os_3(CO)_{11}(P(i\text{-}Pr_3)]$ (23)	1040	2103.5(w), 2064.2(w), 2051.7(m), 2026.2(m), 2015.6(s), 1995.3(w), 1978.6(w)
$[Os_3(CO)_{10}(OP(i\text{-}Pr_3)_2]$ (24)	1202	2095.9(w), 2067.6(m), 2034.1(m), 2017.7(s), 1996.3(m), 1981.6(m), 1964.9(m), 1955.4(w)
$[Os_3(CO)_{11}(OP(i\text{-}Pr_3)]$ (25)	1071	2105.8(w), 2066.5(w), 2052.5(m), 2027.4(m), 2016.2(s), 1996.9(w), 1983.8(w)
$[Os_3(CO)_{10}(PEt_3)_2]$ (26)	1086	2081.9(w), 2065.3(w), 2021.6(m), 1995.1(s), 1957.5(m), 1940.4(w)
$[Os_3(CO)_{11}(PEt_3)]$ (27)	997	2104.6(w), 2065.8(w), 2053.5(m), 2028.1(m), 2016.9(s), 1998.1(w), 1979.9(w)

Discussion

As previously noted the CO stretching frequency for $Ni(CO)_3P$ has been observed to vary with the pKa value of the attached phosphine, with νCO decreasing as the pKa value of the phosphine increases. This study allows a similar treatment to take place as the pKa values of the phosphines utilised ranges from -3.2 ($PMeH_2$) to +8.92 $P(i\text{-}Pr)_3$. The graphs overleaf illustrate the variation of νCO for the *mono* substituted clusters, $[Os_3(CO)_{11}P]$, (Graph 2.1), the disubstituted clusters, $[Os_3(CO)_{10}P_2]$, (Graph 2.2) and the bridged species, $[Os_3(CO)_{11}\mu\text{-}H\mu\text{-}P]$, (Graph 2.3). The stretching frequencies chosen represent the strongest peaks present in the spectra of the three types of system observed, these have been chosen as they are clear even in samples where there was a limited amount of complex avaialble.

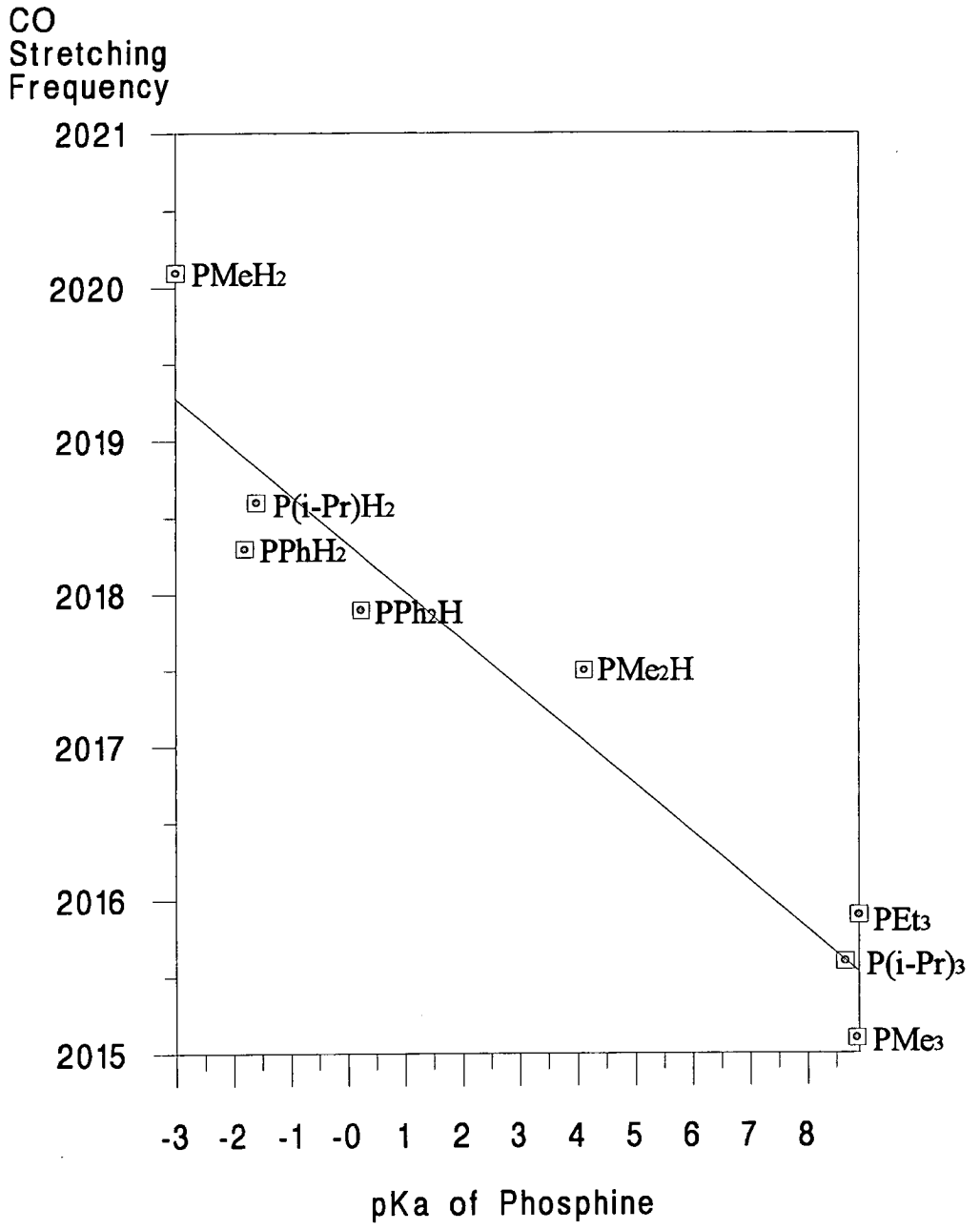

Graph 2.1 : Correlation between νCO and pKa of phosphine for $[Os_3(CO)_{11}P]$

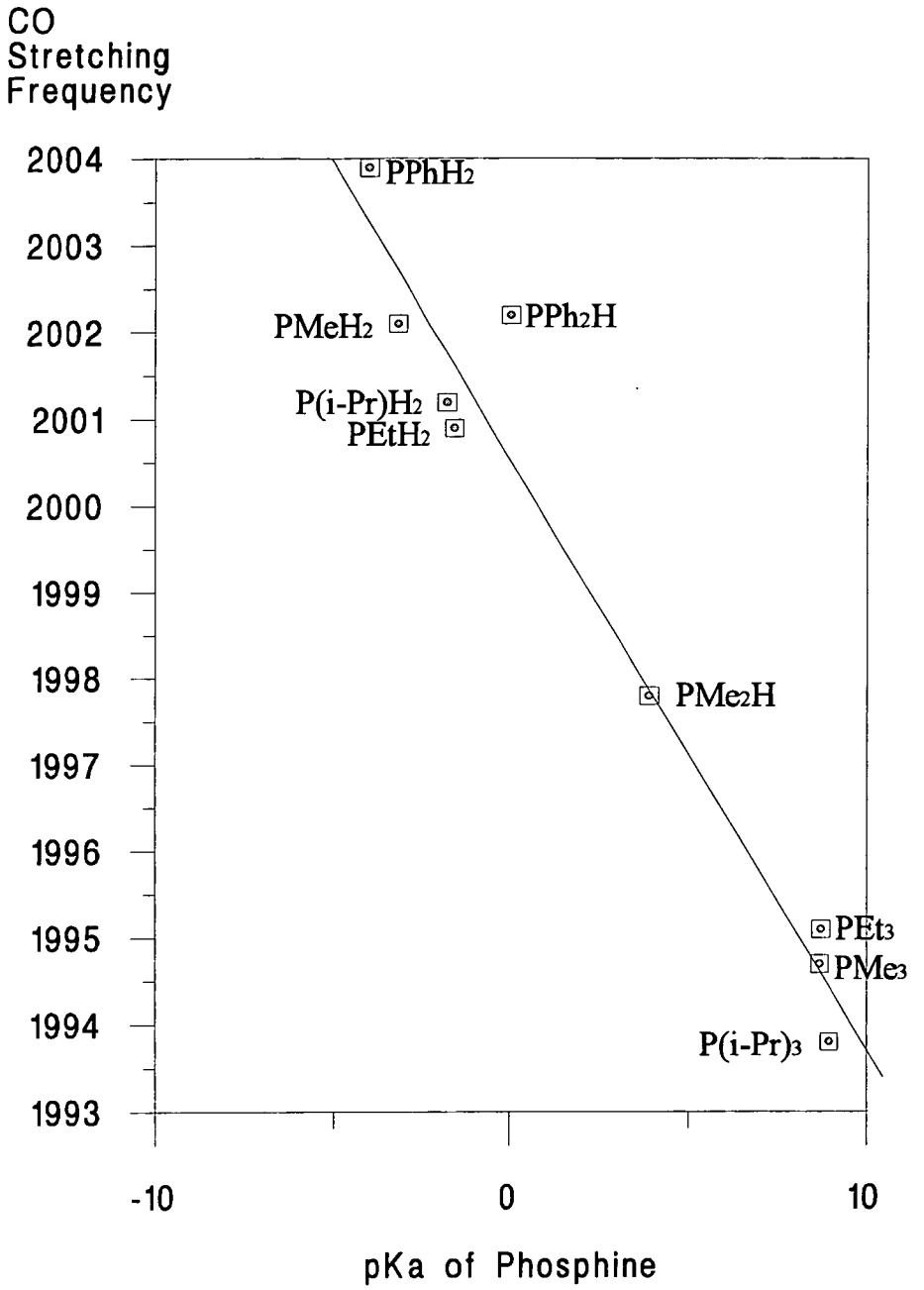

Graph 2.2 : Correlation between νCO and pKa of phosphine for $[Os_3(CO)_{10}P_2]$

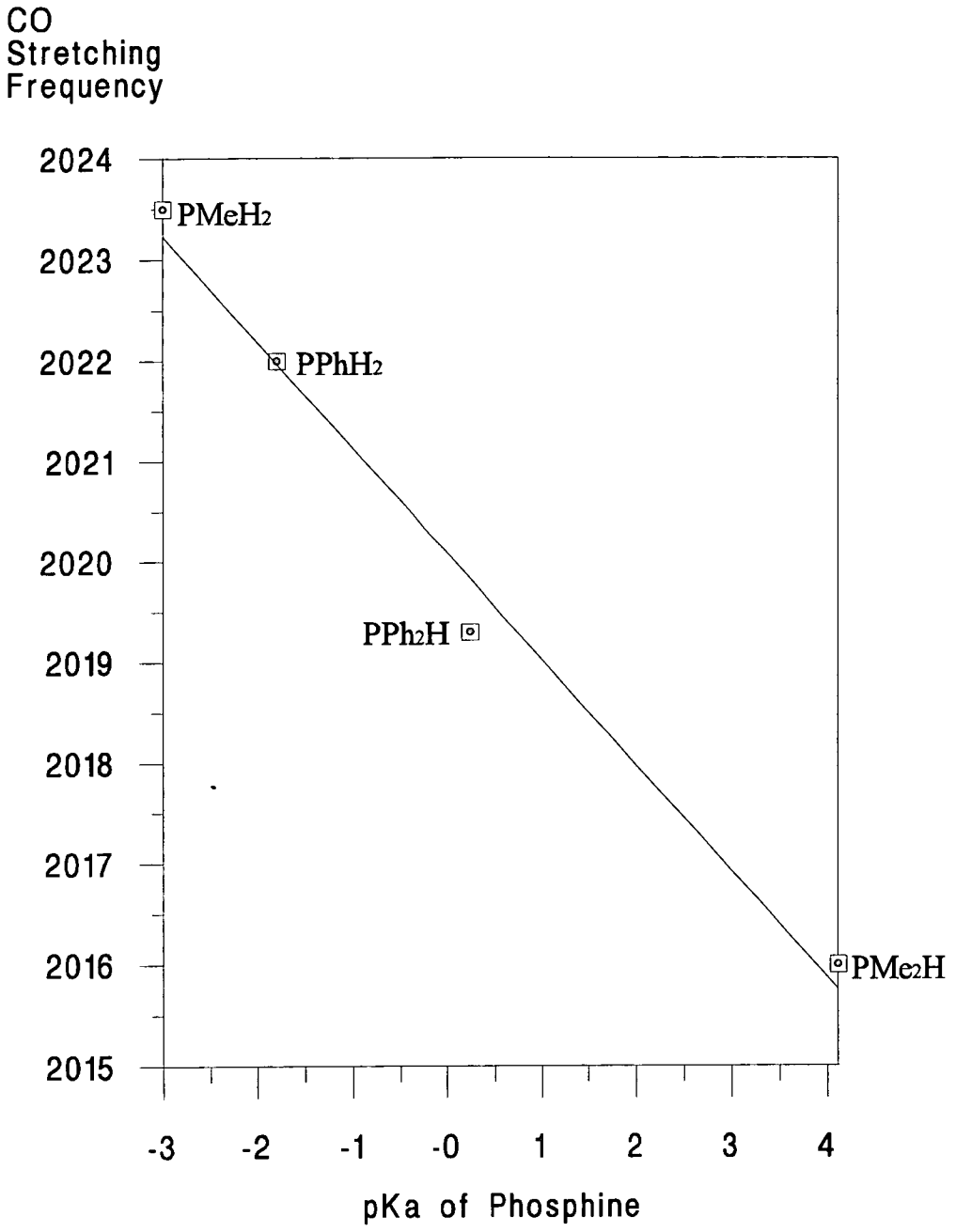

Graph 2.3 : Correlation between νCO and pKa of phosphine for $[Os_3(CO)_{10}(\mu_2\text{-}H)(\mu_2\text{-}P)]$

It can be seen from the graphs given above that the value of νCO decreases with increasing pKa values of the attached phosphines. This is a consequence of the increased electron donicity of the phosphine ligands causing the cluster to become more electron rich, and due to the nature of the synergic bond in the CO ligands attached to the cluster, the value of νCO decreases.

The reactivity of phosphines with triosmium clusters

The range of phosphines selected covers a wide range of pKa values and a wide range of Tolman cone angle values. Tolman[37] concluded that the reactivity of phosphines with $Ni(CO)_4$ to produce species of the type $Ni(CO)_{4-n}P_n$, (n = 1-4), was dictated not by the pKa of the phosphine ligand, but by the steric effect of the phosphine. Giering[38-41] has taken this further with his QALE studies, discussed in chapter one with the proposal of "steric thresholds", which dictate the maximum cone angle for reaction under ambient temperature conditions.

The phosphines under study demonstrate that this hypothesis may be extended to triosmium clusters. By examination of the reactivity of these phosphines at room temperature and at 333K, some idea of their ability to coordinate to a cluster in terms of pKa and cone angle may be gained. The table overleaf, (Table 2.30) summarises the reactivity of the phosphines along with pKa and cone angle data. The pKa values of the phosphines are defined as the dissociation constants of the conjugate acid derivatives of the phosphines and are taken as a measure of the σ donor ability of the phosphine.

Table 2.30 Summarised pKa, cone angle and reactivity data for the reactions of PRR'R'' with triosmium clusters

			Terminal coordination		Bridge formation	
Phosphine	pKa	Cone Angle (Degrees)	Ambient Temp	333K	Ambient Temp	333K
$PMeH_2$	-3.2	107*	NO	YES	NO	YES
PMe_2H	3.91	112*	YES	-	NO	YES
PMe_3	8.65	118	NO	YES	-	-
$P(i\text{-}Pr)H_2$	-1.8	120*	YES	-	NO	YES
$P(i\text{-}Pr)_2H$	N/A	N/A	NO	NO**	NO	NO**
$P(i\text{-}Pr)_3$	8.92	160	NO	YES	-	-
$PEtH_2$	-1.6	116*	YES	-	YES	-
PEt_2H	N/A	N/A	NO	NO**	NO	NO**
PEt_3	8.69	132	NO	YES	-	-
$PPhH_2$	-2	106	YES	-	YES	-
PPh_2H	0.03	126	YES	-	NO	YES

* = Calculated values
** = Decomposed at this temperature

It can be seen that the phosphines which react with the clusters at room temperature span a wide range of pKa values, (-2.0 → +3.91), but all have cone angles of less than or equal to 126°. There are two exceptions to this in $PMeH_2$ and PMe_3, both of which have cone angles of <120° but are at the extremes of pKa in the range studied, (-3.2 and +8.65 respectively).

The formation of bridged species at room temperature appears to be more sensitive to electronic rather than steric effects. Only $PEtH_2$ and $PPhH_2$ form bridged species at room temperature, even though the other primary and secondary phosphines which form terminally bound species at room temperature which fall in the lower end of the cone angle range do not.

These two phosphines fall into fairly narrow range of pKa range, (-1.7 → +0.03), suggesting that the formation of the bridged complexes $[Os_3(CO)_{10}\mu\text{-}H\mu\text{-}PRR']$ is sensitive to the pKa of the incoming ligand. The cone angles of these two phosphines are very similar, however PMe_2H which does not form a bridged species at room temperature has a cone angle of 112° which is lower than both of these.

PMe_2H, however has a pKa value of 3.91, which makes it significantly more basic than either of these two phosphines. This suggests that this is the factor which prohibits the formation of the bridge at room temperature in this case.

At the opposite end of this argument lies PPh_2H, which has a pKa value of 0.03, does not form a bridged complex at room temperature. This phosphine does however have a cone angle of 126°, which will cause the activation energy of bridge formation to lie above that available at room temperature.

It is clear from the evidence available that there is no single factor which dictates the reactivity of phosphines with triosmium clusters. However some degree of understanding has been reached by the reaction of a range of phosphines, spanning a wide range of pKa and cone angle values, with one basic cluster.

1 W. Heiber and H. Stallman, *Z. Electrochem, 1943, 49, 288.*

2 B. F. G. Johnson and J. Lewis, *Inorganic Synthesis, 1971, 13, 92.*

3 E. R. Corey and L. F. Dahl, *Inorg Chem, 1962, 1, 521.*

4 M. R. Churchill and B. G. DeBoer, *Inorg Chem, 1977, 16, 878.*

5 P. Rushman, G. N. van Buuren, M. Shirallan and R. K. Pomeroy, *Organometallics, 1983, 2, 693.*

6 C. R. Eady, B. F. G. Johnson and J. Lewis, *J. Chem Soc, Dalton Trans, 1975, 2606.*

7 A. J. Deeming, B. F. G. Johnson and J. Lewis, *J. Chem Soc, (A), 1970, 2697.*

8 K. A. Azam, C. Choo-Yin and A. J. Deeming, *J. Chem Soc, Dalton Trans, 1978, 1201.*

9 B. F. G. Johnson, J. Lewis and D. Pippard, *J. Orgmet, 1978, 145, C4.*

10 B. F. G. Johnson, J. Lewis and D. Pippard, *J. Chem Soc, Dalton Trans, 1981, 407.*

11 C. E. Anson, E. J. Ditzel, M. Fajardo, H. D. Holden, B. F. G. Johnson, J. Lewis, J. Puga and P. R. Raithby, *J. Chem Soc, Dalton Trans, 1984, 2723.*

12 M. Tachikawa and J. R. Shapley, *J. Orgmet, 1977, 124, C25.*

13 G. Suss-Fink, *Naturforsch, 1980, 35B, 454.*

14 A. J. Deeming, S. Donovan-Muunzi, S. E. Kabir and P. J. Manning, *J. Chem Soc, Dalton Trans, 1985, 1037.*

15 C. G. Pierpont, *Inorg Chem, 1978, 17, 1976.*

16 M. Tachikawa, J. R. Shapley, R. C. Haltiwanger and C. G. Pierpont, *J. Am Chem Soc, 1976, 98, 4651.*

17 A. J. Deeming, *J. Orgmet, 1977, 128, 63.*

18 A. J. Deeming, R. E. Kimber and M. Underhill, *J. Chem Soc, Dalton Trans, 1973, 2589.*

19 M. Tachikawa and J. R. Shapley, *J. Orgmet, 1977, 124, C19.*

20 A. J. Arce and A. J. Deeming, *J. Chem Soc, Dalton Trans, 1982, 1155.*

21 A. J. Deeming, M. B. Hursthouse, D. J. Backer-Dirks and I. P. Rothwell, *J. Chem Soc, Dalton Trans, 1981, 1879.*

22 A. M. Arif, T. A. Bright, D. E. Heaton, R. A. Jones and C. M. Dunn, *Polyhedron, 1990, 9, 1573.*

23 S. B. Colbran, B. F. G. Johnson, J. Lewis and R. M. Sorrell, *J. Orgmet, 1985, 296, C1.*

24 H. G. Ang, B. F. G. Johnson, W. L. Kwik, W. K. Leong, J. Lewis and P. R. Raithby, *J. Orgmet, 1990, 396, C43.*

25 S. B. Colbran, B. F. G. Johnson, F. J. Lahoz, J. Lewis and P. R. Raithby, *J. Chem Soc, Dalton Trans, 1988, 1199.*

26 F. Iwasaki, M. J. Mays, P. R. Raithby, P. L. Taylor and P. J. Wheatley, *J. Orgmet, 1981, 213, 185.*

27 K. Natarajan, L. Zsolani and G. Huttner, *J. Orgmet, 1981, 220, 365*

28 S. B. Colbran, B. F. G. Johnson, J. Lewis and R. M. Sorrell, *J. Chem Soc, Chem Comm, 1986, 525.*

29 C. J. Cardin, S. B. Colbran, B. F. G. Johnson, F. J. Lahoz and J. Lewis, *J. Chem Soc, Dalton Trans, 1988, 173.*

30 B. F. G. Johnson, J. Lewis, B. E. Reichert and K. T. Schorpp, *J. Chem Soc, Dalton Trans, 1976, 1403.*

31 R. E. Benfield, B. F. G. Johnson, P. R. Raithby and G. M. Sheldrick, *Acta Cryst, 1978, B34, 666.*

32 W Ehrenreich, M. Herberbold, H. P. Klein, G. Suss-Fink, U. Thewalt, *J. Orgmet, 1983, 248, 171.*

33 E. Band and E. L. Muetterities, *Chem Rev, 1978, 78, 639.*

34 B. F. G. Johnson, *"Transition Metal Clusters"*, Wiley-Interscience, 1980

35 A. J. Deeming, *Adv in Orgmet Chem, 1986, 26, 1.*

36 R. E. Benfield and B. F. G. Johnson, *Transition Met Chem, 1981, 6, 131.*

37 C. A. Tolman, *J. Am Chem Soc, 1970, 92, 2953.*

38 J. E. Belmonte, M. N. Golovin, M. Rahman and W. P. Giering, *Organometallics, 1985, 4, 1981.*

39 H. Y. Lui, A. Prock, M. Rahman and W. P. Giering, *Organometallics, 1987, 6, 650.*

40 K. Eriks, H. Y. Lui, A. Prock, M. Rahman and W. P. Giering, *Organometallics, 1989, 8, 1.*

41 K. Eriks, H. Y. Lui, A. Prock and W. P. Giering, *Organometallics, 1990, 9, 1758.*

CHAPTER THREE

STABILITY STUDIES ON $[Os_3(CO)_9(\mu_3\text{-}\eta^2\text{:}\eta^2\text{:}\eta^2\text{-}C_6H_6)]$

π-Arene complexes have a long history in the development of organometallic transition metal chemistry, with the first complexes isolated by Hein in 1919[1]. These complexes, $[Cr(\eta^6\text{-}C_6H_6)_2]$, $[Cr(\eta^6\text{-}C_6H_6)(\eta^6C_6H_5Ph)]$ and $[Cr(\eta^6\text{-}C_6H_5Ph)_2]$ were prepared by the treatment of anhydrous $CrCl_3$ with PhMgBr in diethyl ether. At that time they were recognised as the first organochromium species to be isolated but not as π-arene derivatives. This came in the 1950's, when a more systematic study was carried out by Fischer[2,3] and $[Cr(\eta^6\text{-}C_6H_6)_2]$ and $[Cr(\eta^6\text{-}C_6H_6)(CO)_3]$ were more fully characterised, primarily by ir spectroscopy. Many π-arene complexes are now known and several recent reviews[4-6] have described the diversity of binding modes and structures observed in these complexes. Following this pioneering work the structure and reactivity of π-arene complexes of the transition metals have been the subject of intensive study, both crystallographic and theoretical. Of the binding modes known, the most common is η^6-coordination as observed in the complexes $[Cr(\eta^6C_6H_6)_2]$ and $[Cr(\eta^6C_6H_6)(CO)_3]$, isolated and characterised by Hein and Fischer[1-3]. These complexes may be regarded as the forefathers of the numerous sandwich and half sandwich complexes observed for many transition metals.

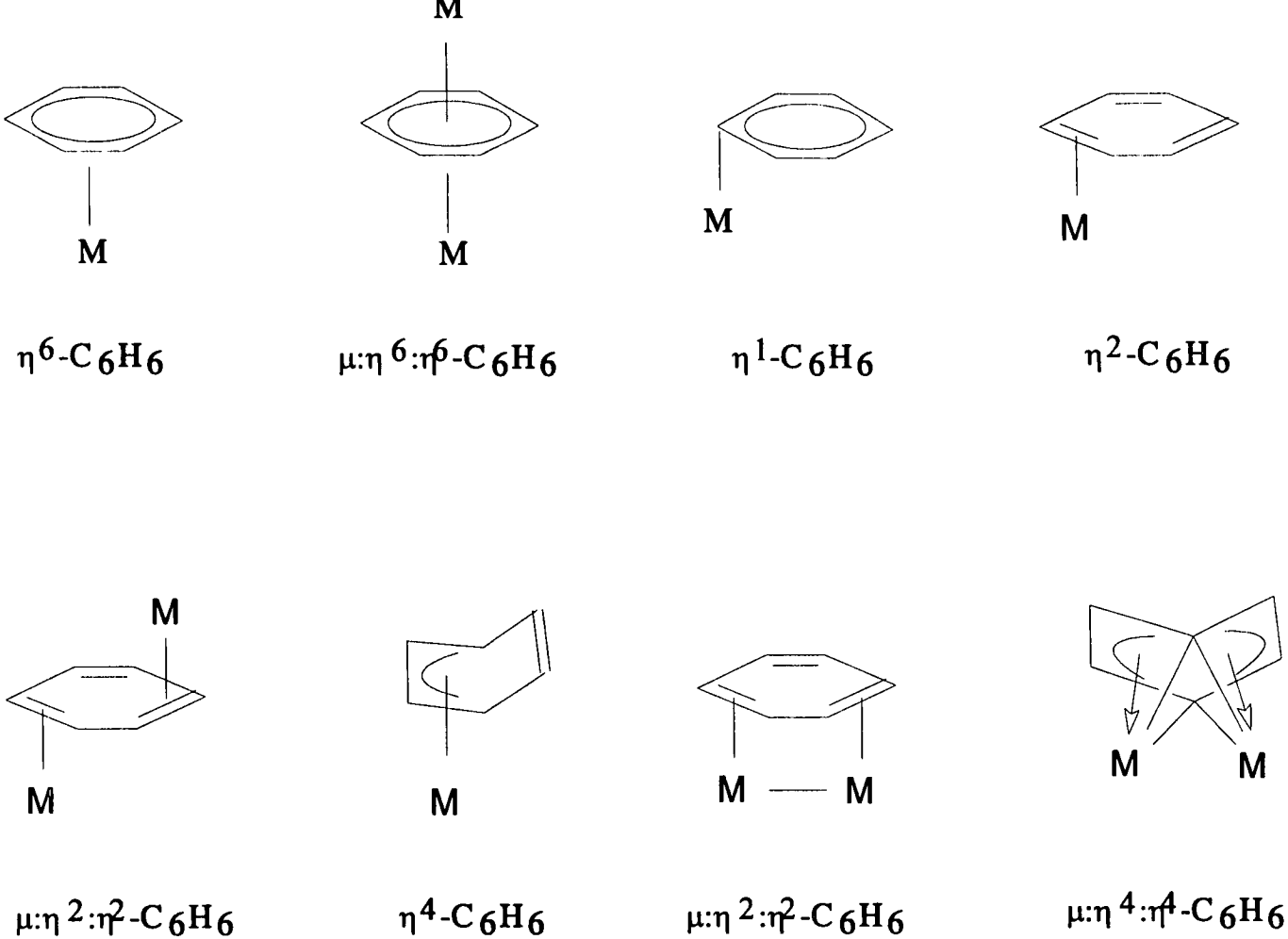

η^6-C_6H_6 μ:η^6:η^6-C_6H_6 η^1-C_6H_6 η^2-C_6H_6

μ:η^2:η^2-C_6H_6 η^4-C_6H_6 μ:η^2:η^2-C_6H_6 μ:η^4:η^4-C_6H_6

Figure 3.1 : Binding modes for π-Arene complexes on transition metal monomers and dimers.

The diagram above, (FIG 3.1), shows the diversity of binding modes and structure types known for π-arene transition metal complexes. The types of π-arene complexes considered here will involve only those with a 6 membered ring π-bonded to a transition metal, either as a monomer or as part of a metal cluster. In order to fully study the interaction of benzene with a metal cluster it is necessary to examine the binding of benzene to monomeric and dimeric metal species.

η^6 Arene binding :

The *bis* benzene species $[Cr(\eta^6\text{-}C_6H_6)_2]$ adopts an eclipsed structure with D_{6h} symmetry (FIG 3.2) in both solid and gas phases. The C-C bond lengths observed in this complex are longer than those of the free ligand by approximately 0.02Å, (1.420Å and 1.398Å respectively), but show little evidence of localised bonding in the benzene.

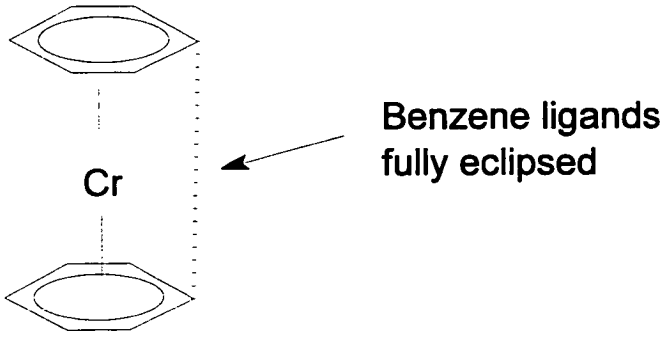

Figure 3.2 : the structure of $[Cr(\eta^6\text{-}C_6H_6)_2]$

The *mono* benzene complex, $[Cr(\eta^6\text{-}C_6H_6)(CO)_3]$, however, adopts a staggered rather than eclipsed structure (FIG 3.3), with C_{3v} symmetry. In this case the benzene ring shows a more significant distortion from the free ligand structure, with alternating long and short C-C bonds of 1.423Å and 1.406Å respectively (compared with an average C-C bond length of 1.398Å for free benzene). This distortion gives the benzene a bond localised cyclohexatriene structure rather than a delocalised aromatic bond system. The CO ligands in the molecule adopt a staggered configuration with the longer bonds being those which eclipse the CO ligands.

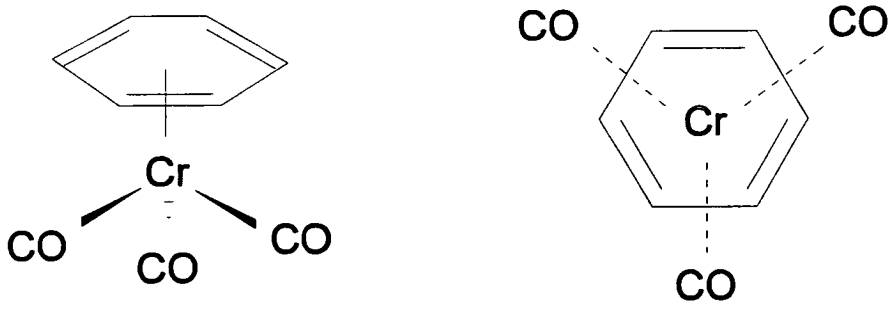

Figure 3.3 : The structure of $[Cr(\eta^6\text{-}C_6H_6)(CO)_3]$, showing staggered configuration

The isolation of benzene in an η^6-terminal binding mode on a ruthenium carbonyl carbide cluster[7,8] similar in structure to the $\eta^6\text{-}C_6H_6$ mode, above, shows that the apical site of a metal cluster can behave in an analogous fashion to an ML_3 fragment in this respect. Many other examples of η^6 coordination for arenes have also been observed in cluster chemistry[9-16], and show structural parallels to $[Cr(\eta^6\text{-}C_6H_6)(CO)_3]$ in terms of the benzene binding.

η^4 Arene binding :

The η^4 binding mode for has never been structurally characterised for benzene itself; however nmr data[17] for $[Os(\eta^6\text{-}C_6H_6)(\eta^4\text{-}C_6H_6)]$ clearly suggest the structure involves an η^4 π-bound benzene (FIG 3.4). In this case the η^4 binding site adopts a 1,3 butadiene type structure with the other 2 carbon atoms in the ring bent away from the metal.

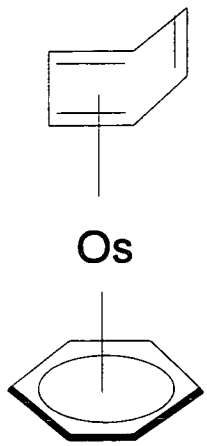

Figure 3.4 : The structure of $[Os(\eta^6\text{-}C_6H_6)(\eta^4\text{-}C_6H_6)]$

η^4 binding of arenes has also been observed in cyclotrimerisation reactions of acetylenes[18] with $[Ru(\eta^6\text{-}C_6H_6)(\eta^4\text{-}C_6H_8)]$. UV irradiation of $[Ru(\eta^6\text{-}C_6H_6)(\eta^4\text{-}C_6H_8)]$ in hexane solution in the presence of substituted acetylenes (RCCR) yields mixed π-arene complexes. These complexes have an η^6 benzene and the substituted arene formed by acetylene trimerisation bound in an η^4 mode.

X-ray study has identified η^4 binding for the perfluoro-hexamethylbenzene species $[Rh(C_9F_7H_6O_2)(\eta^4\text{-}C_6(CF_3)_6)]$[19]. The species is again formed by trimerisation of an acetylene, $(CF_3)CC(CF_3)$, and the crystal structure shows η^4 coordination geometry for the $C_6(CF_3)_6$ ligand. In this case the C_6 ring exhibits bond localisation, as previously observed. The ring is also distorted from planarity, with the η^4 binding unit acting as a 1,3 diene, and with a C_2 unit bent out of the ring plane by 42° away from the metal.

In all of the η^4 bound arene complexes observed the C_6 ring exhibits significant distortions with respect to the free species. The ring loses planarity as a C_2 unit is bent away from the metal, as shown in (FIG 3.4). The ring also exhibits extensive bond localisation with formal single and double C-C bonds being evident. The arene in these cases behaves in a diene like fashion, with the arene ring moving slightly off centre with respect to the η^6 binding mode.

η^2 Arene binding :

η^2 binding has been crystallographically characterised for perfluoro-hexamethylbenzene[20] and for anthracene[21]. In both of these cases the arene behaves in an olefinic fashion rather than as an aromatic ligand.

For the perfluoro-hexamethylbenzene case the species, $[Pt(PEt_3)_2(\eta^4\text{-}C_6(CF_3)_6)]$, has been structurally characterised, (FIG 3.5), showing η^2 binding for the C_6 ring. In this species the ring is highly distorted in that it suffers a significant loss of planarity, as well as extensive bond localisation.

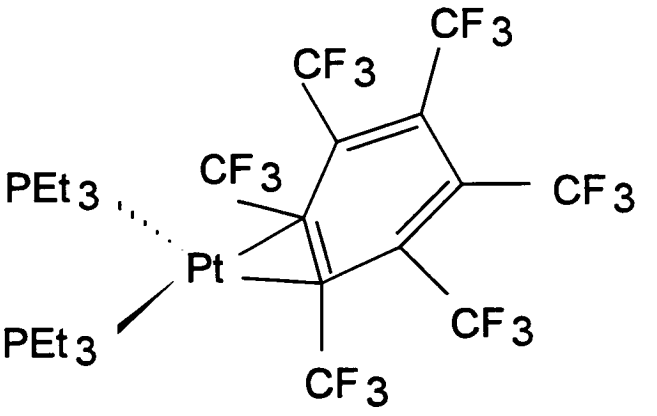

Figure 3.5 : The structure of $[Pt(PEt_3)_2(\eta^4\text{-}C_6(CF_3)_6)]$

The anthracene complex, $[Ni(PCy_3)_2C_{14}H_{10}]$, has one of the outer rings of the anthracene ligand bound in an η^2 fashion, behaving in an analogous fashion to ethylene. The anthracene ligand is distorted in this complex in that it exhibits a torsion of 12.3° around the C_6-C_5 ring junction. Also the bond lengths deviate significantly from the values for free anthracene. The bound ring fragment exhibits bond localisation similar in structure to a 1,3-butadiene moiety.

Benzene has also been observed acting as the bridging ligand in the multiple layer sandwich complex[22] $[(\eta^5\text{-}C_5H_5)V(\mu_2\text{-}\eta^6\text{-}C_6H_6)V(\eta^5\text{-}C_5H_5)]$. Once again the C_6 ring structure in this species shows significant bond localisation; however the ring remains essentially planar in this case. In the species $[\{(\eta^5\text{-}C_5H_5)VH\}_2(\mu_2\text{-}\eta^6\text{-}C_6H_6)]$[23], both of the metal atoms lie on the same side of the C_6 ring, causing a notable distortion from planarity, (FIG 3.6).

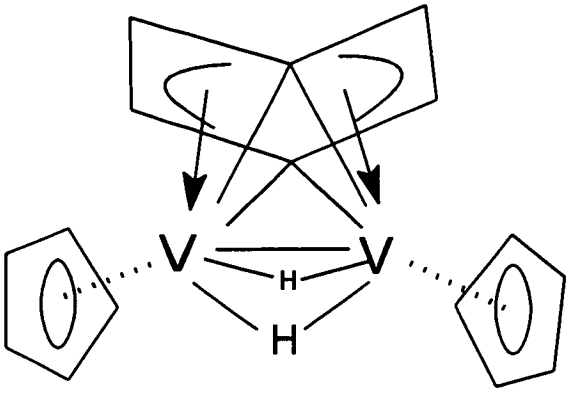

Figure 3.6 : The structure of $[(\eta^5\text{-}C_5H_5)V(\mu_2\text{-}\eta^6C_6H_6)V(\eta^5\text{-}C_5H_5)]$

Arenes as bridging ligands

Benzene has been observed acting as an $\eta^2:\eta^2$ bridge[24] in the rhenium species $[\{(\eta^5\text{-}C_5Me_5)Re(CO)_2\}_2(\mu_2\text{-}\eta^2:\eta^2\text{-}C_6H_6)]$. In this species the benzene shows no loss of planarity but exhibits significant bond localisation, appearing as a cyclohexatriene bridge rather than as an aromatic system, (FIG 3.7).

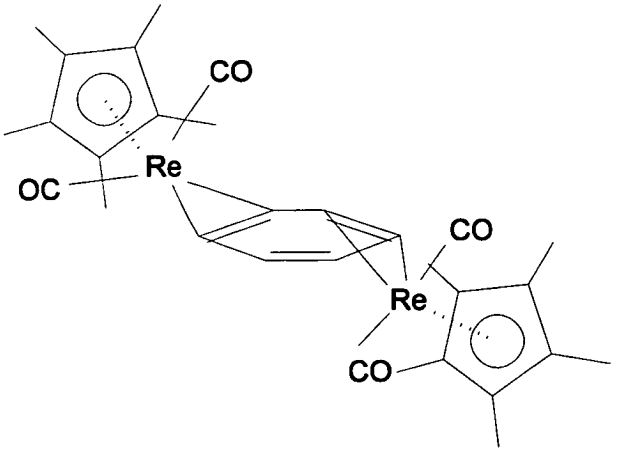

Figure 3.7 : The structure of $[\{(\eta^5\text{-}C_5Me_5)Re(CO)_2\}_2(\mu_2\text{-}\eta^2:\eta^2\text{-}C_6H_6)]$

Arene binding to metal clusters

The occurrence of η^6 binding modes on metal clusters is the most common observed to date. However the identification of a new face capping binding mode for benzene in metal clusters[25,26] has led to the opening of a new area of study. The species, $[Ru_6(CO)_{11}(C_6H_6)_2]$, first isolated in 1985[25,26], has benzene in a new type of binding mode. As well as an η^6 terminal binding mode on an apical site there is also a benzene ligand occupying a face capping position over a metal triangle. This new binding mode, in which the benzene ring is symmetrically placed over a ruthenium triangle in a μ_3-η^2:η^2:η^2 capping fashion has been crystallographically characterised and adopts the structure shown below, (FIG 3.8).

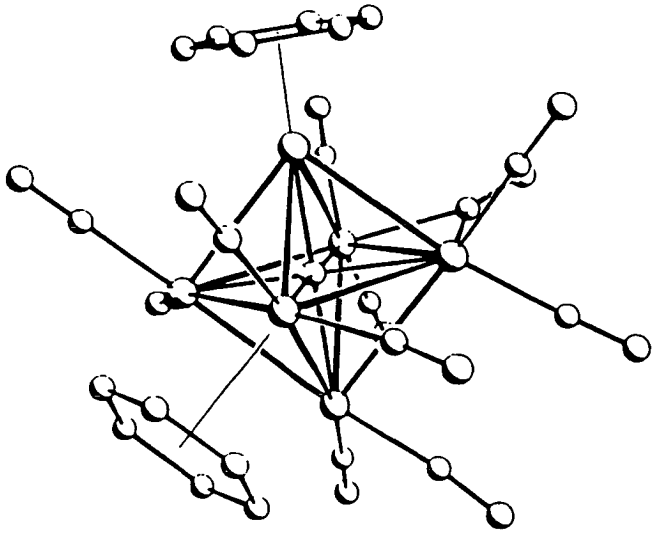

Figure 3.8 : The structure of $[Ru_6(CO)_{11}(C_6H_6)_2]$

The cluster $[Os_3(CO)_9(\mu_3\text{-}\eta^2\text{:}\eta^2\text{:}\eta^2\text{-}C_6H_6)]$ first reported in 1985[25,26] has been structurally characterised by X-ray diffraction. The benzene ligand is formed by stepwise dehydrogenation of a triply bridging cyclohexadienyl ligand. The benzene adopts an $\eta^2\text{:}\eta^2\text{:}\eta^2$ face capping mode similar to the hexaruthenium carbide cluster, above. The molecule has approximate C_{3v} symmetry, with the plane of the benzene carbon atoms skewed 1.1° with respect to the plane of the metal triangle. The C-C bond lengths alternate in a long and short fashion, with the 'coordinated' and 'non-coordinated' distances being 1.41Å and 1.51Å respectively. These bond distances indicate that the bound benzene ligand has a bond localised cyclohexatriene type structure, as shown below (FIG 3.9).

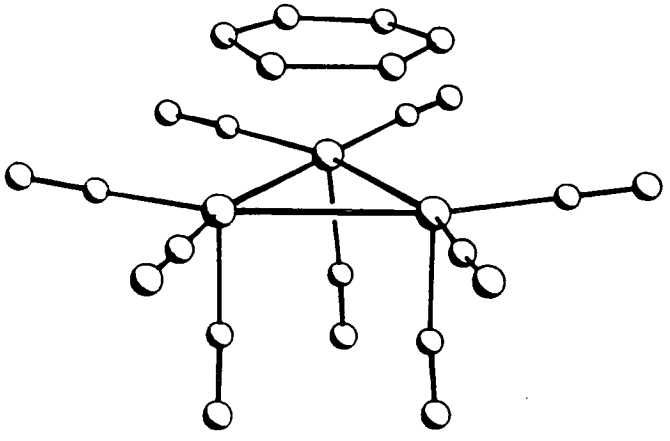

Figure 3.9 : The structure of $[Os_3(CO)_9(\mu_3\text{-}\eta^2\text{:}\eta^2\text{:}\eta^2\text{-}C_6H_6)]$

This species has been the subject of intensive study[26-29] in order to elucidate further the behaviour of face capping cluster bound arenes. This has involved activation of the cluster and a study of the behaviour of some of its derivatives. Investigations into the reactivity of the mono acetonitrile derivative of $[Os_3(CO)_9(\mu_3\text{-}\eta^2\text{:}\eta^2\text{:}\eta^2\text{-}C_6H_6)]$, $[Os_3(CO)_8(MeCN)(\mu_3\text{-}\eta^2\text{:}\eta^2\text{:}\eta^2\text{-}C_6H_6)]$, have shown that it will readily react with 2 electron donor ligands such as olefins, pyridenes, CO or phosphines. The complexes $[Os_3(CO)_8(\eta^2C_2H_4)(\mu_3\text{-}\eta^2\text{:}\eta^2\text{:}\eta^2\text{-}C_6H_6)]$ and $[Os_3(CO)_8(PPh_3)(\mu_3\text{-}\eta^2\text{:}\eta^2\text{:}\eta^2\text{-}C_6H_6)]$ have been characterised by X-ray study[26]. It has been observed for olefin and phosphine substituted derivatives of $[Os_3(CO)_9(\mu_3\text{-}\eta^2\text{:}\eta^2\text{:}\eta^2\text{-}C_6H_6)]$ that the benzene ligand on the cluster face exhibits a rotor like fluxional motion, with the carbon atoms in the benzene cycling in a 1,2 ring hopping motion. This motion has been defined by variable temperature ^{13}C and ^1H nmr studies[27,28] in solution and has also been observed in the solid state *via* Magic Angle Spinning nmr[27,28]. These studies have indicated a low energy barrier to rotation for the benzene (approx 48kJmol^{-1}) in the solution and solid states.

Binding of arenes to metal surfaces

This bonding mode for benzene is similar to one of the modes observed for arenes adsorbed on platinum metal surfaces[30-32]. Studies have also been carried out on coadsorbed mixtures of CO and benzene, on platinum metal surfaces, again showing structural parallels with cluster species[33,34]. This recognition of structural similarity between cluster surfaces and bulk metal surfaces has prompted the theory that a chemisorptive process may be described in terms of localised bonding between the adsorbate ligand and nearest neighbour surface metal atoms.

Observation of benzene bound to a metal surface by LEED studies[30-34] has shown that the benzene adopts a kekule type cyclohexatriene structure, with much longer average bond lengths than in free benzene (1.58±0.15Å and 1.39Å respectively). The kekule distortions show alternating long and short bond lengths of 1.64Å and 1.50Å respectively. These distortions are much more pronounced than those observed for the metal cluster bound benzene, above.

It has been observed[30,34] for benzene bound to platinum metal surfaces that at saturation coverage, (0.9 carbon atoms per metal atom), desorption of benzene occurs between 130°C and 220°C. Also above 220°C benzene decomposition into CH and C_2H fragments competes with desorption of benzene in a 1:1 ratio. Above 260°C, decomposition of benzene on the surface is the primary (>90%) process observed.

Reversible C-H bond breaking has also been observed for benzene on platinum metal surfaces[29]. C-H bond breaking has been observed for face capping cluster bound benzene molecules[35-37]; however there is no evidence that this process is reversible.

Study of the behaviour of surface bound benzene to substitution by tertiary phosphines[30] has shown that at saturation coverage, over 90% of the adsorbed benzene is displaced by trimethyl phosphine.

The formation of a π-bound face capping arene species on a metal cluster allows study of the bound molecule by spectroscopic methods previously unavailable for surface interactions, e.g. nmr. The intention of this work is to attempt to further clarify the relationship between benzene bound to metal clusters and surface bound species by pyrolysis and phosphine displacement studies.

Pyrolysis of $[Os_3(CO)_9(\mu_3\text{-}\eta^2\text{:}\eta^2\text{:}\eta^2\text{-}C_6H_6)]$:

A sample of $[Os_3(CO)_9(\mu_3\text{-}\eta^2\text{:}\eta^2\text{:}\eta^2\text{-}C_6H_6)]$ was placed in a pyrolysis bulb and attached to the vacuum line. The sample was pumped on at $10^{-6}\tau$ for 1 hour and removed from the line and its ir spectrum checked. There was no change observed in the sample over this time. The sample was then reattached to the line and pumped out. The spiral section was sealed off and the sample was heated to a temperature of 210°C at a rate of approximately 1°C/min. There was no evolution of gas observed over the period of heating. However as the temperature was raised above 150°C a yellow crystalline product sublimed out of the sample. The sample was then cooled to room temperature and the sublimate was isolated by cutting out the section of tubing on which it had formed. This mixture was separated by tlc, eluent 60% n-hexane, 40% dichloromethane, affording 2 products as described below.

The sublimate contained a mixture of $[Os_3(CO)_9(\mu_3\text{-}\eta^2\text{:}\eta^2\text{:}\eta^2\text{-}C_6H_6)]$ (90%) and $[H_2Os_3(CO)_9(\mu_3\eta^1\text{:}\eta^2\text{:}\eta^1\text{-}C_4H_6)]$ (10%), a benzyne derivative, (FIG 3.10). The benzyne species has previously been observed[29,35-37], and was identified by ir spectroscopy, $\nu CO(cm^{-1})$ = 2076(m), 2030(s), 1999(m), 1978(w), 1951(w) in dichloromethane. This benzyne derivative has also been observed as the product of the photolysis of $[Os_3(CO)_9(\mu_3\text{-}\eta^2\text{:}\eta^2\text{:}\eta^2\text{-}C_6H_6)]$, (13 hours, 500W tungsten heat lamp)[29].

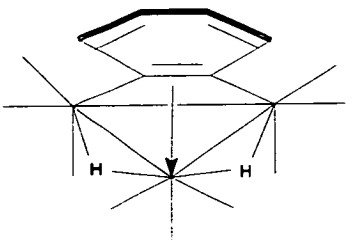

Figure 3.10 : The structure of $[H_2Os_3(CO)_9(\mu_3\text{-}\eta^1\text{:}\eta^2\text{:}\eta^1\text{-}C_4H_6)]$

It was then decided to repeat the reaction in a darkened vessel to ascertain whether the observed isomerisation was photochemical or thermal in nature. The above procedure for pyrolysis was repeated, except that the bulb and spiral section were surrounded with aluminium foil to prevent contributory photolysis influencing the reaction. After heating as before, no pressure increase was observed and the bulb was cooled to room temperature before removal of the foil. Once again a yellow crystalline product had sublimed out of the reaction mixture, which was isolated as before. This mixture was separated by tlc, eluent 60% n-hexane, 40% dichloromethane, again showing the same two products as seen previously, again in the ratio 9:1.

In order to further investigate the possibility of thermal isomerisation between the benzene and benzyne systems a sample of $[Os_3(CO)_9(\mu_3\text{-}\eta^2\text{:}\eta^2\text{-}C_6H_6)]$ was dissolved in toluene. The vessel was then surrounded with aluminium foil to remove any light source and the mixture was refluxed for 1 hour, allowing 2 hours for cooling before the foil was removed. The solvent was removed by placing the solution in a 250ml schlenk bulb and pumping on the sample to dryness, without heating. The resulting yellow crystalline product was then separated by tlc, eluent 60% n-hexane, 40% dichloromethane. This mixture comprised the benzene and benzyne products in the approximate ratio of 9:1. From this it may be deduced that the ligand isomerisation from μ_3 benzene to μ_3 benzyne coordination may be accomplished by thermal as well as photochemical means.

By comparison with the behaviour of benzene bound to a metal surface these pyrolysis reactions have shown three major differences with surface behaviour. Comparison is made for these purposes with saturation coverage of surfaces for ligand behaviour.

(i) The first is that no "desorption" of the benzene has been observed from the cluster. For metal surfaces it was observed that desorption would occur at 130°C and would continue up to 220°C. However no loss of benzene was observed from the cluster species within this temperature range.

(ii) At no point during the pyrolysis reactions was decomposition of the benzene observed. The decomposition process occurs at 200°C for surface bound species, and at 220°C it competes in a 1:1 ratio with desorption. However neither process was observed for cluster bound benzene.

(iii) C-H bond breaking has been observed for both surface and cluster bound benzene at elevated temperatures. However, on cooling the surface bound sample the C-H bond breaking was observed to be reversible. For the cluster bound benzene we have no evidence that this is the case. Unfortunately as we have no methods available to carry out these pyrolyses with direct ir monitoring at elevated temperatures it did not prove possible to ascertain if a higher proportion of the benzyne species is present at higher temperatures.

The reaction of $[Os_3(CO)_9(\mu_3\text{-}\eta^2\text{:}\eta^2\text{:}\eta^2\text{-}C_6H_6)]$ with PEt_3

$[Os_3(CO)_9(\mu_3\text{-}\eta^2\text{:}\eta^2\text{:}\eta^2\text{-}C_6H_6)]$ was placed in a 5mm nmr tube. Excess PEt_3, (0.4mmol) was added and the tube was sealed under vacuum, ($10^{-6}\tau$).

After leaving the tube for 2 hours at ambient temperature the $^{31}P\{^1H\}$ nmr spectrum was recorded, showing that no reaction had occurred. The tube was then heated to 333K for 2 hours, and the $^{31}P\{^1H\}$ nmr spectrum was recorded, again showing that no reaction had occurred. The nmr tube was then irradiated for 2 hours with a mercury UV lamp, (600W). The $^{31}P\{^1H\}$ nmr spectrum was recorded indicating that reaction had occurred.

The $^{31}P\{^1H\}$ nmr spectrum showed a total of eleven peaks, with the lowest frequency resonance being assigned as free PEt_3 on the basis of its chemical shift. The resonances to high frequency occur as described in the table below, (Table 3.1).

Table 3.1 : The room temperature nmr parameters for the reaction of $[Os_3(CO)_9(\mu_3\text{-}\eta^2\text{:}\eta^2\text{:}\eta^2\text{-}C_6H_6)]$ with PEt_3 in dichloromethane

δP (ppm)	Multiplicity	J_{PP} (Hz)	Comments
-19	Triplet	14	Trisubstituted cluster
-15	Doublet	14	Trisubstituted cluster
-8	Singlet	-	*Mono* substituted cluster
+21	Doublet	13	Disubstituted cluster
+38	Doublet	17	Disubstituted cluster
+39	Doublet	17	Disubstituted cluster
+42	Doublet	13	Disubstituted cluster
+54	Singlet	-	*Mono* substituted cluster

From the nmr data obtained it is possible to assign the peaks to different patterns of substitution at the cluster. The triplet/doublet coupling system observed at (δ -19ppm) and (δ -15ppm) has been assigned to a 1,1,2 substitution pattern on a cluster. The singlet peak observed at (δ -8ppm) has been assigned to a *mono* substituted cluster species. The two higher frequency doublets may be assigned in a more specific fashion, owing to the nature of their chemical shift values.

The doublets observed at (δ +21ppm) and (δ +42ppm) have been assigned as arising from a 1,2 substituted species, as the large difference in their chemical shifts suggests that the two phosphines are coordinated to different metals. The other doublets observed at (δ +38ppm) and (δ +39ppm) have been assigned as a 1,1 substituted cluster as the chemical shifts of the phosphines suggests that they share the same metal atom, as they have similar values.

The final resonance observed, the singlet at (δ +54ppm) is very broad suggesting that there is some form of fluxional motion occurring on the cluster. In order to elucidate this the temperature of the probe was lowered in 30K increments, and the spectrum recorded after allowing the sample to temperature equilibrate for 30 minutes.

As the temperature of the sample was lowered below 240K the resonance present at (δ +54ppm) was observed to broaden. The temperature of the probe was then lowered as far as 153K*, when this resonance was observed to split into two separate resonances at (δ +57ppm) and (δ +53ppm). At the lower temperature the other resonances present in the spectrum also sharpened, however no further information could be deduced from this.

* The solvent utilised to allow the sample to be studied at this temperature was a 1:1 mixture of dichloromethane, (deuterated), and diethyl ether.

The room temperature ^1H nmr spectrum of the mixture was then recorded, in order to examine the benzene ligand attached to the cluster. This spectrum showed that, in addition to the resonance expected for the unreacted benzene cluster, (δ +4.46ppm), there were several other sets of peaks present.

Three broad resonances were observed at (δ +3.96ppm), (δ +3.87ppm) and (δ +3.81ppm). These have been assigned to various substitution patterns of the benzene cluster. Also present were several sets of resonances in the aromatic region, which are consistent with benzyne coordination to the cluster. Also present in the proton spectrum were several peaks centred around (δ -17ppm), which are consistent with the bridging hydride ligands formed when the benzene/benzyne coordination change occurs.

From this data it is evident that the photolysis reaction has formed phosphine substituted benzene and benzyne clusters. In order to assign the resonances in the phosphorus spectrum, selective decoupling experiments were carried out. This was achieved by variation of both the decoupler pulse position, and the decoupler power.

These experiments allow observation of the $^2J_{PH}$ couplings from the hydride ligands to the phosphine ligands, whilst coupling to the $-CH_2-$ of the ethyl groups on the phosphorus was eliminated. This was necessary as these couplings are all of the same order, (approximately 10-20Hz), and distinguishing between the couplings to the hydrides and the alkyl groups was not otherwise possible.

This experiment allowed the phosphorus resonances arising from the benzene and benzyne clusters to be differentiated. Unfortunately it is not possible to assign coupling constant values from this type of experiment, all that may be observed in the spectrum is the development of structure in some of the resonances. The table overleaf, (Table 3.2), summarises the information gained from this experiment.

Table 3.2 : The assignment of arene coordination mode from selective decoupling experiment for the reaction of $[Os_3(CO)_9(\mu_3\text{-}\eta^2\text{:}\eta^2\text{:}\eta^2\text{-}C_6H_6)]$ with PEt_3 in dichloromethane

δP (ppm)	Multiplicity	J_{PP} (Hz)	Arene coordination mode
-19	Triplet	14	Benzene
-15	Doublet	14	Benzene
-8	Singlet	-	Benzene
+21	Doublet	13	Benzyne
+38	Doublet	17	Benzene
+39	Doublet	17	Benzene
+42	Doublet	13	Benzyne
+54	Singlet	-	Benzyne

The nmr tube containing the mixture was then opened under N_2 and the products separated by tlc, eluent 40% dichloromethane/40% n-hexane. The ir and mass spectra of the products were recorded, the results of these studies are summarised in the table below, (Table 3.3).

Table 3.3 : The ir and mass spectral parameters for the reaction of $[Os_3(CO)_9(\mu_3\text{-}\eta^2\text{:}\eta^2\text{:}\eta^2\text{-}C_6H_6)]$ with PEt_3

tlc band #	Mass spectrum (Obs/Calc)	ir (νCO/cm^{-1}) (dichloromethane)	Assignment
1	1170/1170	2082.5(m), 2030.9(s), 1999.5(m),1978.6(m), 1961.1(w)	$[Os_3(CO)_6(PEt_3)_3(\mu_3\text{-}\eta^2\text{:}\eta^2\text{:}\eta^2\text{-}C_6H_6)]$ (1)
2	1082/1080	2087.2(w), 2059.2(w), 2008.2(m), 1977.2(s), 1942.5(m)	$[Os_3(CO)_7(PEt_3)_2(\mu_3\text{-}\eta^2\text{:}\eta^2\text{:}\eta^2\text{-}C_6H_6)]$ (2)
3	1080/1080	2046.2(m), 2020.1(s), 1987.9(m), 1970.2(m), 1922.5(w)	$[H_2Os_3(CO)_7(PEt_3)_2(\mu_3\text{-}\eta^4\text{-}C_6H_4)]$ (3)
4	992/990	2052.8(s), 2013.4(s), 1985.7(s), 1970.9(m), 1943.2(w), 1914.5(w)	$[Os_3(CO)_8(\mu_3\text{-}\eta^2\text{:}\eta^2\text{:}\eta^2\text{-}C_6H_6)PEt_3]$ (4)

From the data obtained it is now possible to assign the nmr resonances to individual products. The triplet resonance at (δ -19ppm) and the doublet resonance observed at (δ -15ppm), have been assigned to the 1,1,2 phosphine substituted cluster $[Os_3(CO)_6(PEt_3)_3(\mu_3\text{-}\eta^2\text{:}\eta^2\text{:}\eta^2\text{-}C_6H_6)]$, (1). The two doublets present at (δ +38ppm) and (δ +39ppm) have been assigned as arising from the 1,1 disubstituted cluster $[Os_3(CO)_7(PEt_3)_2(\mu_3\text{-}\eta^2\text{:}\eta^2\text{:}\eta^2\text{-}C_6H_6)]$, (2). The singlet resonance at (δ -8ppm) has been assigned to the *mono* substituted cluster species $[Os_3(CO)_8PEt_3(\mu_3.\eta^2\text{:}\eta^2\text{:}\eta^2\text{-}C_6H_6)]$, (4).

The two benzyne derived clusters observed in the selectively decoupled ^{31}P nmr spectrum have been assigned as follows. The two doublets observed at (δ +21ppm) and (δ +42ppm) have been assigned as arising from the 1,2 substituted benzyne cluster $[H_2Os_3(CO)_7(PEt_3)_2(\mu_3\text{-}\eta^4\text{-}C_6H_4)]$, (3). The singlet resonance at (δ +54ppm) has been assigned to the *mono* substituted benzyne cluster $[H_2Os_3(CO)_8PEt_3(\mu_3\text{-}\eta^4\text{-}C_6H_4)]$, (5). The proposed structures of these complexes are given below, (FIG 3.11).

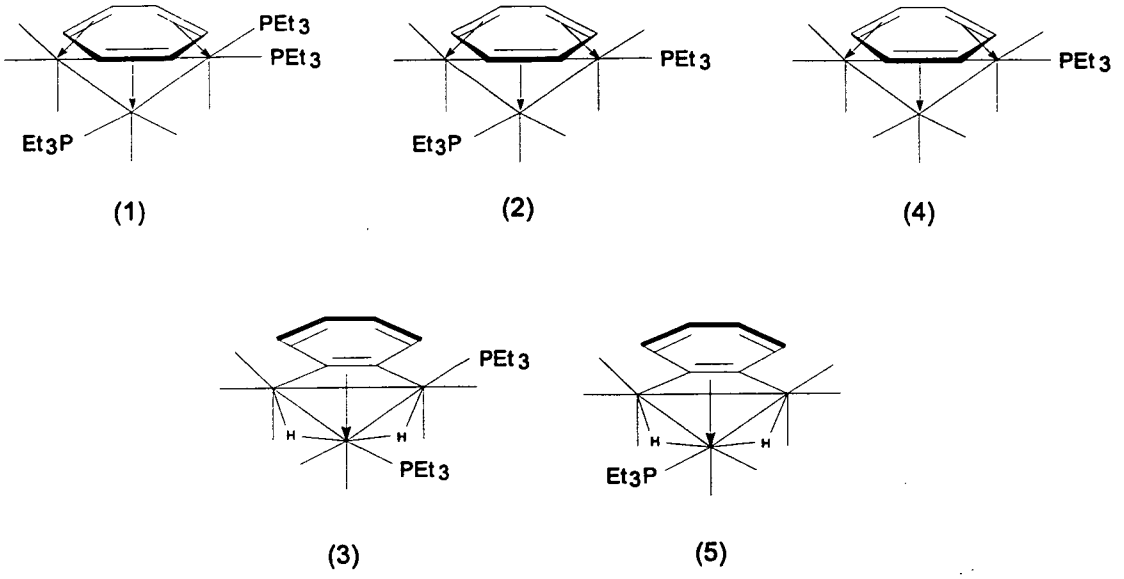

Figure 3.11 : The Proposed Structures Of $[Os_3(CO)_6(PEt_3)_3(\mu_3\text{-}\eta^2\text{:}\eta^2\text{:}\eta^2\text{-}C_6H_6)]$, (1), $[Os_3(CO)_7(PEt_3)_2(\mu_3\text{-}\eta^2\text{:}\eta^2\text{:}\eta^2\text{-}C_6H_6)]$, (2), $[Os_3(CO)_8PEt_3(\mu_3\text{-}\eta^2\text{:}\eta^2\text{:}\eta^2\text{-}C_6H_6)]$, (4), $[H_2Os_3(CO)_7(PEt_3)_2(\mu_3\text{-}\eta^4\text{-}C_6H_4)]$, (3), And $[H_2Os_3(CO)_8PEt_3(\mu_3\text{-}\eta^4\text{-}C_6H_4)]$, (5).

The reaction of $[Os_3(CO)_9(\mu_3\text{-}\eta^2\text{:}\eta^2\text{:}\eta^2\text{-}C_6H_6)]$ with $P(i\text{-}Pr)_3$

$[Os_3(CO)_9(\mu_3\text{-}\eta^2\text{:}\eta^2\text{:}\eta^2\text{-}C_6H_6)]$ was placed in a 5mm nmr tube. Excess $P(i\text{-}Pr)_3$, (0.4mmol) was added and the tube was sealed under vacuum, ($10^{-6}\tau$).

After leaving the tube for 2 hours at ambient temperature the $^{31}P\{^1H\}$ nmr spectrum was recorded, showing that no reaction had occurred. The tube was then heated to 333K for 2 hours, and the $^{31}P\{^1H\}$ nmr spectrum was recorded, again showing that no reaction had occurred. The nmr tube was then irradiated for 2 hours with a mercury UV lamp, (600W). The $^{31}P\{^1H\}$ nmr spectrum was recorded indicating that reaction had occurred.

The $^{31}P\{^1H\}$ nmr spectrum exhibited seven resonances, three singlets and four doublets. The lowest frequency resonance, at (δ +8ppm) has been assigned as free $P(i\text{-}Pr)_3$ on the basis of its chemical shift. The resonances to high frequency occur at the shift values detailed in the table below, (Table 3.4).

Table 3.4 : The room temperature nmr parameters for the reaction of $[Os_3(CO)_9(\mu_3\text{-}\eta^2\text{:}\eta^2\text{:}\eta^2\text{-}C_6H_6)]$ with $P(i\text{-}Pr)_3$ in dichloromethane

δP (ppm)	Multiplicity	J_{PP} (Hz)	Comments
+8	Singlet	-	Free $P(i\text{-}Pr)_3$
+24	Singlet	-	*Mono* substituted cluster
+29	Doublet	26	Disubstituted cluster
+46	Doublet	26	Disubstituted cluster
+56	Doublet	22	Disubstituted cluster
+59	Singlet	-	*Mono* substituted cluster
+63	Doublet	22	Disubstituted cluster

From the nmr data obtained it is possible to assign the peaks to different patterns of substitution at the cluster. The singlet resonance present at (δ +24ppm) may be assigned to a *mono* substituted cluster complex. The two doublet resonances present at (δ +21ppm) and (δ +42ppm) may be assigned to a 1,2 substituted cluster species.

Similarly, the doublets observed at (δ +56ppm) and (δ +63ppm) have been assigned as arising from a disubstituted cluster species. The singlet resonance observed at (δ +59ppm) has bee assigned to a *mono* substituted cluster.

Both of the disubstituted clusters assigned are considered to have a 1,2 substitution pattern, as the large differences in their chemical shifts suggest that the two phosphines are coordinated to different metals in both cases.

The resonance present at (δ +59ppm) was broad at room temperature, suggesting that some fluxional process was occurring. In order to study this further the temperature of the probe was lowered to 213K and the $^{31}P\{^{1}H\}$ nmr spectrum rerecorded.

This spectrum showed that the broad resonance at (δ +59ppm) had resolved into two peaks at (δ +57ppm) and (δ +60ppm). At this temperature there was no appreciable sharpening of any of the other peaks in the spectrum.

The room temperature ^1H nmr spectrum of the mixture was then recorded, in order to examine the benzene ligand attached to the cluster. This spectrum showed that, in addition to the resonance expected for the unreacted benzene cluster, (δ +4.46ppm), there were several other sets of peaks present.

Three broad resonances were observed at (δ +3.94ppm), (δ +3.86ppm) and (δ +3.79ppm). These have been assigned to various substitution patterns of the benzene cluster. Also present were several complex sets of resonances in the aromatic region, consistent with benzyne coordination to the cluster. Also present in the proton spectrum were several peaks centred around (δ -19ppm), which are consistent with the bridging hydride ligands formed when the benzene/benzyne coordination change occurs.

From this data it is evident that the photolysis reaction has formed phosphine substituted benzene and benzyne clusters. In order to assign the resonances in the phosphorus spectrum, selective decoupling experiments were carried out. This was achieved by variation of both the decoupler pulse position, and the decoupler power.

These experiments allow observation of the $^2J_{PH}$ couplings from the hydride ligands to the phosphine ligands, whilst coupling to the $-CH_2-$ of the ethyl groups on the phosphorus has been eliminated. This was necessary as these couplings are all of the same order, (approximately 10-20Hz), and distinguishing between the couplings to the hydrides and the alkyl groups was not otherwise possible.

This experiment allowed the resonances in the phosphorus spectrum arising from the benzene and benzyne clusters to be differentiated. Unfortunately it is not possible to assign coupling constant values from this type of experiment, as all that may be observed in the spectrum is the development of structure in some of the resonances. The table below, (Table 3.4), summarises the information gained from this experiment.

Table 3.4 : The assignment of arene coordination mode from selective decoupling experiment for the reaction of $[Os_3(CO)_9(\mu_3\text{-}\eta^2\text{:}\eta^2\text{:}\eta^2\text{-}C_6H_6)]$ with $P(i\text{-}Pr)_3$ in dichloromethane

δP (ppm)	Multiplicity	J_{PP} (Hz)	Arene coordination mode
+24	Singlet	-	Benzene
+29	Doublet	26	Benzene
+46	Doublet	26	Benzene
+56	Doublet	22	Benzyne
+59	Singlet	-	Benzyne
+63	Doublet	22	Benzyne

The nmr tube containing the mixture was then opened under N_2 and the products separated by tlc, eluent 40% dichloromethane/40% n-hexane. The ir and mass spectra of the products were recorded, the results of these studies are summarised in the table below, (Table 3.4).

Table 3.4 : The ir and mass spectral parameters for the reaction of $[Os_3(CO)_9(\mu_3\text{-}\eta^2\text{:}\eta^2\text{:}\eta^2\text{-}C_6H_6)]$ with P(i-Pr)$_3$

tlc band #	Mass spectrum (Obs/Calc)	ir (νCO/cm^{-1}) (dichloromethane)	Assignment
1	1282/1282	2077.2(m), 2055.0(w), 2030.9(s), 1999.3(w), 1978.8(w), 1959.2(w)	$[Os_3(CO)_7(P(i\text{-}Pr)_3)_2(\mu_3\text{-}\eta^2\text{:}\eta^2\text{:}\eta^2\text{-}C_6H_6)]$ (6)
2	1284/1282	N/A	$[H_2Os_3(CO)_7(P(\text{-}Pr)_3)_2(\mu_3\text{-}\eta^4\text{-}C_6H_4)]$ (7)
3	1035/1032	2045.8(s), 2007.6(s), 1977.5(s), 1964.3(m), 1935.1(w)	$[Os_3(CO)_8(\mu_3\text{-}\eta^2\text{:}\eta^2\text{:}\eta^2\text{-}C_6H_6)P(i\text{-}Pr)_3]$ (8)

From the data obtained it is now possible to assign the nmr resonances to individual products. The two doublets present at (δ +29ppm) and (δ +46ppm) have been assigned as the 1,2 disubstituted cluster $[Os_3(CO)_7(P(i\text{-}Pr)_3)_2(\mu_3\text{-}\eta^2\text{:}\eta^2\text{:}\eta^2\text{-}C_6H_6)]$, (6). The singlet resonance at (δ +24ppm) has been assigned to the *mono* substituted cluster species $[Os_3(CO)_8P(i\text{-}Pr)_3(\mu_3\text{-}\eta^2\text{:}\eta^2\text{:}\eta^2\text{-}C_6H_6)]$, (8).

The two benzyne derived clusters observed in the selectively decoupled ^{31}P nmr spectrum have been assigned as follows. The singlet resonance at (δ +59ppm) has been assigned to the *mono* substituted benzyne cluster $[H_2Os_3(CO)_8P(i\text{-}Pr)_3(\mu_3\text{-}\eta^4\text{-}C_6H_4)]$, (7). The two doublets observed at (δ +56ppm) and (δ +63ppm) have been assigned as arising from the 1,2 substituted benzyne cluster $[H_2Os_3(CO)_7(P(i\text{-}Pr)_3)_2(\mu_3\text{-}\eta^4\text{-}C_6H_4)]$, (9). The proposed structures of these complexes are given below, (FIG 3.12).

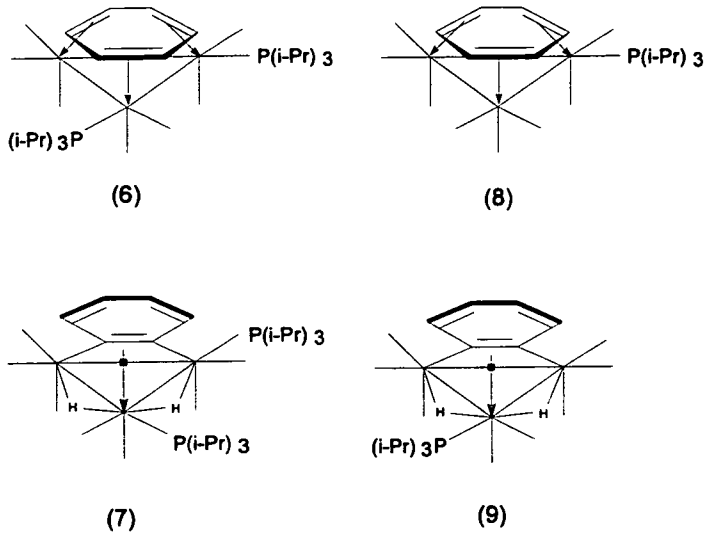

Figure 3.12 : The Proposed Structures Of $[Os_3(CO)_7(P(i\text{-}Pr)_3)_2(\mu_3\text{-}\eta^2\text{:}\eta^2\text{-}C_6H_6)]$, (6), $[Os_3(CO)_8P(i\text{-}Pr)_3(\mu_3\text{-}\eta^2\text{:}\eta^2\text{:}\eta^2\text{-}C_6H_6)]$, (8), $[H_2Os_3(CO)_7(P(i\text{-}Pr)_3)_2(\mu_3\text{-}\eta^4\text{-}C_6H_4)]$, (7), And $[H_2Os_3(CO)_8P(i\text{-}Pr)_3(\mu_3\text{-}\eta^4\text{-}C_6H_4)]$, (9).

Discussion

From these reactions it may be postulated that the benzene bound to an osmium cluster surface in a face capping mode is bound in a different fashion to benzene adsorbed onto a metal surface. The bond lengths for surface bound benzene are considerably longer than the cluster bound ligand, (average bond lengths of 1.58±0.15Å and 1.42Å respectively). This indicates some destabilisation of the benzene on the metal surface with respect to the cluster bound species.

The lack of benzene displacement *via* pyrolysis has also been observed, although C-H bond cleavage has been seen to occur. The other main difference in reactivity is the failure of phosphine ligands to substitute the benzene ligands at the cluster surface. It was observed that even under photolysis conditions PMe_3 failed to react with the cluster in any way, although it will displace benzene from a metal surface very efficiently.

From this data it is suggested that the binding of a benzene ligand in an η^6 fashion to a cluster surface creates a stronger interaction between the metal triangle and the ligand than that observed for benzene adsorbed on a metal surface. From this information it can be seen that while the binding of benzene to a surface is structurally similar to cluster-benzene binding, the analogy begins to break down in terms of reactivity of the bound arene. This may arise from the fact that surface bound benzene may desorb without significant changes to the surface but when bound to a cluster, the loss of the benzene ligand would create a ligand deficient system. This system would be extremely unstable, and the energy barrier to its formation would be very high, possibly explaining the discrepancies in reactivity between the surface and cluster bound arenes.

1 Hein et al., *Chem Ber, 1919, 52, 195.*

2 E. O. Fischer and W. Hafner, *Naturforsch, 1955, B10, 665.*

3 E. O. Fischer and K. Ofle, *Chem Ber, 1957, 90, 2352.*

4 E. L. Muetterties, J. R. Bleeke, E. J. Wucherer and T. A. Albright, *Chem Rev, 1982, 82, 499.*

5 W. E. Silverthorn, *Adv in Organomet Chem, 1975, 13, 47.*

6 A. J. Deeming, *Adv in Organomet Chem, 1988, 26, 47.*

7 R. Mason and W. R. Robinson, *JCS Chem Comm, 1968, 468.*

8 B. F. G. Johnson, R. D. Johnston and J. Lewis, *JCS Chem Comm, 1967, 1057.*

9 S. Z. Goldberg, B. Spivak, G. Stanley, R. Eisenberg, D. M. Braitsch, J. S. Miller and M. Abkowitz, *J. Am Chem Soc, 1977, 99, 110.*

10 P. H. Bird and A. R. Frazer, *J. Orgmet Chem, 1974, 73, 103.*

11 R. O. Gould, C. L. Jones, D. R. Robertson, D.A. Tocher and T. A. Stephenson, *J. Orgmet Chem, 1982, 226, 199.*

12 M. R. Churchill and S. W. Y. Chang, *JCS Chem Comm, 1974, 248.*

13 R. J. Dellaca and B. R. Penfold, *Inorg Chem, 1972, 11, 1855.*

14 M. P. Garcia, M. Green and G. F. Stone, *JCS Chem Comm, 1981, 871.*

15 M. A. Bennet, T. N. Huang and T. W. Turnkey, *JCS Chem Comm, 1979, 312.*

16 T. Arthur, D. R. Robertson, D. A. Tocher and T. A. Stephenson, *J. Orgmet Chem, 1981, 208, 389.*

17 J. A. Bandy, M. L. H. Green, D. O'Hare and K. Prout, *JCS Chem Comm, 1984 1402.*

18 A. Lucherini and L. Porri, *J. Orgmet Chem, 1978, 155, C45, 19.*

19 D. M. Barlex, J. A. Evans, R. D. W. Kemmit and D. R. Russell, *JCS Chem Comm, 1971, 331.*

20 J. Browning, M. Green, B. R. Penfold, J. L. Spencer and F. G. A . Stone, *JCS Chem Comm, 1973, 31.*

21 D. J. Brauer and C. Kruger, *Inorg Chem, 1977, 16, 884.*

22 A. W. Duff, K. Jonas, R. Goddard, H. J. Kraus and C. Kruger, *J. Am Chem Soc, 1983, 105, 5479.*

23 K. Jonas, V. Wiskamp, Y. H. Tsay and C. Kruger, *J. Am Chem Soc, 1983, 105, 5480.*

24 H. van der Heijden, A. G. Orpen, and P. Pasman, *JCS Chem Comm, 1985, 1576.*

25 M. P. Gomez - Sal, B. F. G. Johnson, J. Lewis, P. R. Raithby and A. H. Wright, *JCS Chem Comm, 1985, 1682.*

26 M. A. Gallop, M. P. Gomez - Sal, C. E. Houscroft, B. F. G. Johnson, J. Lewis, S. M. Owen, P. R. Raithby and A. H. Wright, *J. Am Chem Soc, 1992, 114, 2502.*

27 M. A. Gallop, B. F. G. Johnson, J. Lewis and P. R. Raithby , *JCS Chem Comm, 1987, 1809.*

28 M. A. Gallop, B. F. G. Johnson, J. Keeler, J.Lewis, S. J. Heyes and C. M. Dobson, *J. Am Chem Soc, 1992, 114, 2510.*

29 M. A. Gallop, PhD Thesis, *Cambridge, 1988.*

30 M. C. Tsai and E. L. Muetterities, *J. Am Chem Soc, 1982, 104, 2534.*

31 M. C. Tsai, C. M. Friend and E. L. Muetterities, *J. Am Chem Soc, 1982, 104, 2539.*

32 C. M. Friend and E. L. Muetterities, *J. Am Chem Soc, 1981, 103, 773.*

33 M. A. Van Hove, R. F. Lin and G. A. Somorjai, *J. Am Chem Soc, 1986, 108, 2532.*

34 R. F. Lin, G. S. Blackman, M. A. Van Hove and G. A. Somorjai, *Acta Cryst, 1987, B43, 368.*

35 A. J. Deeming, R. E. Kimber and M. Underhill, *JCS Dalton Trans, 1973, 2589.*

36 A. J. Deeming and M. Underhill, *JCS Dalton Trans, 1974, 1415.*

37 R. J. Gousmit, B. F. G. Johnson, J. Lewis, P. R. Raithby and M. J. Rosales, *JCS Dalton Trans, 1983, 2257.*

CHAPTER FOUR

THE PYROLYSIS OF $[Os_6(CO)_{21}]$

The raft cluster $[Os_6(CO)_{21}]$

The so called "raft" cluster $[Os_6(CO)_{21}]$ (FIG 4.1), was first prepared[1,2] when $[Os_6(CO)_{18}]$ was carbonylated by the use of high pressure (50 atm.) CO and elevated temperatures (165°C). A much better synthesis was discovered when an attempt was made to produce mixed metal clusters of osmium and palladium[3]. The reaction of $[Os_3(CO)_{10}(MeCN)_2]$ with $[PdCl_2]$ in dichloromethane produced a dark blue solution which contained a mixture of the of *mono-, bis-* and *tris*-acetonitrile derivatives, $[Os_6(CO)_{21-n}(MeCN)_n]$, (n=1-3). These products may be converted to $[Os_6(CO)_{21}]$ (1) by bubbling CO through a solution containing this mixture of acetonitrile derivatives when the CO displaces the (MeCN) ligands. Upon further study[2] of the reaction it was observed that the $[PdCl_2]$ was only required in catalytic amounts to cause the triosmium species to dimerise and form the raft. This dimerisation is believed to arise from the formation of ligand deficient triosmium species, presumably catalysed by the palladium chloride. Howevèr, this mechanism has not been fully elucidated to date.

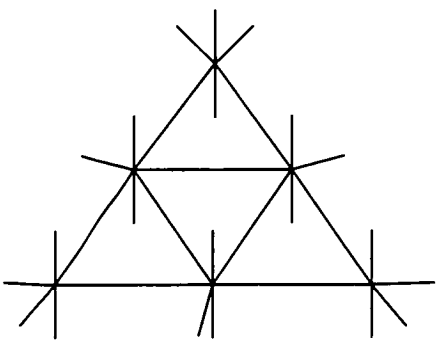

Figure 4.1 : The Proposed Structure Of The Raft Cluster $[Os_6(CO)_{21}]$

Whilst the reaction with $[PdCl_2]$ provides a good yield of the activated raft clusters (75-80%), the remainder of the products are a mixture of Os_3 and Os_5 derivatives as well as $[Os_6(CO)_{18}]$. This may be overcome by using the more soluble $[Pd(OAc)_2]$ instead of the $[PdCl_2]$, which gives a higher yield of the acetonitrile substituted raft clusters (approx 95%), with the only other products present being Os_3 derivatives which are easily separated on a silica column, eluent 60% n-hexane/40% dichloromethane.

Although the exact molecular structure of this raft cluster has not been determined by X-ray diffraction methods, its structure has been inferred from studies on the analogous clusters $[Os_6(CO)_{21-n}(PR_3)_n]$ (n=1-6)[1], in that the metal framework adopts a planar raft arrangement. Further studies on this cluster have shown that it undergoes CO elimination upon heating to form the known cluster $[Os_6(CO)_{18}]$, and that the reverse reaction can be carried out by heating $[Os_6(CO)_{18}]$ under high CO pressure, (FIG 4.2).

A) Decarbonylation:

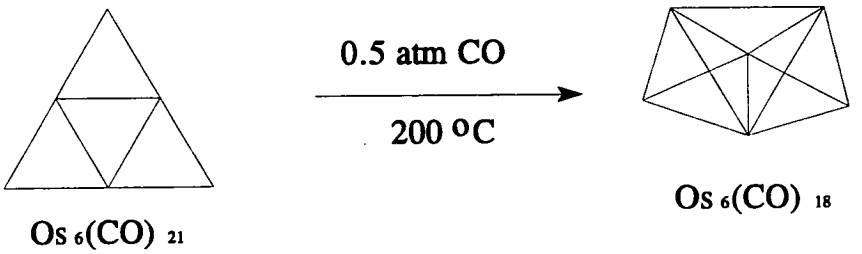

B) Carbonylation:

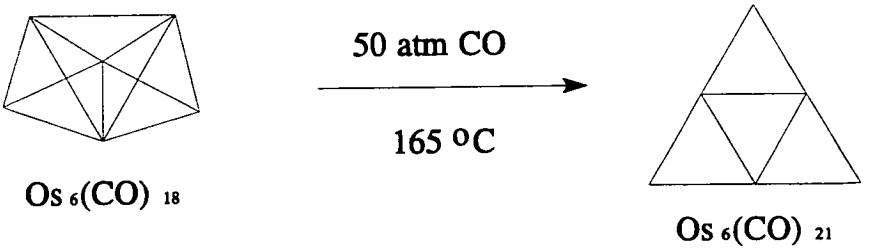

Figure 4.2 : Reversible Carbonylation Of $[Os_6(CO)_{18}]$

Pyrolysis of $[Os_6(CO)_{21}]$:

In order to investigate the mechanism of decarbonylation in a more detailed and systematic way, the reaction was carried out on a sealed high vacuum ($10^{-6}\tau$) line with pressure monitoring *via* a null zero spiral deflection gauge. The monitoring of pressure was carried out to ascertain whether the CO loss was a stepwise or gradual process.

50mg of $[Os_6(CO)_{21}]$ was placed in a pyrolysis bulb and attached to the spiral section of the line. The sample was pumped on for 1 hour at $10^{-6}\tau$, after which it was removed and the ir spectrum recorded. This showed that no CO loss occurred at room temperature at this pressure. The sample was then attached to the line again and pumped on for a further 30 minutes. The sample tube was immersed in an oil bath and the temperature was increased gradually (approx 1^0C every minute). The pressure was monitored over time and the reaction showed a stepwise loss of 3 aliquots of CO at the temperatures detailed below.

Table 4.1 : Pyrolysis data for $[Os_6(CO)_{21}]$

Temperature	Observation
105°C	1st CO aliquot evolved
165°C	2nd CO aliquot evolved
210°C	3rd CO aliquot evolved

These losses of CO are thought to be associated with a systematic closure of the planar metal framework, as a three stage mechanism (Scheme 1), to form $[Os_6(CO)_{18}]$. This mechanism involves the formation of two proposed intermediates, $[Os_6(CO)_{19}]$ (2) and $[Os_6(CO)_{20}]$ (3).

Species (2) is best described as a tetrahedron of osmium atoms, with two edge bridging $[Os(CO)_4]$ units. Species (3) may be described as a trigonal bipyramid of osmium atoms with one edge bridging $[Os(CO)_4]$ unit.

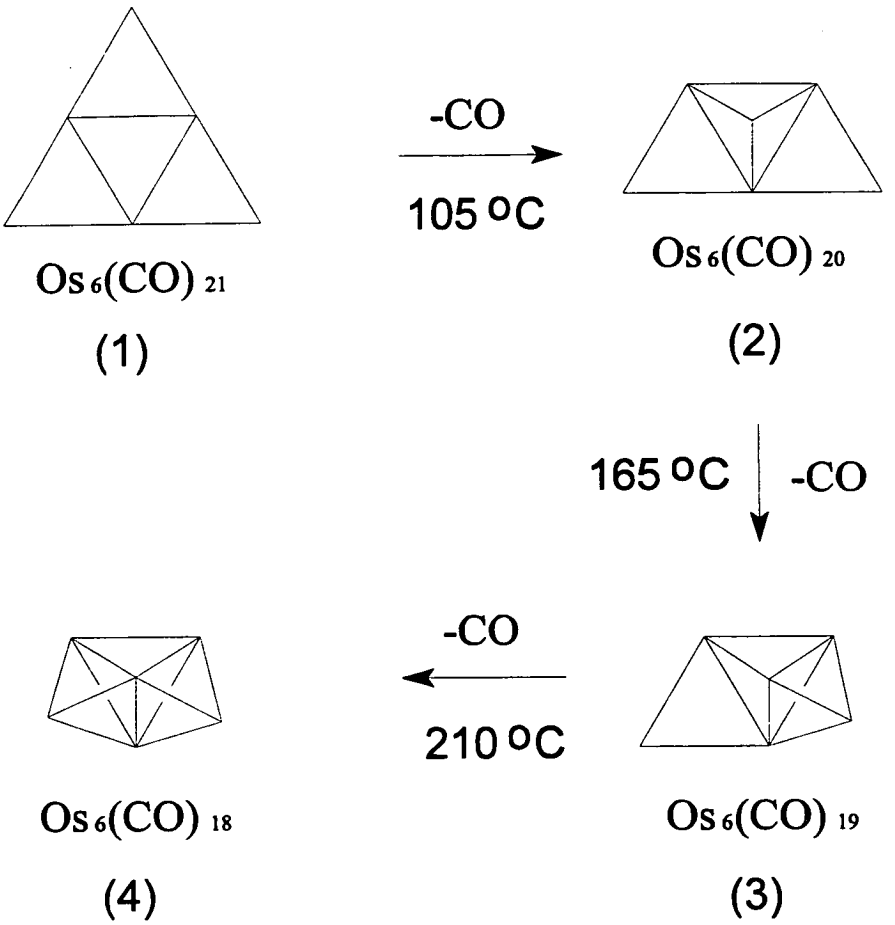

Scheme 4.1 : Proposed Foldup Mechanism Of Metal Framework

The reaction was then repeated with the intention of isolating the proposed intermediate species (2) and (3). This was done by heating a sample of $[Os_6(CO)_{21}]$ until the first CO loss was observed and removing the sample from the vacuum line. This was repeated with a separate sample, heated until the first and second CO losses had been observed.

However neither species (2) or (3) could be isolated from these mixtures, it was therefore assumed that these species were unstable and would rearrange rapidly to either $[Os_6(CO)_{18}]$ or $[Os_6(CO)_{21}]$. Full analysis of these mixtures after the reaction revealed only $[Os_6(CO)_{18}]$ and $[Os_6(CO)_{21}]$.

Upon analysis of the final reaction mixture it was observed that $[Os_6(CO)_{18}]$ was present in high yield (80%), but no $[Os_6(CO)_{21}]$ could be detected. The remainder of the mixture was an insoluble black material, which exhibited no carbonyl stretches in its ir spectrum. Mass spectral analysis of this substance showed no evidence of a parent complex, only fragments representing Os^+. It is assumed that the black solid is some form of osmium complex, as metallic osmium itself would not give rise to any peaks in a mass spectrum. It is not possible to elucidate the nature of this complex due to its lack of solubility, and the absence of any spectral data.

In order to further investigate this stepwise process a sample of $[Os_6(CO)_{21}]$ was attached to the vacuum line and heated until the first CO loss was observed. The temperature was maintained at 105°C and the pressure monitored. Over a period of 2 hours a gradual loss of CO from the cluster was observed, until total conversion to $[Os_6(CO)_{18}]$ had occurred, confirmed by ir spectroscopy. This would appear to indicate that once the first loss of CO from the raft has occurred, then the stable thermodynamic product is $[Os_6(CO)_{18}]$.

This hypothesis is supported by observation of the MALDI[4,5] laser desorption mass spectrum of $[Os_6(CO)_{21}]$, (FIG 4.3). This spectrum exhibits a parent ion peak at M/e = 1730, and subsequent loss of at least eleven CO ligands. A peak was also observed at M/e = 1648, which has been assigned to the cluster $[Os_6(CO)_{18}]$. This peak is approximately 50 times as intense as the parent peak which possibly indicates preferential stability of the daughter product.

The peak at m/e = 1704 is also considerably stronger than the parent peak, indicating that species (2) shows some preferential stability. This intermediate has been observed during high pressure ir studies on the carbonylation of $[Os_6(CO)_{18}]^{2-}$ when it was observed as a deposit on the inside of the ir cell, but was never fully characterised.

Whilst the MALDI spectrum shows agreement that the species under study is $[Os_6(CO)_{21}]$, the peaks are not as well defined as a FAB spectrum would give. This is a consequence of the nature of the ionisation in this type of spectroscopy. MALDI gives rise to $(M+H)^+$, $(M-H)^-$ and $M^{\cdot+}$ ions, causing peak broadening, though in this case the peaks for $(M-H)^-$ ions cannot possibly be observed. The MALDI spectrum shown (FIG 4.3) shows only gaussian peaks, with no internal resolution available in the peaks. This gives rise to "errors" in the peak positions, with the mass values given not being exactly as calculated, e.g. the parent ion peak at m/e=1730 should be at m/e=1728, assuming a CO ligands has been lost, similarly the peak attributable to $[Os_6(CO)_{18}]$ should be at m/e=1644.

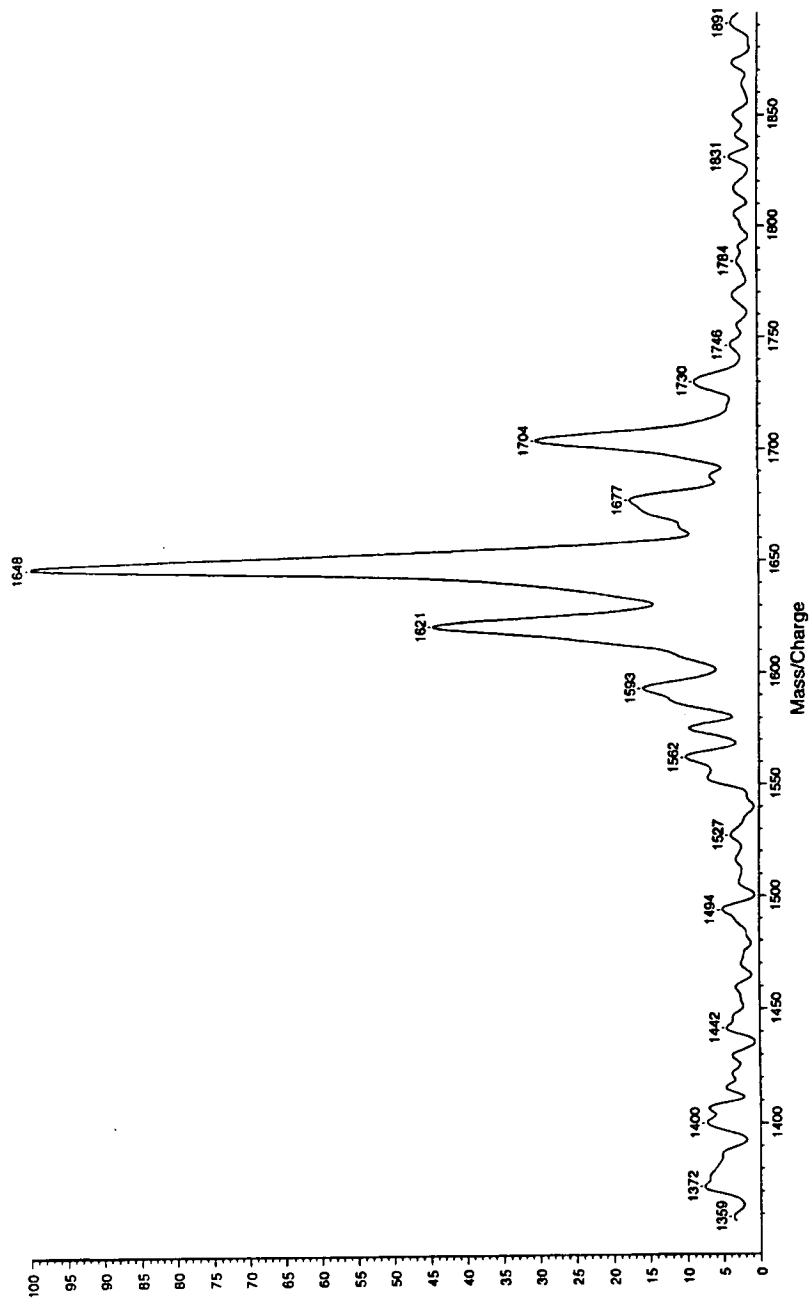

Figure 4.3 : The MALDI Spectrum Of $[Os_6(CO)_{21}]$

However, it was observed that as the temperature was raised above 165°C, additional decomposition of the reaction mixture occurred, and a pale lemon yellow crystalline product sublimed onto the surface of the pyrolysis tube. None of the crystals which were produced were of suitable quality for X-ray diffraction. This material proved to be a mixture of compounds and after separation by tlc, eluent 65% n-hexane/35% dichloromethane, the ir and mass spectra were recorded. The table below, (Table 4.2), summarises the spectroscopic data available for these clusters.

Table 4.2 : ir and mass spectroscopic data for pyrolysis products

Complex	$\upsilon CO/cm^{-1}$ In dichloromethane	Parent ion (calculated value)
$Os_3(CO)_{12}$	2068(s), 2034(s), 2013(m), 1999(m)	906 (906)
$Os_6(CO)_{18}$	2107.5(w),2075.9(s), 2060.8(s), 2038.3(s), 2027.8(m), 2000.4(w), 1956.9(w)	1648 (1648)
$Os_3(CO)_{12}C$	2115.3(w), 2077.2(s), 2068.1(s), 2025.5(s), 1985.6(w)	918(918)

Analysis of the mixture showed the presence of a novel new cluster species, only present in very low yield (<5%) in the mixture. This species was, on the basis of mass spectral analysis, formulated as $[Os_3(CO)_{12}C]$ (4). Accurate mass determinations support this formulation with agreement to less than 1ppm from calculated mass values. These determinations were carried out both for the parent ion and the peak corresponding to the first CO loss from the cluster.

The analysis of two peaks in this manner was carried out to eliminate the possibility that the parent peak arose from the presence of $[Os_3(CO)_{11}(MeCN)]$. This has a nominal mass difference of 1 from species (4), which would make differentiation of the two impossible by nominal mass measurements.

The presence of $[Os_3(CO)_{11}(MeCN)]$ has been discounted on two counts. Firstly, accurate mass determination exhibits a difference of less than 1ppm from that calculated for (4), whereas they are approximately 500ppm different from the calculated value for $[Os_3(CO)_{11}(MeCN)]$. Secondly, if $[Os_3(CO)_{11}(MeCN)]$ was present it might be assumed, given the lability of the MeCN ligand that this would be the first ligand lost, giving an initial mass loss of 42 amu, not 28 as would be expected for loss of a carbonyl. Therefore, the accurate mass determinations allow us to discount the presence of $[Os_3(CO)_{11}(MeCN)]$, and to assign the new cluster as species (4). The table below, (Table 4.3), summarises the exact mass data acquired for the parent peak and first CO loss.

Table 4.3 : Exact mass data for sublimed products

Species	Calculated mass	Experimental Mass
$Os_3(CO)_{12}C$	921.820631	921.820630
$Os_3(CO)_{11}C$	890.822780	890.822781
$Os_3(CO)_{11}(MeCN)$	921.821158	N/A

From the mass spectrum (4) has been assigned as $[Os_3(CO)_{12}C]$ However the parent ion peak in the mass spectrum is by far the weakest present, and a much stronger peak is observed at m/e = 890, which may be tentatively assigned to the ion of formula $[Os_3(CO)_{11}C]^+$.

This species is believed to be the new ketenylidene cluster, $[Os_3(CO)_{10}CCO]^+$ arising from the thermal decomposition of species (4). It has not been possible to confirm this by thermal decomposition of a sample of (4), due to the small amount of sample produced.

The formation of species (4) is assumed to arise from decomposition of (2) or (3), as the pyrolysis of $[Os_6(CO)_{18}]$ does not give rise to any detectable ketenylidene derivatives after pyrolysis (200°C for 2 hours at $10^{-6}\tau$). The assignment of these species as ketenylidene derivatives has been made by analogy with known cluster species of similar formulation, in that the cluster has an "extra" carbon atom present with respect to the oxygen content, ie. contains either one "CCO" unit or a carbide. The carbide has been discounted as a possibility because there is not enough physical space in the metal framework to accommodate an extra carbon atom. Ketenylidene derivatives of metal clusters are well established[6-12], and cluster (4) is possibly related to derivatives of $[Fe_3(CO)_{12}]$ or $[Co_3(CO)_9CCl]$. The species $[Fe_3(CO)_9CCO]^{2-}$ is well known and has been fully characterised by X-ray study[6] (FIG 4.4), but the neutral species $[Fe_3(CO)_{10}CCO]$ has not been reported.

The chemistry of $[Co_3(CO)_9CCl]$ and its derivatives has been investigated in some detail and a ketenylidene species, $[Co_3(CO)_9CCO]^+$ has been reported[9], although no X-ray structural data has been obtained, (FIG 4.5). The structure of the cobalt species has been assigned by analogy with a series of complexes based on the $[Co_3(CO)_9CR]$ cluster. All X-ray structures obtained for species in this series exhibit a μ_3 carbon cap on the face of the metal triangle.

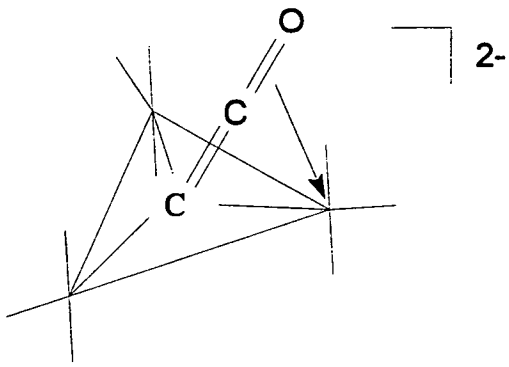

Figure 4.4 : The Structure Of $[Fe_3(CO)_9CCO]^{2-}$

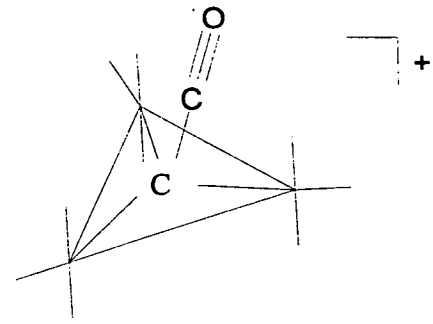

Figure 4.5 : The Structure Of $[Co_3(CO)_9CCO]^{+}$

Both of these ketenylidene species have a μ_3 capping CCO group located on the face of the metal triangle.

In (4) we have a species related to the parent binary carbonyl $[Os_3(CO)_{12}]$, but with several structural possibilities. By comparison with the known ketenylidene species, above, a structure involving one of the 2 electron carbonyl ligands replaced with a μ_3-CCO group (a), possibly with a μ_2-CO group present (b), is proposed, (FIG 4.6).

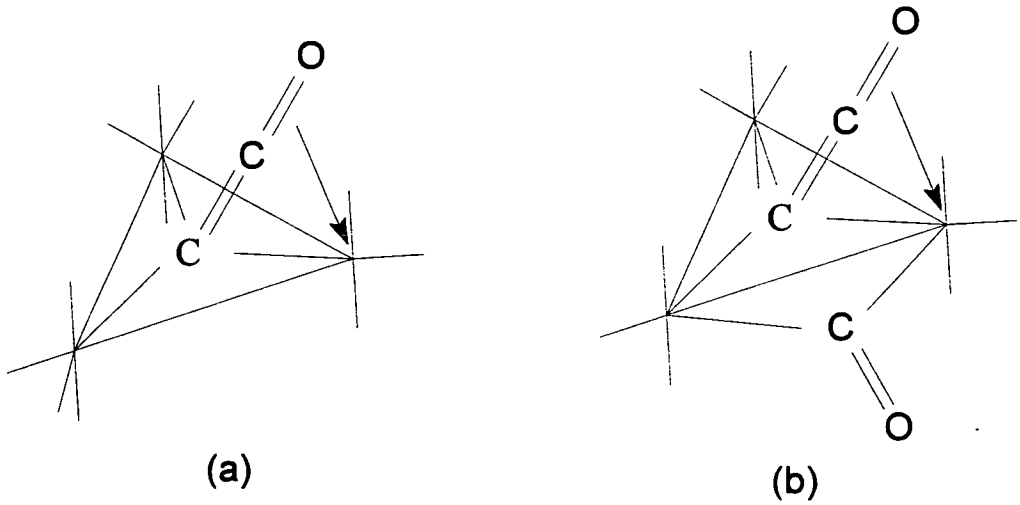

Figure 4.6 : Possible ketenylidene structures for $[Os_3(CO)_{12}C]$

Another type of structure to be considered involves comparison to $[Fe_3(CO)_{12}]$ itself with a μ_2-CCO group and a μ_2-CO group bridging one edge of the metal triangle, this proposed structure is given below, (FIG 4.7).

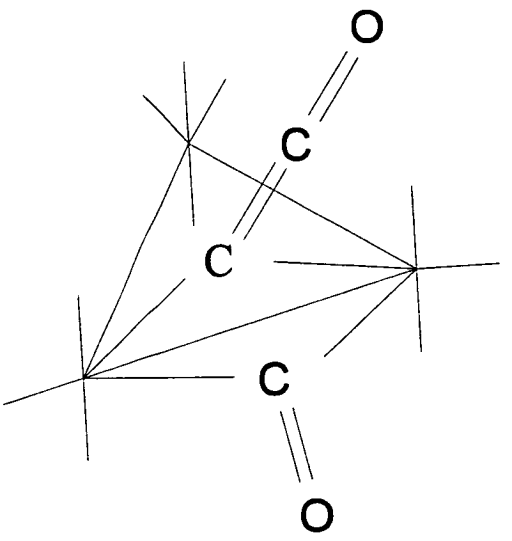

Figure 4.7 : The Proposed Structure Of $[Os_3(CO)_{12}C]$ With μ_2-CCO Ligand

This structure is thought to be more likely than those given in FIG 4.6, as the electron count on all three osmium atoms totals 18, giving a stable closed shell configuration.

The structures of the first derivative of (4), $[Os_3(CO)_{10}CCO]^+$, both without a bridging CO ligand (a) and with a μ_2-CO ligand (b) are given overleaf, (FIG 4.8).

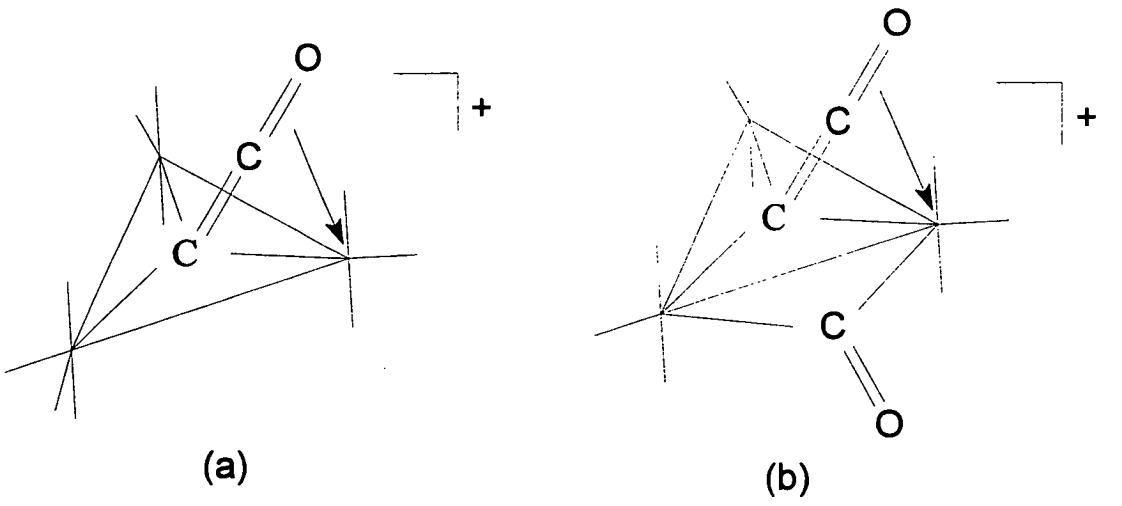

Figure 4.8 : Possible ketenylidene structures for $[Os_3(CO)_{10}CCO]^+$

Of the two structures given it is assumed (b) is the more likely as the electron count on the osmium atoms comes to two with 18 electrons, and one with only 17, accounting for the +ve charge. Structure (a), however has all three metal atoms in an electron deficient state, this has been assigned as being less stable than (b).

Attempts to stabilise (4), and facilitate crystallisation by reaction with 1.1 equivalents of Me_3NO and triphenyl phosphine resulted in the formation of no stable phosphine derivatives, and caused decomposition of (4). It must be assumed that the abstraction of one CO ligand by the amine oxide results in rapid cluster degradation as none of the products of this reaction appeared to be metal cluster based.

Activation of $[Os_6(CO)_{21}]$:

The reaction of $[Os_3(CO)_{10}(MeCN)_2]$ with palladium acetate in dichloromethane gives a mixture of activated raft clusters which were then almost impossible to separate as mentioned before. In order to investigate the reactions of the activated raft more systematically, it was decided to manufacture the parent binary carbonyl, $[Os_6(CO)_{21}]$, and to then activate it by use of trimethylamine oxide. This would allow the reactions of the *mono* and *bis* activated clusters to be investigated separately.

Preparation of $[Os_6(CO)_{19}(MeCN)_2]$:

The resultant solution was a deep emerald green colour, not deep blue as expected. An attempt to separate the reaction mixture by tlc, eluent 60% n-hexane/40% dichloromethane, was then carried out. The tlc had only one band evident which was deep green in colour. The ir and mass spectra of this complex were then taken giving no further information into the composition of this species.

The green complex was then refluxed with triphenyl phosphine in dichloromethane for 1 hour. After this time the deep green colour had changed to turquoise. The mixture was then separated by tlc, eluent 60% n-hexane/40% dichloromethane. This yielded a yellow product, identified by ir and mass spectroscopy as $[Os_3(CO)_{10}(PPh_3)_2]$ and a blue band identified as $[Os_6(CO)_{19}(PPh_3)_2]$ in a 2:1 ratio. From this it can be seen that significant degradation of the cluster metal framework has occurred (approximately 50% of the starting material has decomposed).

The reaction was then repeated in the presence of $[Pd(OAc)_2]$ in an attempt to stabilise the raft cluster. However this had the reverse effect on the reaction, causing total breakdown of the raft to $[Os_3(CO)_{10}(MeCN)_2]$.

Conclusion

From the evidence given it can be seen that the $[Os_6(CO)_{21}]$ raft system, whilst stable as a binary carbonyl, is otherwise a highly reactive species. The cluster will readily isomerise to $[Os_6(CO)_{18}]$ if it loses ligands in the solid phase. It has also been observed that replacement of CO with the more labile MeCN causes the cluster to isomerise in solution, once more to form $[Os_6(CO)_{18}]$.

It has also been observed[13] that further addition of CO to the raft cluster causes breakdown of the raft to $[Os(CO)_5]$ and $[Os_5(CO)_{19}]$.

Coupled with this hypothesis the fact that the presence of $[Pd(OAc)_2]$ causes more extensive breakdown of the cluster than amine oxide alone, reinforces the theory that the dimerisation of two triosmium units may proceed *via* the formation of ligand deficient species.

References :

1 R. J. Goudsmit, Ph.D thesis, Cambridge, 1982.

2 J. N. Nicholls, D. H. Farrar, P. F. Jackson, B. F. G. Johnson and J. Lewis, *J. Chem Soc, Dalton transactions, 1982, 1395.*

3 R. J. Goudsmit, J. G. Jeffrey, B. F. G. Johnson, J. Lewis, R. C. S. M^{c}Queen, A. J. Whitmire and J. C. Lui, *J. Chem Soc, Chem Comm, 1986, 24.*

4 U. Bahr, M. Karas and F. Hillenkamp, *Fresenius, J. Anal Chem, 1994, 783.*

5 P. Juhasz and C. E. Costello, *Rapid Comm in Mass Spectrometry, 1993, 343.*

6 J.W. Kolis, E. M. Holt and D.F. Shriver, *J. Am. Chem Soc. 1983, 105, 7307.*

7 S. Ching, J. W. Kolis, E. M. Holt and D. F. Shriver, *Organometallics, 1988, 7, 892.*

8 D. Seyferth, J. E.Hallgren and C. S. Eschbach, *J. Am. Chem Soc. 1974, 96, 1730.*

9 D. Seyferth, G. H. Williams and C. L. Nivert, *Inorganic Chemistry, 1977, 16, 758.*

10 J. A. Hriljac and D. F. Shriver, *Organometallics, 1985, 4, 2225.*

11 J. A. Hriljac, P. N. Swepston and D. F. Shriver, *Organometallics, 1985, 4, 158.*

12 D. Seyferth, *Adv Organomet Chem, 1976, 14, 97.*

13 D. H. Farrar, B. F. G. Johnson, J. Lewis, N. Nicholls, P. R. Raithby and M. J. Rosales, *JCS Chem Comm, 1981, 273.*

CHAPTER FIVE

EXPERIMENTAL

Apparatus for preparation

Reagents were handled using two different methods during the course of this work. Volatile compounds were handled on a glass high vacuum line on which samples for nmr spectroscopic studies were sealed. Air and moisture sensitive compounds were handled utilising a schlenk system. All nmr samples were made up in 5mm pyrex tubes, extended with 5mm pyrex tubing and attached to the vacuum line via a B10 ground glass joint

The vacuum line consisted of detachable pyrex sections, to facilitate regular cleaning, connected by ground glass joints lubricated with Apiezon L grease, with Apiezon N grease used on the stopcocks. Vacuum was obtained by a glass 3 stage mercury diffusion pump backed by a rotary oil pump, this combined system providing a vacuum of $\sim 10^{-6}\tau$. The quality of vacuum on line was monitored by a pirani gauge. The quantity of a volatile reagent on line was monitored by means of a null zero spiral deflection gauge, operating with mirror, lamp and scale. Pressure was monitored on line by a mercury manometer. Samples of highly volatile (boiling point <273K) phosphorus compounds were stored in traps on line cooled to 79K. Less volatile phosphorus compounds and nmr solvents were stored in ampoules equipped with greaseless taps which were attached to the line prior to use. The volumes of the individual line sections were determined using a molecular weight bulb of known volume, allowing quantitative measurement of volatile reagents.

The schlenk system comprised a vacuum manifold and an inert gas manifold fitted with three way taps which allowed either vacuum or inert gas (N_2 or Ar) to be applied to a sample. Vacuum was provided by a rotary oil pump giving $\sim 10^{-2}\tau$. Commercial oxygen free, white spot nitrogen was supplied to the line.

Instrumentation

All ^{31}P nmr spectra were recorded in CD_2Cl_2, referenced to 85% H_3PO_4. All ^{1}H nmr spectra were recorded in $CDCl_3$, referenced to Me_4Si. The nmr spectra were recorded on a Brucker WP200SY 200MHz multinuclear nmr spectrometer, to observe ^{31}P, (81.02MHz) and ^{1}H, (200.13MHz). The ir spectra were recorded on a Perkin Elmer 1600 series fourier transform ir spectrometer in matched 0.1mm path length solution ir cells, (KBr window).

The preparation of $[Os_3(CO)_{10}(MeCN)_2]$

$[Os_3(CO)_{12}]$ (500mg, 0.55mmol) was dissolved in dichloromethane (140ml) and acetonitrile (70ml) and placed in a 500ml round bottomed, 3-necked, quickfit flask. $(CH_3)_3NO$ (125mg, 1.155mmol) was dissolved in acetonitrile (60ml), and added dropwise over 1 hour with stirring. The solution was then stirred for a further 2 hours and then filtered through a short silica column to remove excess $(CH_3)_3NO$. Pure $[Os_3(CO)_{10}(CH_3CN)_2]$ (0.5g, 95%) was collected by removal of solvent on a rotary evaporator. All operations were carried out under a flow of N_2 gas. The purity of the product was checked by ir spectroscopy.

$\nu CN(cm^{-1})$ = 2360(s), 2340(s) in dichloromethane

$\nu CO(cm^{-1})$ = 2106(w), 2052(m), 2029(m), 2016(s), 1983(w), 1968(w) in dichloromethane

The preparation of $[Os_3(CO)_9(\mu_3\text{-}\eta^2\text{:}\eta^2\text{:}\eta^2\text{-}C_6H_6)]$

$[Os_3(CO)_{12}]$ (500mg, 0.55mmol) was dissolved in 250ml of n-octane and placed in a 500ml round bottomed, 3-necked, quickfit flask and heated to reflux. H_2 was bubbled through the solution for 5 hours. The solution was then concentrated to approximately 60ml and 1,3 cyclohexadiene (C_6H_8) (1.5ml, 2mmol) was added, and the mixture refluxed for 1 hour. The solid was filtered off and redissolved in 20ml dichloromethane. Triphenylcarbenium (trityl) tetrafluoroborate $[(C_6H_5)_3C^+BF_4^-]$, (50mg, 1.5mmol) was added and the solution refluxed for 30 minutes and the resultant precipitate was filtered off. This solid was suspended in 50ml of dichloromethane and diazabicyclo[5.4.0]undec-7-ene (DBU), (0.15ml, 0.5mmol) was added, the mixture was then stirred for 1 hour.

Pure $[Os_3(CO)_9(\mu_3\text{-}\eta^2\text{:}\eta^2\text{:}\eta^2\text{-}C_6H_6)]$ then precipitated out of solution in the form of yellow microcrystals, overall yield 60%. The product was characterised by ir and nmr spectroscopy.

$\nu CO(cm^{-1})$ = 2076(m), 2030(s), 1999(m), 1978(w), 1951(w) in dichloromethane

δH = 4.46ppm

The preparation of $[Os_6(CO)_{18}]$

$[Os_3(CO)_{12}]$ (500mg, 0.55mmol) was sealed in an 85ml carius tube at $10^{-6}\tau$. The tube was heated in a furnace to 483K for 12 hours. The reaction products were removed from the tube under a flow of N_2 gas and dissolved in ethyl acetate. The mixture was filtered to remove any solid residues, and was then cooled to 253K for 24 hours during which time all of the unreacted $[Os_3(CO)_{12}]$ crystallised out. This was then removed by filtration. The solution was then cooled to 253K and maintained at that temperature for 2 weeks, during which time the pure $[Os_6(CO)_{18}]$ crystallised out, leaving small amounts of tetra- and pentanuclear osmium clusters in solution, yield 80%. The product was characterised by ir and FAB mass spectroscopy.

$\nu CO(cm^{-1})$ = 2108(w), 2077(s), 2063(s), 2040(m), 2007(m), 1955(w) in dichloromethane

M^+ = 1644, (3-NOBA Matrix)

The preparation of $[Os_6(CO)_{21}]$

$[Os_3(CO)_{10}(MeCN)_2]$ (500mg, 0.53mmol) was dissolved in 150ml dichloromethane and placed in a 500ml, round bottomed, 3-necked quickfit flask. $Pd(OC_2H_5)_2$ (10mg, 0.07mmol) was added as a catalyst and the mixture stirred overnight. The resulting deep blue solution was concentrated to approximately 2ml and the products separated by tlc, eluent 70% dichloromethane/15% n-hexane/5% carbon tetrachloride. The blue band consisted of a mixture of $[Os_6(CO)_{20}(MeCN)]$ and $[Os_6(CO)_{19}(MeCN)_2]$. This mixture was isolated from the plates and dissolved in 100ml of dichloromethane, and placed in a 250ml, round bottomed, 3-necked quickfit flask. CO was bubbled through the solution for 2 hours and the resulting solid $[Os_6(CO)_{21}]$, filtered off, yield 90%. All operations were carried out under N_2 gas. The product was characterised by ir and laser desorption mass spectroscopy.

$\nu CO(cm^{-1})$ = 2103(m) ,2092(w), 2064(m),2035(m), 2018(s), 1997(m), 1983(w), 1967(w), 1964(w), 1957(w), 1895(w) as Nujol mull

M^+ = 1730, MALDI spectrum

The preparation of $[Os_6(CO)_{19}(MeCN)_2]$

$[Os_6(CO)_{21}]$, (500mg, 0.32mmol), was placed in a 500ml round bottomed quickfit flask. Acetonitrile, (100ml), and dichloromethane, (100ml), were added to the flask. $(CH_3)_3NO$, (125mg, 1.155mmol) was dissolved in acetonitrile, (60ml), and added dropwise over 1 hour with stirring. The solution was then stirred for a further 2 hours and filtered through a short silica column to remove excess $(CH_3)_3NO$.

The preparation of PH_3

5g of Ca_3P_2 was ground to a fine powder and placed in a 250ml round bottomed, 3-necked, quickfit flask. This was attached to a glass high vacuum line via swivel link connectors. 10ml of degassed H_2O was placed in a pressure equalised dropping funnel and added dropwise to the vessel over 1 hour. The PH_3, contaminated with P_2H_4 and H_2O was collected online in a series of traps cooled to 79K. The PH_3 was purified by concentrating all of the samples into one trap, placing a slush bath at 177K around the trap and distilling the pure PH_3 into a trap cooled to 79K, yield 97%. All operations were carried out under $10^{-6}\tau$. The purity of the product was checked by ir and nmr spectroscopy.

The preparation of $PMeH_2$

200ml of trimethyl phosphite was refluxed with 1.5g of KI for 20 hours under a flow of N_2 gas. The solution was then cooled to room temperature and the KI was filtered off.

25ml of the resulting methyl dimethyl phosphonate $[(CH_3)P(OCH_3)_2O]$ was dissolved in 100ml THF and placed in a pressure equalised dropping funnel, 9g of $LiAlH_4$ and 100ml THF were placed in a 500ml, round bottomed, 3-necked quickfit flask. The flask was attached to a glass high vacuum line via swivel links and a dry ice condenser. The pressure equalised dropping funnel was then attached to the flask and the system was flushed with N_2 gas. An ice/salt bath (ca. 260K) was placed round the flask and the pressure in the system was reduced to $2 \times 10^{-1}\tau$. The THF/phosphonate mixture was added to the flask dropwise over 2 hours; once the reaction mixture began to effervesce a slow bleed of N_2 gas was passed through the reaction vessel, allowing the pressure to rise to $5 \times 10^{-1}\tau$, and maintaining that pressure.

Once the addition was complete the vessel was warmed to room temperature and the system was through pumped to boil the product out of solution. The product was trapped on line at 79K, along with approximately 50ml of THF. The mixture was fractionated through a trap held at 163K to separate small amounts of PH_3 which formed. The trapped mixture of product and THF was then separated by fractionating through a trap held at 157K which retained the THF. The pure product was then isolated in a trap at 79K, yield 87%. The purity of the product was checked by ir and nmr spectroscopy.

The preparation of PMe_2H

24g of Mg was placed in a 2.5l round bottomed, 3-necked, quickfit flask. 1.25l of diethyl ether was also placed in the flask. 84ml of iodomethane was added dropwise over 2 hours and stirred for a further 2 hours. 51ml of $SPCl_3$ was added dropwise over 3 hours and stirred for a further 2 hours. The mixture was then added to a 5l beaker half filled with a mixture of crushed ice, 700ml of 1M H_2SO_4 and H_2O. The white precipitate of $[P_2S_2(CH_3)_4]$ was filtered off and recrystallised from diethyl ether.

5g of $[P_2S_2(CH_3)_4]$ was dry mixed with 0.25g of $LiAlH_4$ and ground together thoroughly. The mixture was placed in a 250ml round bottomed,3-necked, quickfit flask attached to a glass high vacuum line via swivel links. A pressure equalised dropping funnel was connected to the flask and charged with 25ml of degassed di-n-butyl ether. This was added dropwise to the mixture over 2 hours with stirring. The product, contaminated with di-n-butyl ether was collected in a series of traps cooled to 79K. Purification was carried out by concentrating all of the fractions into one trap, placing a slush bath at 209K around the trap and distilling the pure $PH(CH_3)_2$ into a trap cooled to 79K, yield 79%. All operations were carried out under $10^{-6}\tau$. The purity of the product was checked by ir and nmr spectroscopy.

The preparation of PMe_3

24g of Mg was placed in a 1l round bottomed, 3-necked, quickfit flask. 500ml of diethyl ether was also placed in the flask. 96ml of iodomethane was added dropwise over 2 hours and the mixture stirred for a further 2 hours. 63ml of $P(OC_6H_5)_3$ was added dropwise over 3 hours. The product was trapped out in the form of a silver iodide adduct. The adduct was formed by bubbling the product gas through a solution containing 10g of potassium iodide and 14g of silver iodide. The phosphine/silver iodide adduct precipitated out as a pale yellow powder. The product was collected by filtration and dried carefully. All operations were carried out under a flow of N_2 gas.

To liberate the product the adduct was placed in an ampoule attached to the vacuum line and heated. Pure $P(CH_3)_3$ was collected in a trap cooled to 79K, yield 74%. All operations were carried out at $10^{-6}\tau$. The purity of the product was checked by ir and nmr spectroscopy.

The preparation of KPH_2

456mg (13mmol) of potassium was broken up and rolled into small cylinders and placed in an ampoule which was attached to a glass vacuum line and evacuated. Approximately 20ml of NH_3 was condensed into the ampoule at 79K giving a deep blue solution. 13mmol of PH_3 was then condensed into the ampoule and the mixture was warmed to 195K and stirred for 2 hours, during which time the solution turned pale yellow. The NH_3 and excess PH_3 were removed under vacuum at 195K over 24 hours. The resulting KPH_2 (10 mmol, yield 77%) was then used immediately due to its instability. All operations were carried out at $10^{-6}\tau$.

The preparation of $PEtH_2$

10 mmol of KPH_2 was prepared using the above method. Excess (approximately 2:1 ratio) bromoethane was condensed into the ampoule and left overnight at room temperature. The resulting mixture of $PH_2(C_2H_5)$, bromoethane and PH_3 was condensed into a trap cooled to 79K. The PH_3 contamination was removed by placing a trap cooled to 177K around the sample and pumping on the sample for 1 hour. The bromoethane was removed by fractionation through a trap cooled to 227K, yield 85%. All operations were carried out at $10^{-6}\tau$. The purity of the product was checked by ir and nmr spectroscopy.

The preparation of PEt_2H

24g of Mg was placed in a 2.5l round bottomed, 3-necked, quickfit flask. 1.25l of diethyl ether was also placed in the flask. 84ml of bromoethane was added dropwise over 2 hours and stirred for a further 2 hours. 51ml of $SPCl_3$ was added dropwise over 3 hours and stirred for a further 2 hours. The mixture was then added to a 5l beaker half filled with a mixture of crushed ice, 700ml of 1M H_2SO_4 and H_2O. The white precipitate of $[P_2S_2(C_2H_5)_4]$ was filtered off and recrystallised from diethyl ether.

5g of $[P_2S_2(C_2H_5)_4]$ was dry mixed with 0.25g of $LiAlH_4$ and ground together thoroughly. The mixture was placed in a 250ml round bottomed, 3-necked, quickfit flask attached to a glass high vacuum line via swivel links. A pressure equalised dropping funnel was connected to the flask and charged with 25ml of degassed di-n-butyl ether. This was added dropwise to the mixture over 2 hours with stirring. The product, contaminated with diethyl ether, was collected in a series of traps cooled to 79K. Purification was carried out by concentrating all of the fractions into one trap, placing a slush bath at 209K around the trap and removing the diethyl ether under vacuum, yield 82%. All operations were carried out under $10^{-6}\tau$. The purity of the product was checked

by ir and nmr spectroscopy.

The preparation of PEt_3

24g of Mg and 500ml of diethyl ether were placed in a 1l round bottomed, 3-necked, quickfit flask. 100ml of iodoethane was added dropwise over 2 hours and stirred for a further 2 hours. 63ml of $P(OC_6H_5)_3$ was added dropwise over 3 hours. The $P(C_2H_5)_3$ was purified by filtering off the MgI_2, under a flood of N_2 gas and distilling off the $(C_2H_5)_2O$. The $P(C_2H_5)_3$ was then distilled under vacuum utilising an air leak with a flow of N_2 gas (B.Pt. 140°C @ $10^{-1}\tau$), yield 60%. All operations were carried out under a flow of N_2 gas. The purity of the product was checked by ir and nmr spectroscopy.

The Preparation of $P(i\text{-}Pr)H_2$

10mmol of KPH_2 was prepared using the above method. Excess (approximately 2:1 ratio) $i\text{-}C_3H_7Cl$ was condensed into the ampoule at 79K and left for 3 hours at room temperature. The mixture of $PH_2(i\text{-}C_3H_7)$, C_3H_7Cl and PH_3 was condensed into a trap cooled to 79K. The PH_3 contamination arises from traces of HCl in the C_3H_7Cl, and is removed by placing a trap cooled to 177K around the mixture and pumping on the sample for 1 hour. The $i\text{-}C_3H_7Cl$ was removed by fractionation through a trap cooled to 227K, yield 89%. All operations were carried out at $10^{-6}\tau$. The purity of the product was checked by ir and nmr spectroscopy.

The Preparation of $P(i\text{-}Pr)_2H$

1.5ml of $PCl(i\text{-}C_3H_7)_2$ was dissolved in 50ml of $(C_2H_5)_2O$ and placed in a pressure equalised dropping funnel attached to a 100ml, round bottomed, 3-necked, quickfit flask. 0.75g of $LiAlH_4$ was added to the flask and a condenser was fitted. The solution was then added dropwise to the flask over 2 hours, monitoring the reaction by ir spectroscopy to observe the disappearance of the P-Cl stretch (approx. $550cm^{-1}$) and the growth of the P-H stretch (approx. $2350cm^{-1}$) in the mixture. Once the P-Cl stretch was no longer evident in the ir the mixture was condensed on to a glass high vacuum line. The diethyl ether was removed by fractionation through a trap cooled to 227K which trapped the $PH(i\text{-}C_3H_7)_2$ but not the solvent, yield 94%. The reduction of the chlorophosphine species was carried out under N_2. The purification of the product was carried out under $10^{-6}\tau$. The purity of the product was checked by ir and nmr spectroscopy.

The preparation of PPh_2H

456mg of potassium and 120mg of sodium were placed in a schlenk tube and heated under a flow of N_2 gas until a melt was obtained. 1g of PPh_3 was added to the melt and stirred under N_2 for 1 hour, resulting in formation of $K^+ (PPh_2)^-$. The melt was cooled to room temperature and n-butanol was slowly dripped into the tube to destroy any remaining metal and to protonate the $(PPh_2)^-$ groups. The solution was then filtered to remove any metal oxides and the n-butanol was distilled off. The pure product was obtained by distillation under vacuum (B.Pt. 150°C @ $10^{-1}\tau$), yield 88%. The purity of the product was checked by ir and nmr spectroscopy.

Reagent purification

Crude PPh_3 was purchased from the Aldrich Chemical Company and purified by means of recrysallisation from ethanol to remove traces of $OPPh_3$. PH_2Ph and $P(i\text{-}Pr)_3$ were purchased from the Aldrich Chemical Company and used without further purification. The cluster $[Os_3(CO)_{12}]$ was purchased from the Oxchem chemical company and used without further purification.

Table 5.1 : Spectroscopic data for free phosphines			
Phosphine	δP (ppm)	$^1J_{PH}$ (Hz)	νPH (cm^{-1})
PH_2Me	-161	199	2324.5
$PHMe_2$	-94	191	2280.1
PMe_3	-62	N/A	N/A
PH_2Et	-126	190	2297.4
$PHEt_2$	-58	197	2284.1
PEt_3	-20	B/A	N/A
$PH_2(i\text{-}Pr)$	-103	195	2292.0
$PH(i\text{-}Pr)_2$	-37	201	2269.9
$P(i\text{-}Pr)_3$	+8	N/A	N/A
PH_2Ph	-122	205	
$PHPh_2$	-40	214	
PPh_3	-6	N/A	N/A

The nmr experiment for the reaction of phosphines with $[Os_3(CO)_{10}(MeCN)_2]$

$[Os_3(CO)_{10}(MeCN)_2]$, (94mg, 0.1mmol), was dissolved in CD_2Cl_2 and placed in a 5mm pyrex nmr tube. The tube was then attached to the vacuum line and the solvent degassed by a repeated freeze/thaw method. A 0.2mmol sample of phosphine was condensed into the tube at 77K. The tube was then sealed under vacuum and stored at 77K until required. Due to the involatile and stable nature of PPh_3 the phosphine was weighed out and placed in the tube with the cluster sample and sealed as normal. The table below, (Table 5.2) summarises the yields of products obtained for the different phosphines before and after heating to 333K.

Table 5.2 : Product yields for the reaction of $[Os_3(CO)_{10}(MeCN)_2]$ with Phosphines

Phosphine	Room Temperature		333K		Mono Substituted
	1,2 Product	Bridged	1,2 Product	Bridged	
$PMeH_2$	N/A	N/A	80%	6%	8%
PMe_2H	N/A	N/A	45%	7%	7%
PMe_3	N/A	N/A	38%	N/A	6%
$PEtH_2$	77%	9(6)%*	62%	18(12)%*	8%
PEt_3	N/A	N/A	29%	N/A	5%
$P(i\text{-}Pr)H_2$	88%	N/A	79%	8%	8%
$P(i\text{-}Pr)_3$	N/A	N/A	20%	N/A	5%
$O{=}P(i\text{-}Pr)_3$	N/A	N/A	14%	N/A	4%
$PPhH_2$	84%	7(3)%*	79%	11(4)%*	6%
PPh_2H	N/A	N/A	84%	4%	8%

* : Numbers in parenthesis are for the proposed intercluster bridging units.

The table above gives percentage yields of products obtained as a proportion of total nmr signal intensity in the spectra.

Courses Attended

Attendance at U.S.I.C. Conferences, 1991-93.

Attendance at Chemistry of the copper and zinc triads conference, 1992.

Attendance at Inorganic section group meetings, 1991-94.

Cluster Chemistry - Professor B. F. G. Johnson.

X-Ray and Laser safety - University of Edinburgh safety department.

Electron spin resonance spectroscopy - Dr R. E. P. Winpenny.

Introduction to nmr spectroscopy - Dr I. H. Sadler, Dr D. Reed and Dr J. Parkinson.

Heavy metals in the environment - Professor M. Schröder.

Surface chemistry and catalysis - Dr G. S. McDougall.